Design of a Residential Air Source Heat Pump for Extremely Cold Climates

by

Wahid Besada

A thesis submitted to the
School of Graduate and Postdoctoral Studies in partial
fulfillment of the requirements for the degree of

Master of Applied Science in Mechanical Engineering

Faculty of Engineering and Applied Science

University of Ontario Institute of Technology (Ontario Tech University)

Oshawa, Ontario, Canada

May 2023

THESIS EXAMINATION INFORMATION

Submitted by: **Wahid Besada**

Master of Applied Science in Mechanical Engineering

Design of a Residential Air Source Heat Pump for Extremely Cold Climate

An oral defense of this thesis took place on 24-May-2023 in front of the following examining committee:

Examining Committee:

Chair of Examining Committee	Dr. Amirkianoosh Kiani
Research Supervisor	Dr. Martin Agelin-Chaab
Examining Committee Member	Dr. Bale Reddy, Ontario Tech University
Thesis Examiner	Dr. Xianke Ling, Ontario Tech University

The above committee determined that the thesis is acceptable in form and content and that a satisfactory knowledge of the field covered by the thesis was demonstrated by the candidate during an oral examination. A signed copy of the Certificate of Approval is available from the School of Graduate and Postdoctoral Studies.

ABSTRACT

Air source heat pumps are energy efficient systems suitable for space heating applications, however, their performance drastically degrades in low ambient temperatures. An innovative design is proposed in this thesis that can switch operating modes to allow efficient heating operation in an ambient temperature range of -50 °C to +20 °C. The proposed design is modeled and analyzed in detail, and the system performance is applied to weather data of two northern Canadian cities. The results show remarkable performance improvement, with around 30% annual energy savings compared to similar systems available in the market. The coefficient of performance is above 2.0 and 1.5 for temperatures as low as -30 °C and -50 °C, respectively. In addition, the heating capacity is almost steady despite decreasing lower ambient temperatures, thereby solving one of the biggest challenges of this technology and eliminating the need for auxiliary heating systems, as is the current practice.

Keywords: Heat pump; residential heating; cold climate; air source; weather data.

AUTHOR'S DECLARATION

I hereby declare that this thesis consists of original work which I have authored. This is a true copy of the thesis, including any required final revisions, as accepted by my examiners.

I authorize the University of Ontario Institute of Technology (Ontario Tech University) to lend this thesis to other institutions or individuals for the purpose of scholarly research. I further authorize the University of Ontario Institute of Technology (Ontario Tech University) to reproduce this thesis by photocopying or by other means, in total or in part, at the request of other institutions or individuals for the purpose of scholarly research. I understand that my thesis will be made electronically available to the public.

Wahid Besada

STATEMENT OF CONTRIBUTIONS

I hereby certify that I am the sole author of this thesis and that no part of this thesis has been published or submitted for publication. I have used standard referencing practices to acknowledge ideas, research techniques, or other materials that belong to others. Furthermore, I hereby certify that I am the sole source of the creative works and/or inventive knowledge described in this thesis.

ACKNOWLEDGEMENTS

First and foremost, I would like to thank my supervisor Dr. Martin Agelin-Chaab for his encouragement, guidance, and support, which played a major role for this work to materialize.

A great appreciation for the whole Ontario Tech staff for creating this productive, collaborative, and friendly environment. It was always a pleasure to be around.

A special Thank You to my wife for her patience and support. And to my children for adding joy to my life. I will forever love you.

And thanks to everyone who added to my knowledge throughout my career.

TABLE OF CONTENTS

LIST OF TABLES

LIST OF FIGURES

LIST OF ABBREVIATIONS AND SYMBOLS

Abbreviations

ΔT_1	Temperature difference between fluids at heat exchanger inlet, °C
ΔT_2	Temperature difference between fluids at heat exchanger exit, °C
ΔT_{lm}	Logarithmic temperature mean difference, °C
a_1	Building load equation slope
b_1	Building load equation intercept
BL	Building load, kW
C_D	Degradation coefficient, unitless
COP	Coefficient of performance, unitless
c_p	Fluid specific heat at constant pressure, kJ/kg K
D	Rotor diameter in turbomachinery, m
E	Consumed energy, kJ
EER	Energy efficiency ratio, Btu/W.hr
F	Factor depending on compressor volumetric efficiency
H	Heat load total, kJ
h_i	Specific enthalpy at state i, kJ/kg K
HH	Heating hours, hr
HLH	Heating load hours, hr
$HSPF$	Heating seasonal performance factor, Btu/W.hr
K_{HE}	Heat exchanger characteristic constant, kJ/s K
$\dot{m}$	Mass flowrate, kg/s
N	Rotation speed, 1/min
p	Pressure, Pa
P	Power consumption, kW
p_1	Vapor pressure at compressor inlet, Pa
p_2	Vapor pressure at compressor exit, Pa
PF	Power factor, unitless

PLF	Part load factor, unitless
Q	Heat energy, kJ
$\dot{Q}$	rate of heat transfer, kW
QR	Capacity ratio, capacity as a ratio to capacity at -20 °C ambient.
RPM	Revolutions per minute, 1/min
$SEER$	Seasonal energy efficiency ratio, Btu/W.hr
$SCOP$	Seasonal coefficient of performance, unitless
s_i	Entropy at state *i,* kJ/K
t_D	Refrigerant saturated discharge temperature at compressor discharge, °C
T_L	Temperature of low temperature region, °C
T_H	Temperature of the high temperature region, °C
t_S	Refrigerant saturated suction temperature at compressor suction, °C
U	Overall heat transfer coefficient, kW/m^{2}K
V	Normal air velocity in fans, m/s
$\dot{W}$	power consumption, kW

Symbols

η	Efficiency
γ	fluid polytropic constant
ε	Compressor clearance volume ratio
ψ	Fan head coefficient
ϕ	Fan flowrate coefficient
Δ	Differential
ρ	Density, kg/m^3
τ	Heating time, hr

Subscripts

aux	Auxiliary
c	Compression
H	High temperature

Hp	High pressure
HP	Heat pump
i	Fluid state number
ID	Indoor
inj	Injection
j	Temperature bin number
L	Low temperature
Lp	Low pressure
lm	Logarithmic mean
OD	Outdoor
p	polytropic
s	Isentropic
$std.$	Standard
t	total
v	Volumetric

Superscripts

C	Cooling mode
H	Heating mode

Chapter 1. Introduction

1.1 Background

Heat pump systems are designed based on the refrigeration cycle to deliver heat energy from a low temperature region to a high temperature region. In particular, the heat pump absorbs heat energy from the low temperature region, does work on it, and then delivers this total energy (energy absorbed and energy from work) to the higher temperature region.

Heat pumps are categorized depending on the low temperature source of energy into:

1. Air source, the heat is absorbed from the ambient air.
2. Water source heat is absorbed from a water source.
3. Ground source, the heat is absorbed from the underground.

Heat pumps are also categorized based on the heating application, either air (or space) heating or water heating. Air heating applications are used to directly heat the space. Water heating applications can also utilize the hot water in a secondary circulation system for space heating.

Heat pumps can be used in residential, commercial, or industrial space heating applications. Capacities can vary from 5 kW up to 100 kW. They are often designed to fulfil both heating and cooling needs. Thus, just one piece of equipment is needed to provide heating in winter and cooling in summer [1].

The refrigeration cycle, heat pump and air conditioning are based on the theoretical reverse Carnot cycle. The actual cycle deviates from the theoretical one to form the vapor-compression refrigeration cycle. The system is considered an air conditioner when the energy absorbed from the cold region is the one utilized and considered a heat pump when the energy rejected by the warm region is the one utilized [2].

1.1.1 Vapor Refrigeration Cycle

The purpose of a refrigeration cycle is to absorb heat energy from a low temperature region and reject it at a higher temperature region. This process is against the natural flow of heat energy from high temperature to low temperature. According to the Second Law of

thermodynamics, work must be done, and this work is used to compress the working fluid, refrigerant, from a low pressure to a higher pressure during this cycle.

1.1.1.1 Carnot Refrigeration Cycle

The Carnot Refrigeration Cycle is a theoretically reversible cycle operating between two thermal reservoirs at different temperatures. The cycle is executed by circulating refrigerant fluid through four components: 1) Compressor, 2) Condenser, 3) Evaporator, and 4) Turbine. All processes are considered internally reversible. Also, heat transfer between the warm and cold regions and the respective heat exchanger, the condenser and the evaporator occurs with no temperature difference. Figure 1.1 shows an illustration of such a system between a warm region at temperature T_H and a cold region at temperature T_L, along with the relevant Temperature-Entropy (T-s) diagram.

The process is described as follows:

i. The vapor-liquid mixture refrigerant at state 1 enters the compressor, where it undergoes an isentropic compression process to state 2. The temperature and pressure of the refrigerant rise from T_L to T_H.
ii. The saturated vapor at state 2 enters the condenser and leaves as a saturated liquid at state 3. During this process, heat is rejected adiabatically from the refrigerant to the hot region at temperature T_H. Both pressure and temperature of the refrigerant remain constant during this process.
iii. Saturated liquid at state 3 undergoes an isentropic expansion process in the turbine to a vapor-liquid mixture at state 4. The refrigerant temperature and pressure fall back from T_H to T_L.
iv. The liquid-vapor refrigerant mixture at state 4 enters the evaporator and leaves at state 1. During this process, heat is absorbed adiabatically by the refrigerant from the cold region at temperature T_L. The temperature and pressure do not change during this process.

The coefficient of performance of the cycle (COP), by definition, is the ratio of the heat energy gained to the net-work input required to achieve that gain. If the cycle is considered a refrigeration cycle, then the heat gain is the amount of heat absorbed by the refrigerant in

the evaporator (Process 4-1), whereas the heat gain in a heat pump application is that rejected to the warm region (Process 2-3).

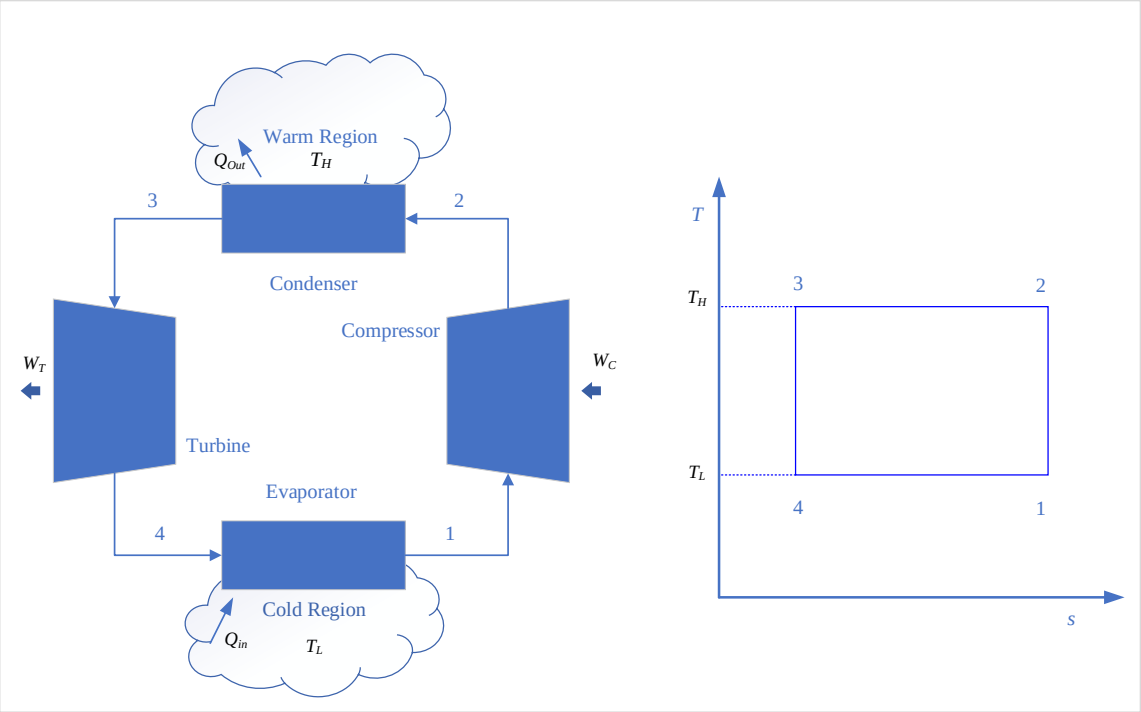

Figure 1.1: Carnot refrigeration cycle.

Hence, the COP of the cycle when operating as an air conditioner or a refrigerator is as follows [2]:

$$COP^C = \frac{T_L}{T_H - T_L} \tag{1.1}$$

And when operating as a heat pump is:

$$COP^H = \frac{T_H}{T_H - T_L} \tag{1.2}$$

This represents the maximum theoretical coefficient of performance possible for such a system running between T_L and T_H.

It is noticed that in the heat pump operation of this system, the COP value must be greater than 1.

1.1.1.2 Vapor-Compression Cycles

There are three major impractical aspects within the Carnot Cycle described above.

i. To build a practical-sized heat exchanger, there must be a reasonable temperature difference between the fluids passing across the heat exchanger to achieve the desired heat energy transfer between the fluids. Therefore, the temperature of the refrigerant in the condenser T_C must be above the warm region temperature T_H. Also, the refrigerant temperature in the evaporator T_E must be lower than that of the cold region T_L. See Figure 1.2

ii. The compression of vapor-liquid mixture at state 1 in the Carnot Cycle is not attainable by normal compressors because compressors are usually designed to compress only fluids in the gaseous state. This means that liquid-vapor mixture must leave the evaporator after all the liquid is evaporated, and the state of the refrigerant is at least saturated vapor.

iii. The amount of work generated during the expansion process is relatively small therefore sacrificing the work generated by the turbine and using a throttling device is more economical.

Applying the above-mentioned changes result in the so-called ideal vapor-compression refrigeration cycle, see Figure 1.2

The process of the cycle is described as follows:

1-2s: Isentropic compression

2s-3: Heat rejection at constant pressure

3-4: Throttling process,

4-1: Heat absorption at constant pressure.

The following assumptions have been made:

- All processes are internally irreversible except processes 3-4.
- No pressure drops between components.
- Stray heat transfer to surroundings is ignored.
- The compression process is isentropic.

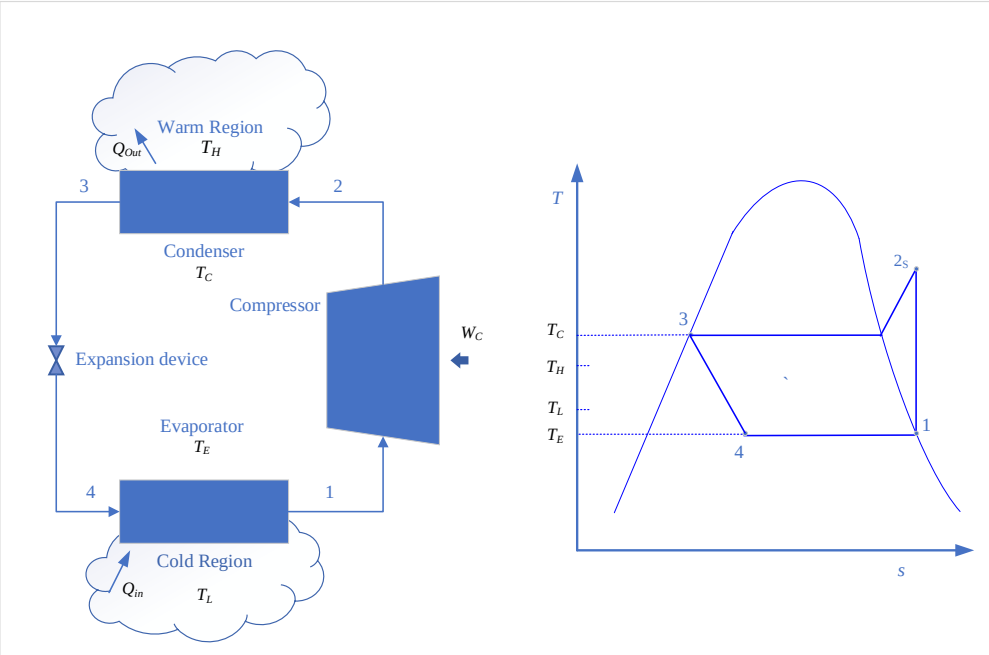

Figure 1.2: Ideal vapor-compression refrigeration cycle.

The coefficient of performance of this system is therefore calculated as [2]

- In cooling mode

$$COP^{C} = \frac{h_1 - h_4}{h_{2s} - h_1} \tag{1.3}$$

- In heating mode

$$COP^{H} = \frac{h_2 - h_3}{h_{2s} - h_1} \tag{1.4}$$

It was mentioned earlier that the COP of the Carnot cycle is the maximum that could be achieved. Thus, the COP values obtained from Equations 1.3 and 1.4 will always be lower than that obtained from Equations 1.1 and 1.3 for the same system operating between the same T_H and T_L.

There are a few assumptions that make the ideal vapor-compression refrigeration cycle described above practically unattainable. In evaluating the actual vapor-compression refrigeration system, the actual processes should be considered.

- The refrigerant entering the compressor is superheated as it is safer and more practical for the operation of the compressor. That is to ensure that even with a loss of a few degrees of the refrigerant temperature, it will still enter the compressor in a gaseous form.
- The compression and expansion processes are not isentropic but rather adiabatic. Heat loss from the compressor body or the expansion device is ignored.
- Refrigerant leaving the condenser in a sub-cooled liquid state ensures that all vapor is condensed and only liquid is being sent to the throttling device.

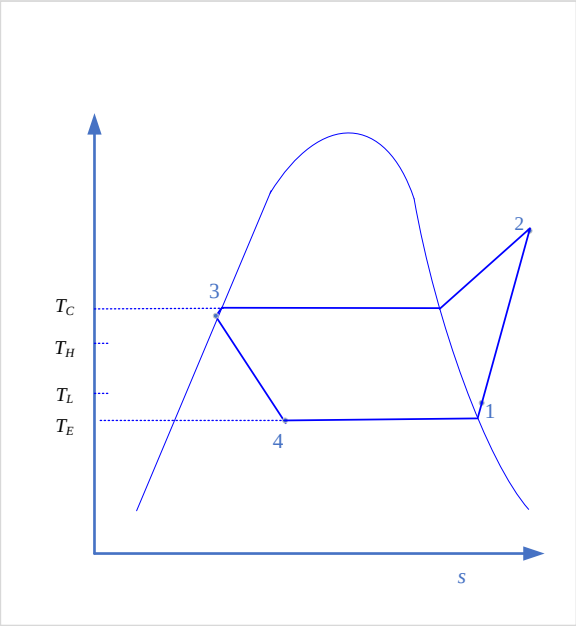

Figure 1.3: T-s diagram for actual vapor-compression refrigeration cycle.

$$\dot{Q}_C = \dot{m} \cdot (h_2 - h_3) \tag{1.5}$$

$$\dot{Q}_E = \dot{m} \cdot (h_1 - h_4) \tag{1.6}$$

$$\dot{W} = \dot{m} \cdot (h_2 - h_1) \tag{1.7}$$

$$COP^{H} = \frac{h_2 - h_3}{h_2 - h_1} \tag{1.8}$$

$$COP^{C} = \frac{h_1 - h_4}{h_2 - h_1} \tag{1.9}$$

1.1.2 Effect of Compression Ratio on Compressor Efficiencies

1.1.2.1 Isentropic Efficiency

The compression ratio plays a significant role in determining the compression process's overall isentropic efficiency. The thermodynamic analysis of a polytropic compression process for ideal gas results in the following equation [3]:

$$\eta_c = \left[\left(\frac{p_2}{p_1}\right)^{\frac{\gamma-1}{\gamma}} - 1\right] / \left[\left(\frac{p_2}{p_1}\right)^{\frac{\gamma-1}{\eta_P \gamma}} - 1\right] \qquad (1.10)$$

The equation shows that the work done during the compression process for a certain gas depends only on the compression ratio.

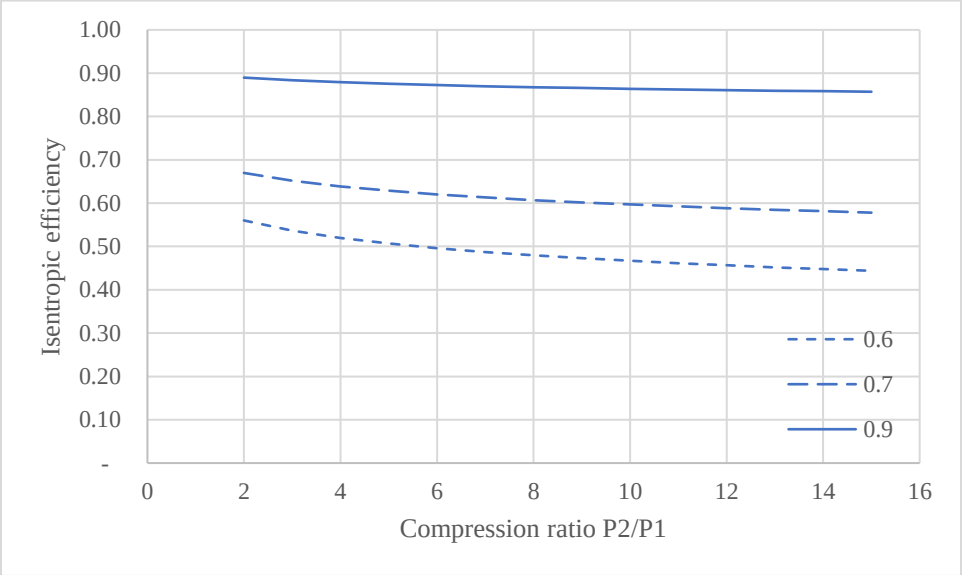

Figure 1.4: Relationship between overall isentropic efficiency, pressure ratio and polytropic efficiency for γ=1.4.

The plot shown in Figure 1.4 was done by applying Equation 1.10 for various pressure ratios and polytropic efficiencies using γ =1.4. It shows how the isentropic efficiency deteriorates with an increased pressure ratio. This means that the compression process consumes less energy if the compression process is divided into smaller steps. That is why there is always a practical cap on the economic compression ratio of the compressor. For the air conditioning and refrigeration industry, a compression ratio of less than 1:12 is desirable, while 1:15 would be permitted just for short intervals of time [4].

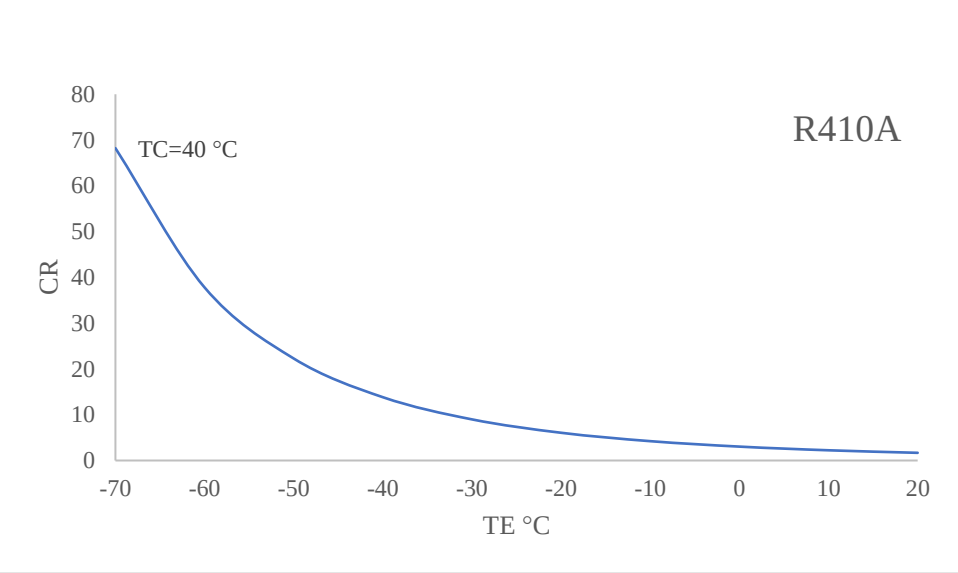

Figure 1.5: Compression ratio (CR) for refrigerant R410A at different evaporator temperatures (TE) and 40 °C condenser temperature (TC).

1.1.2.2 Volumetric Efficiency

The compressor volumetric efficiency is defined as the actual volume of gas entering the compression compartment of the compressor during the suction process divided by the swept volume.

For practical reasons, there is always some residual gas left in the compression compartment of the compressor that does not get out of the compressor at the end of the compression process. This eventually reduces the amount of gas volume flow rate in the system as compared to the theoretical one based on the swept volume [5], [6], [7].

The theoretical formula for volumetric efficiency is [6]

$$\eta_v = 1 - \left(\left(\frac{p_2}{p_1} \right)^{\frac{1}{\gamma}} - 1 \right) \cdot \varepsilon \qquad (1.11)$$

This shows that the main factor that affects the volumetric efficiency of a given compressor is the pressure ratio. Thus, one of the biggest challenges when operating a compressor at high compression ratios, like the case of a heat pump compressor running at extremely low ambient temperature, is that the compressor's capability to circulate the fluid deteriorates, which results in a significant drop in the heating capacity.

1.1.3 Cascade Refrigeration System

As explained earlier, when the compression ratio exceeds a certain value, it becomes uneconomic to do it in one stage. For this reason, cascade refrigeration systems were introduced to ultra-low temperature applications. These kinds of systems can operate in hot ambient temperature, 45 °C and can provide refrigeration temperatures down to -50 to -100 °C. -35 to -50 °C is common in industrial freezing applications. Depending on the system design, the number of cascade stages can be selected, ranging from two to as high as six in some designs.

A simple cascade system consists of a low temperature vapor-compression refrigeration system that absorbs heat to its evaporator from the low temperature region and rejects heat through an intermediate cascade heat exchanger. The heat rejected in the intermediate cascade heat exchanger is absorbed by the refrigerant of another vapor-compression refrigeration system acting as the system's evaporator. The condenser of this other system, in turn, rejects heat to the high temperature region through its condenser. Eventually, heat energy is moved from an ultra-low temperature region to a high temperature region in multiple stages [8].

The two systems can circulate two different kinds of refrigerants. Depending on the application, the system designer has the flexibility to select the refrigerants that better fulfill the requirements of each system independently. This could enhance the overall performance of the system.

The T-s diagram of a simple cascade system is shown in Fig 1-6. The thermodynamic analysis for this system follows the same equations as for the single-stage actual cycle. The total power consumption of the system is the addition of the power consumption of each compressor. The useful heating effect is the one rejected by the high-pressure system only.

In addition, an energy balance calculation should be done for the intermediate heat exchanger.

Then the Thermodynamic equations become:

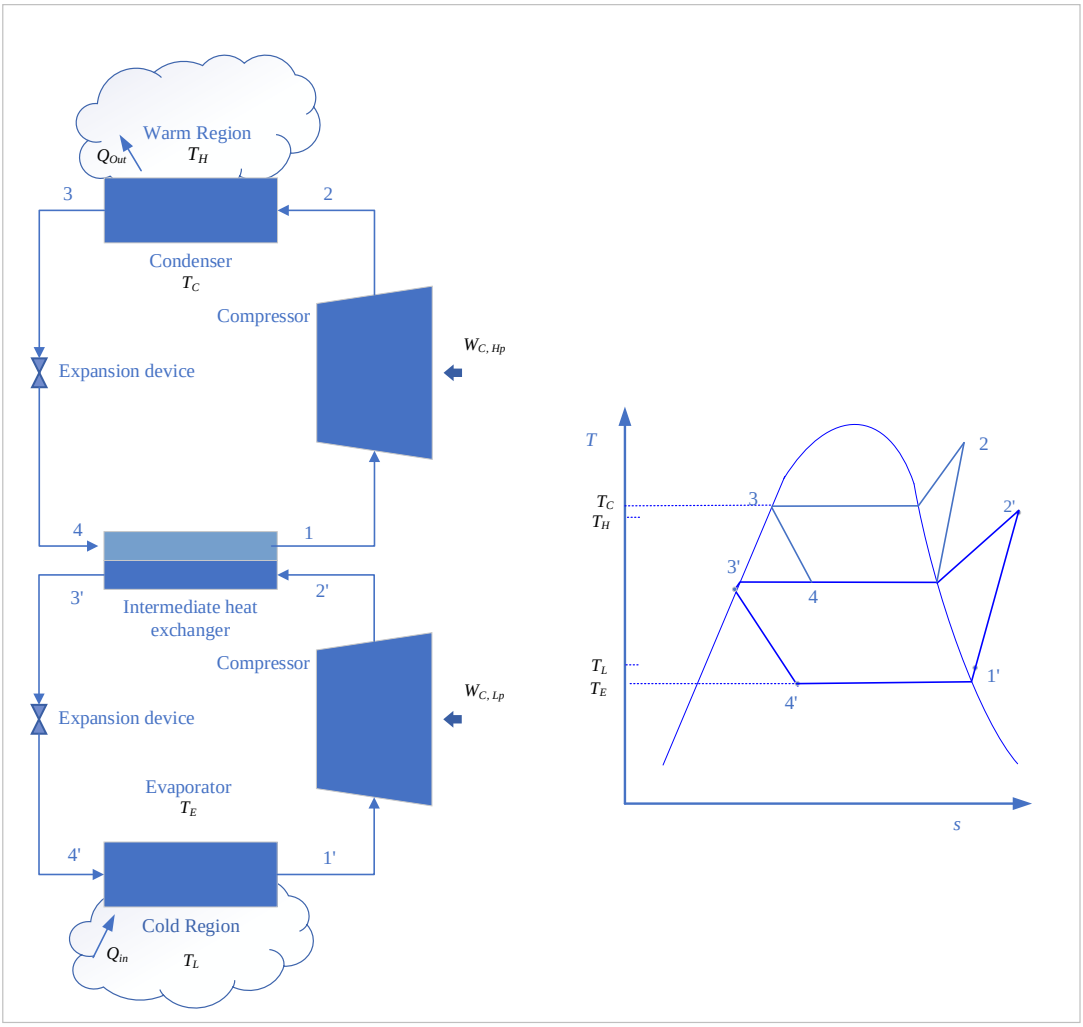

Figure 1.6: Simple cascade system.

$$\dot{m}_{Lp} \cdot (\dot{h_{2'}} - h_{3'}) = \dot{m_{Hp}} \cdot (h_1 - h_4) \tag{1.12}$$

$$COP^H = \frac{\dot{m_{Hp}} \cdot (h_2 - h_3)}{\dot{m}_{Lp} \cdot (h_{2'} - h_{1'}) + \dot{m_{Hp}} \cdot (h_2 - h_1)} \tag{1.13}$$

$$COP^C = \frac{\dot{m_{Lp}} \cdot (h_1 - h_4)}{\dot{m}_{Lp} \cdot (h_{2'} - h_{1'}) + \dot{m_{Hp}} \cdot (h_2 - h_1)} \tag{1.14}$$

1.1.4 Ambient Temperatures and Climate Regions

The USA Department of Energy (DOE) divides the country into six climate regions (see Figure 1.7). Air conditioners and heat pump manufacturers reference these regions in

calculating and rating the seasonal performance of their units for sale in North America. Canada is considered Region V which is the coldest of the six regions [9].

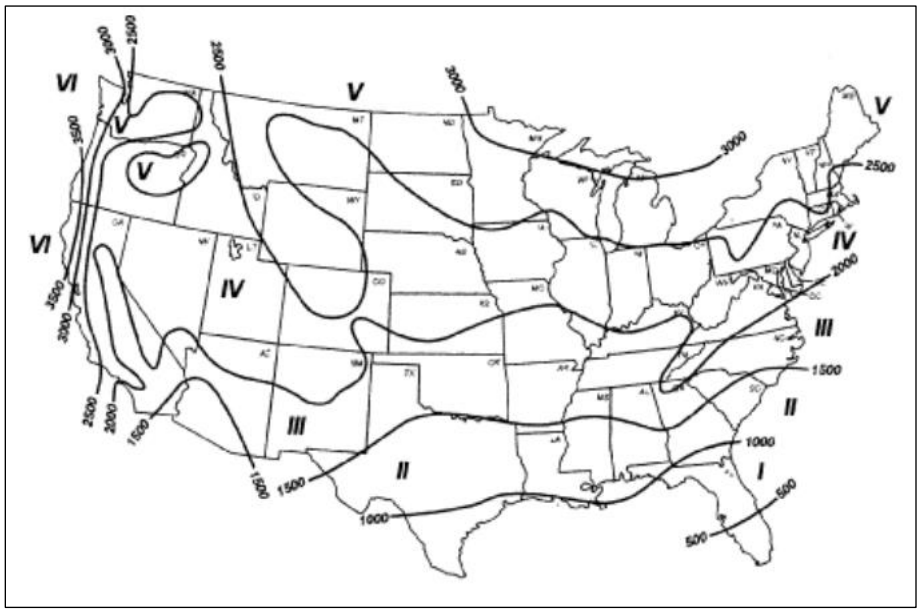

Figure 1.7: The United States of America, Heating Load Hours, and Climate Zones [9].

However, studying northern Canadian cities shows that they cannot be categorized into Region V during the heating season. Winter temperatures drop way below the minimum temperature in Region V. Also, the heating hours are much longer [10].

Compare a northern Canadian city like Whitehorse, YT, which has heating hours of 8318 viz-a-viz the 2202 heating hours for Region V. Also, Figure 1.11 shows the wide gap between the two temperature patterns. Moreover, the heating design temperature for Whitehorse, YT is -38.1 °C, whereas it is only -10 °F [-23.3 °C] for Region V. See Figure 1.8.

Appendix A includes the heating hours for the USA zones obtained from Appendix M1 to Subpart B of Part 430 from the USA electronic Code of Regulations [9]. Appendix B shows the weather data for Whitehorse, YT, Canada. Data obtained from the ASHRA Weather Data Viewer 2021 [11].

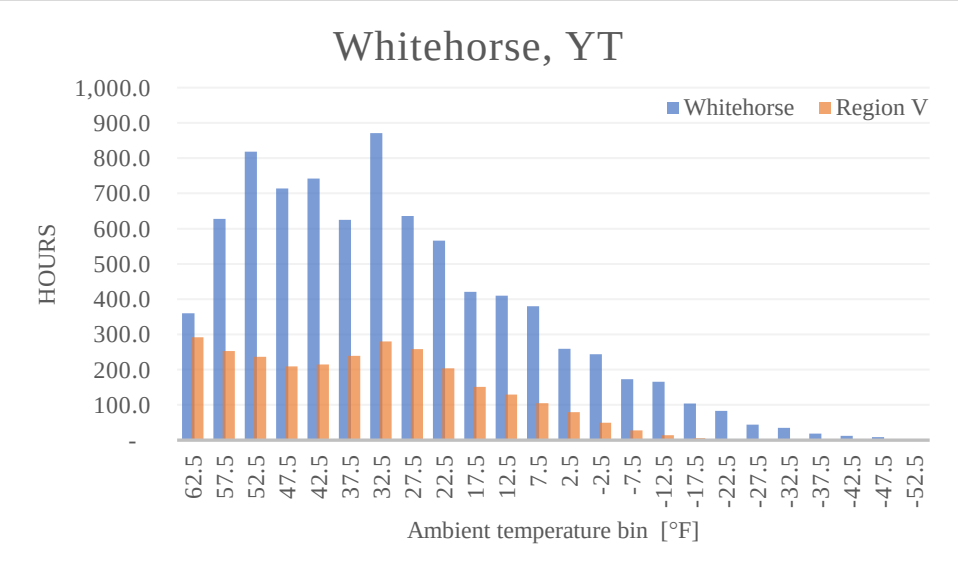

Figure 1.8: Heating hours for each ambient temperature bin in °F, Whitehorse YT & Region V, compiled from data in appendices A and B.

There is limited research in the open literature on air source heat pumps for the extremely cold northern Canadian climate. The author can only speculate that it is probably due to the small market potential because of the relatively smaller population compared to the large population of the United States of America. That is why the focus of the present study is to evaluate the seasonal performance in actual northern Canadian cities.

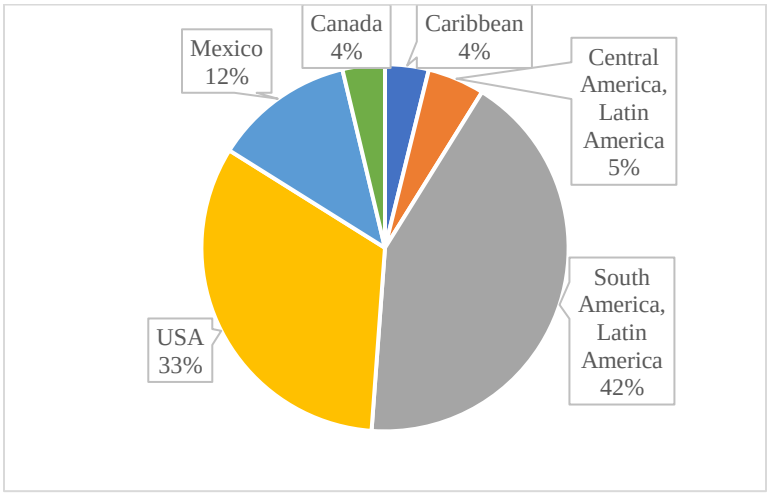

Figure 1.9: Population distribution of the Americas, data from the US Census Bureau's world population [12].

1.2 Motivation

According to Natural Resources Canada, in 2018, two-thirds of the total residential energy used was dedicated to space heating, Figure 1.10. Unfortunately, half of this energy is generated from burning fossil fuels, such as natural gas, propane, oil, etc., with electricity making up only a quarter of the total energy used (Figure 1.11. Interestingly, as seen in Figure 1.12, there has not been any significant change in the pattern of the energy sources used for residential space heating in the past two decades [13], [14].

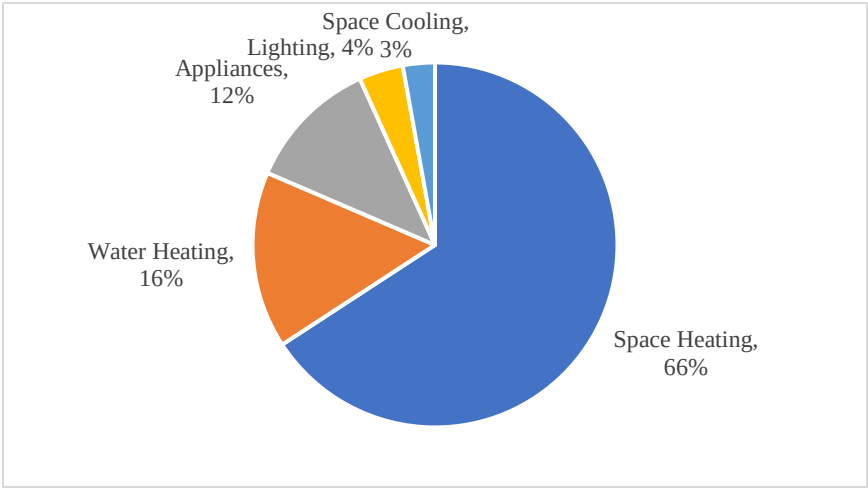

Figure 1.10: Residential energy usage by end-use in Canada 2018.

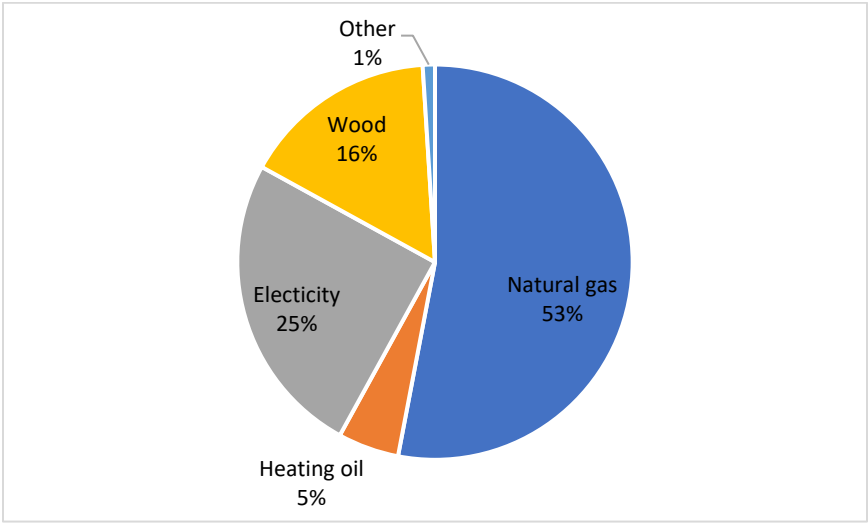

Figure 1.11: Residential space heating by energy sources in Canada, 2018.

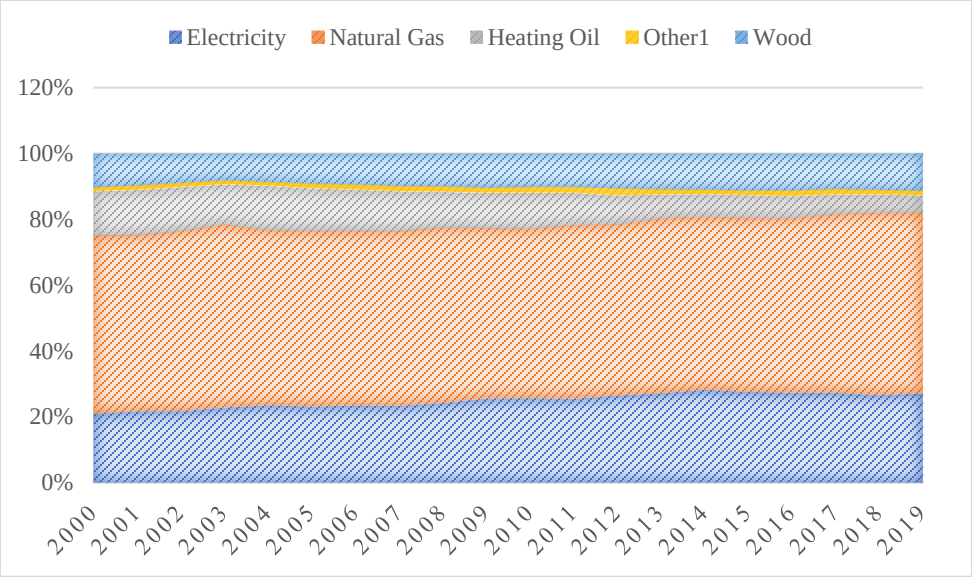

Figure 1.12: Residential space heating energy use by energy source by year.

Canada's long term aspirational goal for space heating is that all space heating equipment meet an efficiency[1] greater than 100% by 2035. Also, one of the midterm goals that should be reached by 2025 is to achieve a residential cold climate air source heat pump with a seasonal coefficient of performance greater than 2.75 that can be cost-efficient from a manufacturing, installation, and operation standpoint [15].

All available fossil fuel burning equipment that is commonly used in Canadian homes, like gas furnaces, gas boilers, wood stoves, gas or wood fireplaces, etc., has an efficiency limit of 98% at the most [16]. On the other hand, the efficiency of electric resistance heating, like an electric baseboard or electric heater air handler, is capped at a theoretical maximum efficiency of 100%. These limitations leave these kinds of equipment behind the aspirational goals of Canada and open the door for further exploration of solutions that can utilize renewable energy sources.

Heat pumps provide a promising solution for achieving efficiencies above 100%. Theoretically, air source heat pumps add heat energy extracted from the outdoors to the

[1] Efficiency is the term that appeared in the Canadian government document. The author would like to comment that the term COP is more engineering appropriate, as efficiencies cannot technically be greater than 100%.

electric energy consumed in the compression process and deliver as the heating energy to the space, and thus, the energy delivered is always greater than the energy consumed.

1.3 Objective

Based on the motivation presented above, therefore, the overall objective of this thesis is to propose and model novel efficient air source heat pumps for extremely cold climate applications. The specific objectives are as follows:

1. Design and analyze a vapor-compression system that can operate in ambient temperatures from -50 °C to +20 °C and provide the full heating load required for space heating without violating the compressor operating range specified by the manufacturer. The system can also provide cooling in the summer and can perform defrost functions. In addition, it must have efficiency above 100%.
2. Develop a modeling algorithm to calculate the system performance at any outdoor temperature.
3. Apply the system performance numbers to model the seasonal energy usage in an extremely cold weather Canadian city and calculate the seasonal heating coefficient of performance and compare it to other systems available.

1.4 Thesis Structure

The rest of the thesis is structured as follows:

Chapter 2 contains the literature review of heat pump technologies and their adaption to cold climate heating applications, as well as the challenges involved. Chapter 3 presents the thermodynamic analysis of various refrigeration systems and modeling of their performance. Then, the proposed system description. Chapter 4 reports the results and presents detailed analyses and discussions of the results. Finally, Chapter 5 provides the concluding summary and remarks on this study, as well as recommendations for future work.

Chapter 2. Literature Review

2.1 Basic Heat Pump Design

As explained earlier, the heat pump is designed based on the refrigeration cycle. What distinguishes a heat pump from an air-conditioner is the heat energy utilized; either the rejected heat, then it is a heat pump or the absorbed heat, then it is an air-conditioner. To achieve both functions by the same system, a 4-way reversing valve is used. Figure 2.1 shows the system with the 4-way valve directing the flow of refrigerant in each mode of operation [17].

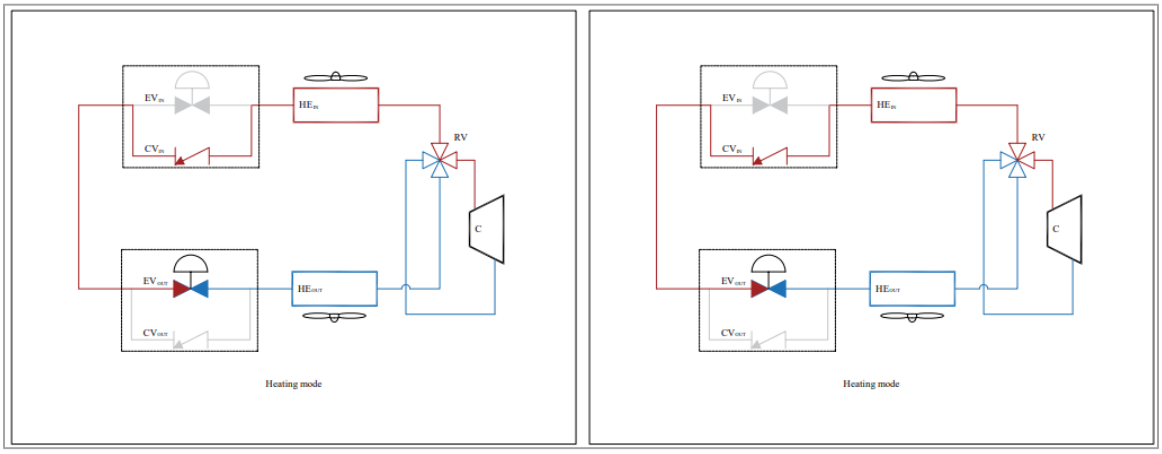

Figure 2.1: Single-stage heat pump system diagram showing refrigerant flow in heating and cooling modes of operation [17].

The 4-way reversing valve, as shown in Figure 2.2, is designed to switch the flow between the suction port and the discharge port by moving a slider inside a cylinder. The slider is moved by a pilot mechanism that is actuated by a solenoid. Through a control signal sent to the solenoid coil, the mode of operation can be switched between heating and cooling [17], [18].

This is a very economical way to have both heating and cooling functions using just one piece of equipment rather than having two separate pieces of equipment.

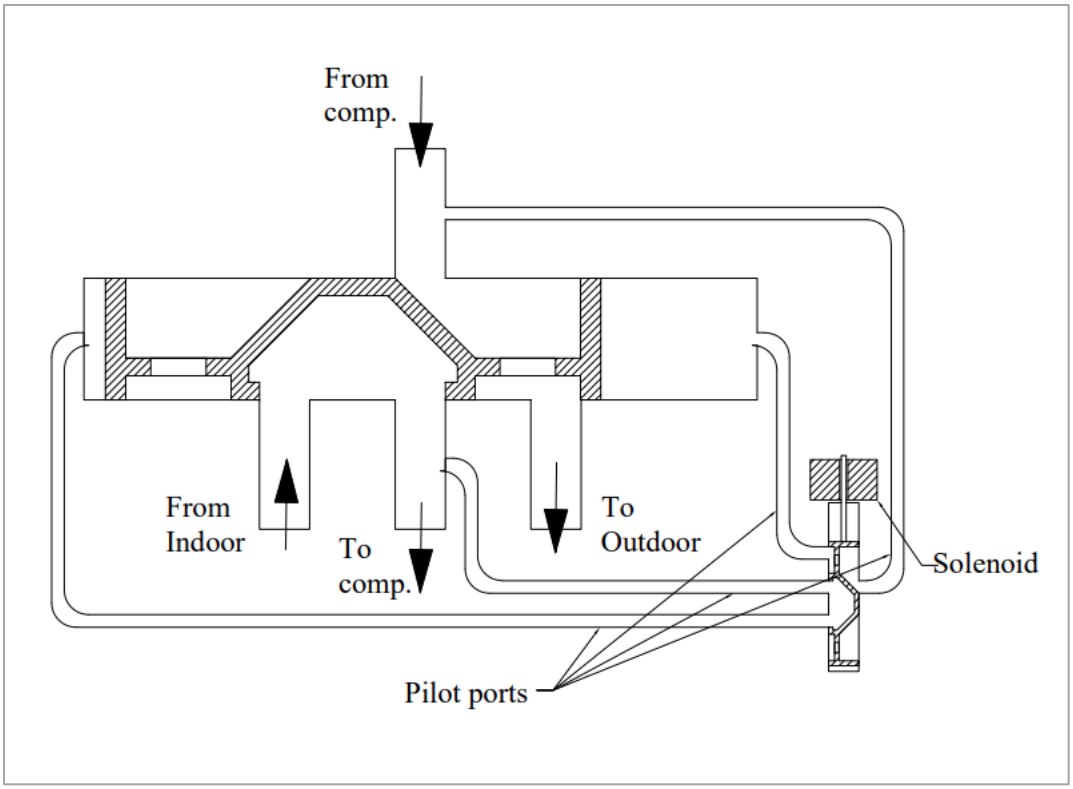

Figure 2.2: 4-Way reversing valve, pilot-operated.

2.2 System Components

Five main components are necessary to operate a vapor-compression refrigeration cycle, compressor, condenser, evaporator, expansion device, and refrigerant. Some other components are often added to the system to add safety measures or to optimize operation and performance.

2.2.1 Compressors

The compressor is considered the heart of the vapor-compression cycle. It pumps the refrigerant and cycles it across the system components. Refrigeration compressors using refrigerants are categorized in many ways. The term compressor often refers to both the compressor and the motor that drives it.

2.2.1.1 Classification Based on the Compressor and Motor Housing

A. Open-drive type compressors: this kind has the compressor only inside the housing. A shaft comes out of the housing that should be coupled to a motor shaft by means of either a clutch, a coupling, or a system of pulleys. This type is

particularly useful in transport refrigeration and air conditioning. The shaft can get its rotation from the engine. This type is also used in commercial and industrial refrigeration applications, but due to the complexity of the design of the shaft seal and the coupling mechanism, they are never used in residential air-conditioning applications [17].

B. Hermetic type compressors: the compressor mechanism along with the motor of this type are all enclosed inside one shell. The motor-compressor is connected to a source of electricity to get it running. It provides a much easier economic solution if compared to the open type. The oil necessary to lubricate the compressor is included in the sump of the compressor shell. This makes the oil part of the system, where it flows with the refrigerant and needs to circulate back to the compressor [19]. Accordingly, systems utilizing this kind of compressor take special design considerations to address the oil return to the compressor [20]. The cold refrigerant, as it returns to the compressor, passes over the motor windings and provides means of cooling them. The downside of this kind of compressor is that it is not serviceable. Once it is broken, it must be replaced. Almost all residential air-conditioning applications utilize this kind of compressor.

C. Semi-hermetic type compressors: Like the hermetic type compressor, this one also has both compressor and motor inside one housing. However, the housing would have some access to the internal component and allows this kind of compressor to be serviceable [17], [19].

2.2.1.2 Classification Based on the Compression Mechanism

A. Reciprocating type compressors: this type of compressor uses a piston, cylinder, crankshaft, and connecting rod to perform the compression process along with suction and discharge valves to allow for suction at low-pressure and discharge at higher pressure [5]. This type is prevalent in commercial refrigeration and freezing applications. They are capable of efficiently handling medium to high compression ratios. They were also commonly used in air-conditioning applications until recently. However, manufacturers managed to upgrade the scroll and rotary types to replace the reciprocating type in all current residential air-conditioners [6].

B. Rotary type compressors: See Figure 2.3, this compressor has a disc-shaped rotor concentric with the shaft. They have been placed off-centre with the cylinder. A vane is pushed at the disc by means of a spring to split the cylinder into two compartments. When rotating, the disc creates a gap with the cylinder. The gap keeps decreasing in volume in the direction of rotation and increasing on the other side. The refrigerant enters the cylinder through a valve to one side of the cylinder, and as it rotates, the volume keeps decreasing, resulting in the compression process. Eventually, the compressed gas leaves the cylinder through a discharge valve. This type of compressor is compact in size, economical, and efficient. It is commonly used in residential air-conditioning and heat pump applications [17], [19].

C. Scroll type compressors: See Figure 2.3, the compression takes place between two spiral shaped mechanisms. One of them is fixed, and the other goes in orbital motion. The orbiting motion creates pockets between the spirals that decrease in volume with the motion until it gets to the exit of the spiral and discharges at high pressure. The flow, in this case, is almost continuous, not intermitted like the reciprocating or rotary types. Also, there are no suction or discharge valves. This type has a relatively higher efficiency when compared to the other types. They are becoming so common nowadays in residential and commercial applications. However, one of the biggest disadvantages is that they struggle to handle higher compression ratios, which complicates their use in freezing equipment for example [17][19].

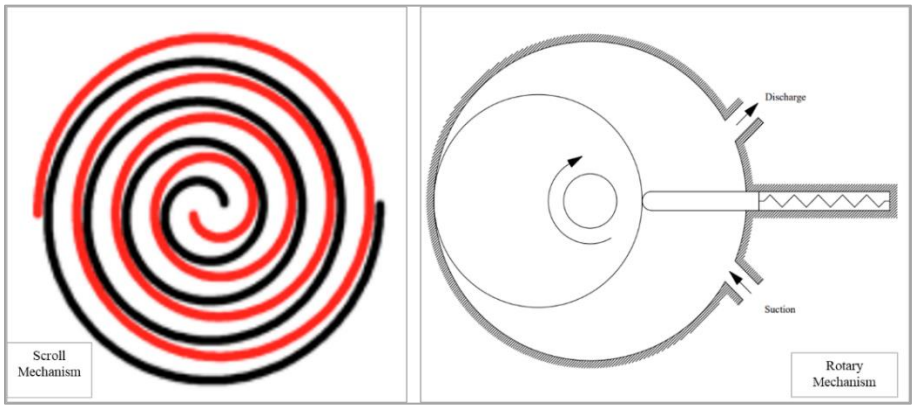

Figure 2.3: Schematic of scroll and rotary compression mechanisms in compressors.

2.2.1.3 Classification Based on the Motor Speed

A. Fixed speed compressors: The motor of this kind of compressor is usually an induction type motor with just one fixed speed of rotation[21].
B. Variable speed compressors: they are designed so that they will be connected to a variable frequency drive that allows control of the rotational speed of the compressor and, thus, its capacity [22].

Both fixed speed and variable speed types can be used in any application. The variable speed offers higher control over the system's capacity and performance. Obviously, this comes at a price of more complicated and more expensive equipment. It then becomes a question of whether to invest in a variable speed system to target higher efficiencies or accept the efficiency at the fixed speed.

2.2.1.4 Classification Based on Compression Stages

A. Single-stage compressors: it has only one compression process. The refrigerant enters the compressor through the suction port, gets compressed, then discharged from the discharge port [21], [23]. The single-stage compression has the limitation of the maximum compression ratio that the compressor can handle. It is acceptable for refrigeration or freezing applications but not for deep freezing, the compression ratio makes its operation inefficient.
B. 2-Stage compressors: the compression is done in 2-stages. Refrigerant enters the compressor through the suction port at the lowest system pressure. The refrigerant is then compressed in part of the compressor, 2 out of 4 cylinders, for example. Then, the refrigerant goes out of the compressor housing, where it undergoes some sort of cooling by some of the system refrigerants. The cooled refrigerant then enters the second stage of compression, the 2 remaining cylinders in this example, to complete the compression process to the discharge pressure. By doing so, the compression process at higher compression ratios becomes attainable. This makes them a good choice for deep freezing applications [17], [19], [23].

There are also other types of compressors that are used in industrial applications, like centrifugal compressors and the screw type compressors. They address much higher

capacity requirements, so they are outside the scope of this thesis. Therefore, they will be excluded from this review.

The review of available compressor technologies shows that:

- Compressors are developed for certain application ranges and for specific refrigerants that can match this range.
- For air source heat pumps and air conditioning applications, the hermetic scroll or rotary compressor is the common type for its efficiency and lower cost.
- To achieve higher compression ratios and avoid decrease in efficiency, compressors are designed in 2-stages where an intercooler can occur.
- There is no single compressor that can operate for all ranges of temperatures and all refrigerants. To be able to run reliably and efficiently, the compressor must run within its application limits and with the proper refrigerant.

2.2.1.5 Low Condensing Temperature Compressor Application

Low condensing pressure is defined as running the compressor at a saturated condensing temperature lower than the traditional 21 °C (70 °F). By doing so, both efficiency and capacity increase. Moreover, an increase in the overall durability of the compressor because of lower discharge pressure and temperature.

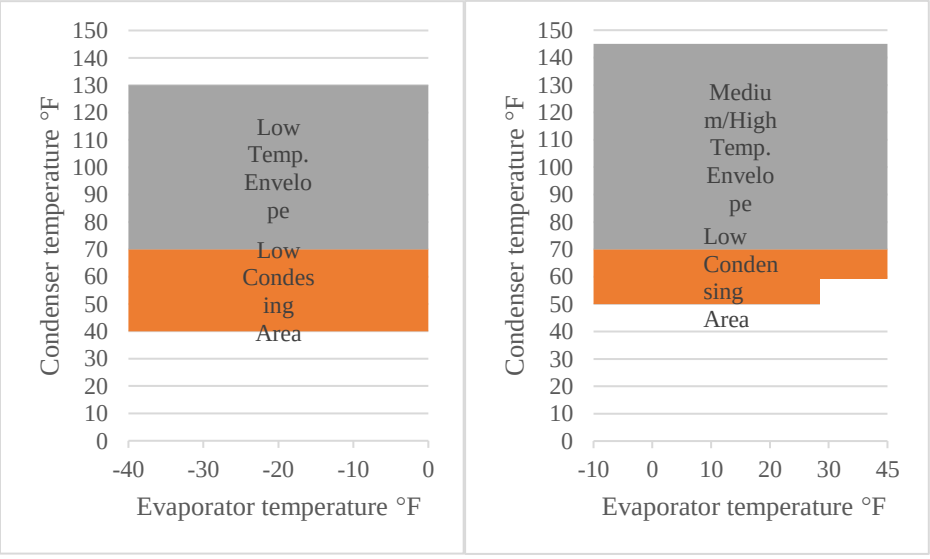

Figure 2.4: Low condensing temperature compressor application limits, for refrigerants R-404A/507 [24].

Special considerations must be taken when running a compressor at a low condensing temperature. Under low condensing pressure, oil circulation tends to be higher. The oil then might get logged, which could degrade the system's performance. Properly sized oil separators and suction line design are crucial to the proper operation [24].

2.2.2 Expansion Devices

If the compressor is considered the heart of the system, the expansion devices, or metering devices, by analogy, can be thought of as the system brain. They are the system components that control the refrigerant flow in the system. This will eventually translate to the amount of cooling or heating energy for the system. The types of metering devices applied to air-conditioners, heat pumps, refrigerators, and freezers are as follows:

2.2.2.1 Capillary Tubes

Capillary tubes are the simplest and most economical expansion devices. By running the refrigerant across a capillary tube having a specific diameter and length, the required pressure-drop could be achieved due to the friction losses that the refrigerant experiences inside the capillary tube. As the size of the capillary is fixed, once installed in the system, the pressure drop is uncontrolled at various operating conditions. This is one of the biggest disadvantages of this type of metering. That is why they are mostly used in small systems with a minimum variation in operating conditions. An example of that is the domestic refrigerator or freezer, where the set temperature of the cabinet is fixed when it is expected to be installed in a house or so, with an almost steady room temperature [25].

2.2.2.2 Piston Orifice

The piston orifice is commonly used in residential central air conditioners and heat pumps. They comprise a fixed diameter orifice, like the capillary tube, but in a compact design. Their design allows flow in the reverse direction, which is why they can be used in heat pump applications. However, they still have the same disadvantage of inflexibility in a wide application range as the capillary tube [26].

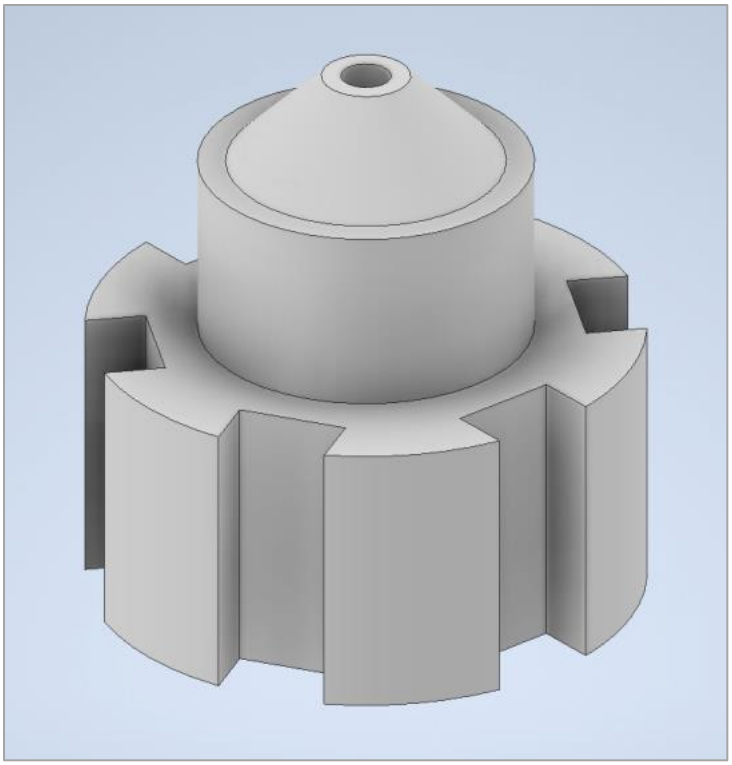

Figure 2.5: Piston orifice expansion device [27].

2.2.2.3 Thermostatic Expansion Valves

Thermostatic expansion valves (TXV) are throttling devices designed with an internal orifice that can adjust its diameter based on the sensed pressure and temperature. Pressure from the suction line is applied to one side of the diaphragm. Pressure on the other side of the diaphragm is a result of the temperature of a fluid filled bulb attached to the suction pipe. The two forces should balance if the system refrigerant is at saturation. An additional spring excerpts an extra force to the suction-pressure side of the diaphragm, closing the orifice a bit more and forcing a specific amount of superheat. Changes in suction pressure and temperature move the diaphragm that drives a needle that could control the size of the orifice. Accordingly, a steady superheat at the evaporator outlet or compressor inlet could be achieved. That ensures that 1) only vapor enters the compressor and 2) all latent refrigerant heat of vaporization is utilized in the evaporator. Figure 2.6 shows an illustration of the thermostatic expansion valve design[17].

Theoretically, the bulb charge is the same as the system charge. However, manufacturers tend to develop special thermostatic charges to enhance the valve performance and, thus,

the overall system performance. Practically, there is no single thermostatic charge that can work efficiently for all evaporating temperatures of a specific refrigerant. The applications are divided into 1) air conditioning and heat pumps and 2) refrigeration, which is further categorized into: a) commercial refrigeration temperature, b) low temperature refrigeration and c) extremely low temperature refrigeration. Manufacturers published superheat characteristics curves for each thermostatic charge that help select the proper one for a specific application.

Some liquid thermostatic charges are designed so that the whole bulb charge totally evaporates at a specific temperature. This stops the valve from opening further at higher temperatures. This provides the Maximum Operating Pressure (MOP) of the evaporator. This is particularly helpful in air conditioning applications as it keeps the pressure low enough during pull down time so that the compressor does not get overloaded. MOP is also beneficial in freezer systems where after defrosting cycle, the evaporator temperature becomes so high so, and the MOP limits the valve from opening, which could lead to excess refrigerant flow and the risk of liquid flooding back to the compressor.

There are some thermostatic charges that are specifically developed for extremely low temperatures -40 °C to -73 °C evaporating temperatures. These thermostatic charges have superheated characteristics tailored to provide more accurate superheat control at extremely low pressure and temperature.

Adsorption type thermostatic charges are made of non-condensable vapor, so they do not have a MOP. They fit right in medium temperature applications installed in lower ambient temperatures [28].

This kind of metering device provides better control over a wide range of operating conditions. It is commonly used in air-conditioning, refrigeration, and freezing for commercial and sometimes residential applications. A study by Sunu et al. compared the performance of a thermostatic expansion valve and a capillary tube in the air condition system and found an improvement in COP of about 21% in favor of the thermostatic expansion valve [19], [25].

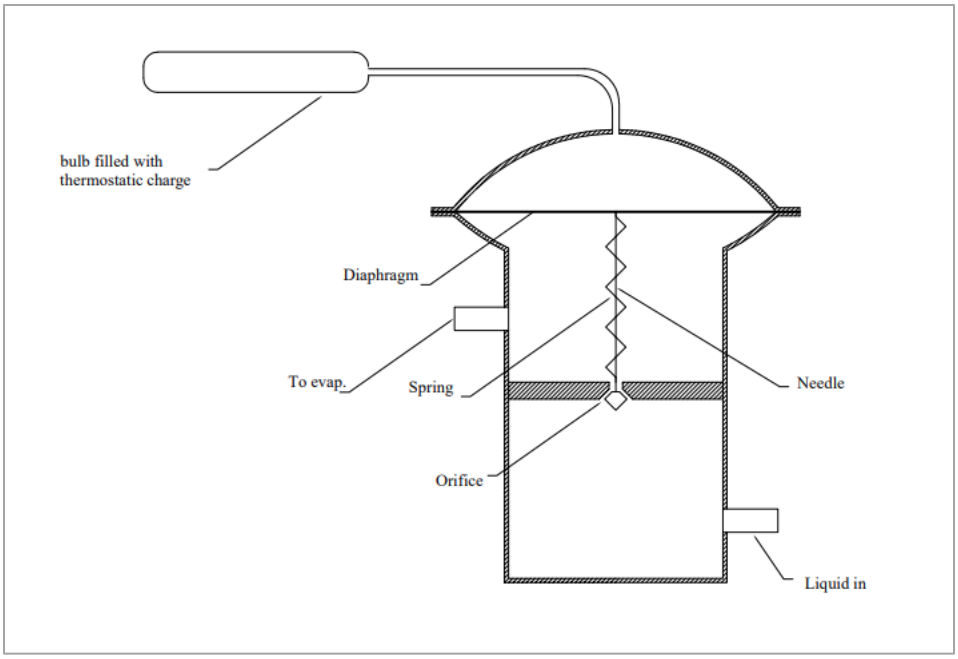

Figure 2.6: Schematic od a thermostatic expansion valve [17] [27].

2.2.2.4 Electronic Expansion Valves

Like the thermostatic expansion valve, the electronic expansion valve (EEV) is constructed with a variable diameter orifice that is controlled by moving a needle. The electronic expansion valves utilize a stepper motor that drives the needle across the orifice opening to control its diameter. By feeding temperature signals from temperature sensors and pressure signals from pressure transducers to a control board running a certain control logic, the movement of the needle can be controlled. This kind of metering device gives the most accurate control of the superheat and, thus, refrigerant flow. Apparently, it is more expensive and more complicated to set up and operate. It is commonly used in high efficiency air-conditioning and refrigeration equipment as it helps improve the overall efficiency of the equipment [29], [30].

Being a newer device when compared to the TXV, and as it involves electronic controls and control algorithms, there are so many research studies that cover this area. Apart from the mechanical design of the EEV, the control algorithm plays a crucial role in their operation. The study by Xia Y. and Deng S. is an example of the influence of the operating characteristics of the EEV [29]. The EEV will always provide better control over the

system and better performance. However, it complicates the system design and increases the system cost.

2.2.3 Condenser and Evaporator Heat Exchangers

In air source heat pumps and air conditioners, both indoor and outdoor heat exchangers also could be referred to as condensers and evaporators, exchange heat between air on the outside and refrigerant on the inside. The main construction design in this field of application is the tube and fin heat exchanger and the microchannel heat exchanger.

The tube and fin design comprises tubes, usually either copper or aluminum, where the refrigerant flows inside them. On the outer side, fins are attached to the tubes to provide a larger surface area. For residential applications, tube sizes range between 5-mm, 7-mm, 3/8” and 5/16”. While the fin density is commonly within 20 fins per inch (FPI) in air conditioning applications. However, in freezing applications, it can be as low as 3 FPI [31], [32]. Manufacturers develop fin shapes and forms, like wavy, louvered, sinusoidal, flat, and lanced, to get the best heat exchange capacity while minimizing the air pressure loss across the fins.

A comprehensive study by Sadeghianjahromi and Wang compares the performance of the fin and tube heat exchanger with the different mechanisms discussed above [31]. It is understood that there is no single design that can fit all applications. While the fin and tube type heat exchanger is almost the sole choice, so far, for residential air source heat pumps, designers select between the various mechanisms to fulfil the required function and economic cost.

Microchannel is a variation of the tube and fin heat exchanger. Instead of tubes, they utilize less than 1-mm channels, hence the name microchannel, for the refrigerant flow. The channels are connected from the outside via fins. The advantage of the microchannels over the tubes is that they provide more surface contact between the refrigerant and the surface, therefore, a better heat exchange efficiency. Commonly the material of this type of heat exchanger is aluminum. Although lightweight and robust, they are more difficult to braze. On the other hand, the lower internal volume requires a lower refrigerant charge. This type of heat exchanger is favourable for automotive air-conditioning and transport refrigeration. However, there are also some residential air-conditioners that are using them [33].

Some studies are conducted to utilize this type in heat pump applications, but still not that common. Shao et al. conducted a study to compare the performance of heat pumps using fin and tube vs. microchannel heat exchangers under frost conditions. Although microchannel heat exchangers tend to improve performance, the performance is degraded with frost build up. Their study showed potential improvement could be achieved by different refrigerant distribution methods [34], [35]. The main issue with the microchannel type of heat exchanger is the frost build up and the defrosting. This problem is exacerbated in a cold climate operation where frost build up is expected to be high.

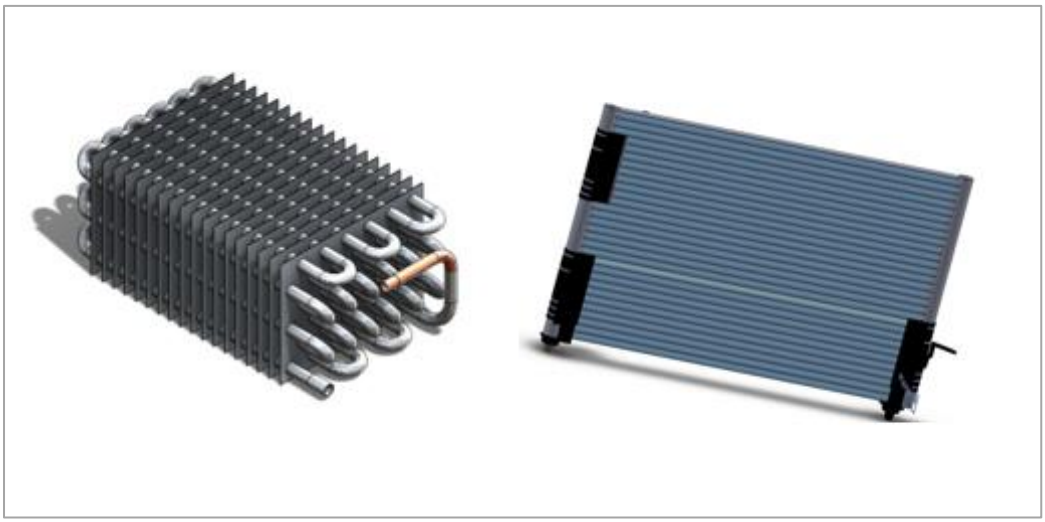

Figure 2.7: Fin-and-tube heat exchanger, Left. Microchannel heat exchanger, right [36].

Reviewing the products of residential air conditioner and heat pump manufacturers, it could be found that some, like YORK, utilize the microchannel heat exchanger for some of their air conditioners but not heat pumps [37].

2.2.4 Refrigerants

Refrigerants are the working fluids for the vapor-compression refrigeration cycle, which is the basis for air-conditioning and heat pumps. There is no single fluid that can satisfy all the attributes desired for a refrigerant. That is why manufacturers come up with different blends so that thousands of refrigerants are available in the market. The properties of each blend are designed to satisfy some areas of performance, obviously at the cost of less important factors. So, each blend of refrigerant would target an application. The critical point of the refrigerant must be sufficiently higher than the highest operating

pressure/temperature of the application. Viscosity, density, conductivity, saturation temperature/pressure, and latent heat of boiling/condensation are all properties that can influence the overall system performance. It is safe to say that there is no single refrigerant that can work efficiently for all applications; there must be some tradeoffs [38].

Table 2.1: Refrigerant safety group classifications according to their toxicity and flammability [39].

	Toxicity	
	Low	High
High Flammability	A3	B3
Flammable	A2	B2
Lower Flammability	A2L	B2L
No Flame Propagation	A1	B1

ASHRAE standard 15 and 15.2 [40] classifies the refrigerants according to their flammability and toxicity levels. See Table 2.1 [39].

Refrigerants are grouped based on their chemical composition into the following:

- CFC = Chlorofluorocarbons. These refrigerants include Chorine, Florine, and Carbon. Examples are R11, R12, R502. This kind has been banned because of its harmful effect on the ozone layer.
- HCFC = Hydrochlorofluorocarbons, they substituted CFCs. They include less Chlorine than CFCs which makes them less harmful to the Ozone layer. A good example is R22.
- HFC= Hydrofluorocarbons. They do not include any Chlorine; they have zero Ozone Depletion Potential (ODP). Examples are, R32, R125, R134a, R404A, R407C, and R410A.

A refrigerant may be either a pure compound or a mixture or blend of two or more refrigerants. A zeotropic mixture, although made of multiple refrigerants, tends to evaporate with constant pressure and temperature in the whole liquid-vapor mixture region.

Azeotropic mixtures have gliding evaporation and condensing temperatures. The highest volatile component evaporates first and the least volatile one last. The opposite happens during the condensation process. This results in a range of evaporating or condensing temperatures at a certain pressure. This range is called the glide. These types of refrigerants need to be charged to the system in liquid form to keep the consistency of the mixture. As a result of that, in systems where liquid refrigerant is allowed to collect somewhere in the system, like the suction accumulator, receiver, etc., the flowing refrigerant might change in composition. This could result in unpredicted performance. Similarly, a refrigerant leak might lead to the same issue, which might require the reclaim and recharge of the full refrigerant amount [41], [42].

The refrigerant widely used these days in the residential air-conditioning application is R410A. It is a composition of R-32/125 (50/50) [38]. This refrigerant falls under the safe A1 category. Also, for low temperatures applications R404A, R-125/143a/134a (44/52/4) has gained popularity. Both fall under the safe A1 category, which makes them safe to handle.

Another important factor that gained attention more recently is the Global Warming Potential of refrigerants (GWP).

The warming effect of carbon dioxide is baselined at a GWP value of 1.0. The GWP number for any other fluid represents the ratio of its warming effect to that of the baseline.

Governments around the globe are issuing more stringent rules to limit the global warming effects resulting from using refrigerants. In the US, EPA (Environment Protection Agency) issued SNAP rule 23 (Significant New Alternative Policy) to provide a list of low GWP approved refrigerants [43]. In Europe, F-gas regulation and, in Canada, Greenhouse Gas Offset Credit System Regulations set a maximum limit on the GWP of refrigerants per sector, as shown in the tables below [44], [45].

Table 2.2: USA, SNAP rule 23, Acceptable alternatives of refrigerants [43].

Application	Substitute
Residential and light commercial air conditioning and heat pumps	R452B, R454A, R454B, R454C, R457A
Residential and light commercial air conditioning and heat pumps excluding room air conditioners	R32
Retail food refrigeration, medium temperature, standalone	R448A, R449A, R449B

Table 2.3: F-Gas Regulation No 517/2014, European Union, GWP limit by application [45].

Application	GWP limit
Air conditioner with < 3kg refrigerant	750
Self-contained refrigeration	150
Centralized refrigeration, ≥ 40 kW	100
Mobile room air conditioning	150
Domestic refrigeration	150

Table 2.4: Canada Green House Gas Offset System, GWP limit by application[44].

Application	GWP limit
Stand-alone medium temperature refrigeration system	1400
Stand-alone low temperature refrigeration system	1500
Centralized refrigeration system	2200
Condensing unit	2200
Chiller	750
Commercial AC	2000
Heat Pumps	2000

R410A is the main player in the residential air conditioning and heat pump industry. However, with the newer direction to lower Global Warming, more refrigerants are hitting the market with lower (GWP). R32, R454B are among the front-line candidates to replace R410A. Research is ongoing to validate the performance of this kind of refrigerants [46], [47], [48]. As these refrigerants fall under the A2L category, they must be treated with more care. Compressor manufacturers and refrigeration component manufacturers, in general, develop products specifically designed for them. The newer UL 60335-2-40 safety standard applies more stringent safety measures to mitigate the risk resulting from their flammability [49].

Table 2.5: GWP for some refrigerants [50].

Refrigerant	Composition	GWP
R410A	R32-/R-125(50/50)	1,923.50
R404A	R125/R-143a/R134a (44/52/4)	3,942.80
R-454B	R-32/R-1234yf (68.9/31.1)	466.76
R-32	Difluoromethane	677.00

Few refrigerants in the market are designed for ultra-low temperature applications below -50 °C. In their research, Mota-Babilioni et al. pointed to the limited available refrigerants in the market that are designed for -80 °C operation, R-469A, R-472A, and R-473A. The requirements of lower GWP, as explained earlier, put more limitations on the use of such refrigerants. They studied thirteen fluids in multiple blends to achieve the performance requirements at ultra-low temperature applications [51].

There are two refrigerants that are being widely used in ultra-low temperature applications, R-23, and R-508B. With a boiling point a bit below -80 °C at zero gage pressure, the risk of running the system under a vacuum is eliminated. These refrigerants are commonly used in medical applications, like the storage of blood components. The disadvantage is that they have a high GWP of around 14000. Apparently, this is way above the accepted targets outlined earlier [52].

Research in this area is still so young compared to that on air-conditioning or refrigeration applications. That is expected given the limited market size of the ultra-low temperature applications as compared to the huge challenge that faces researchers to develop lower GWP refrigerants for the air conditioning and refrigeration industry.

2.2.5 Additional System Components

2.2.5.1 Suction Accumulators

As mentioned earlier, compressors are designed to handle vapor or gas only; thus, the system often includes a suction accumulator to ensure only refrigerant gas is sucked into the compressor.

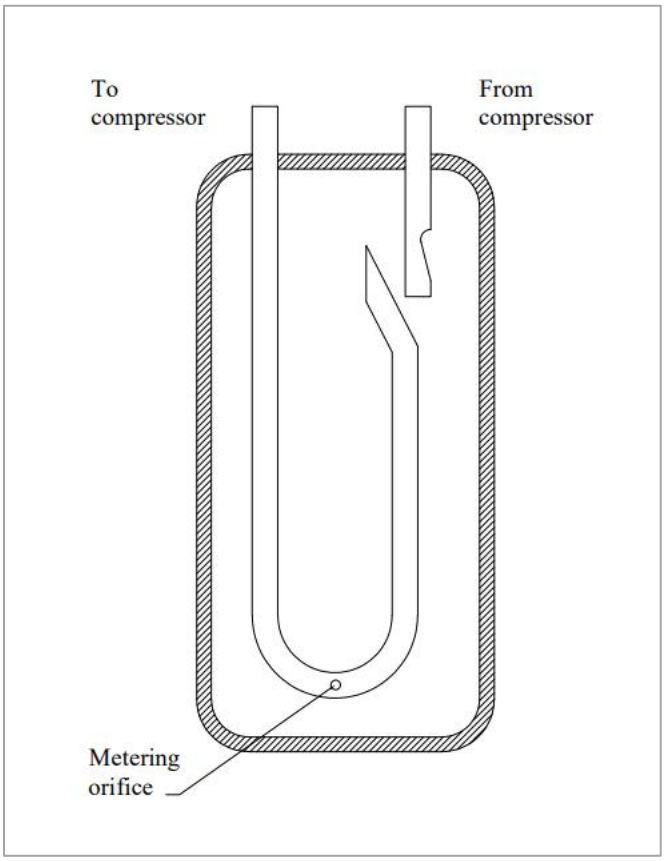

Figure 2.8: Schematic for a suction accumulator [53].

The design of a suction accumulator comprises a U-shaped tube inside a vertical container that is used as the exit port. The inlet to the suction accumulator is admitted through the top of the container. This allows any liquid entering the suction accumulator to accumulate at the bottom of the container. The exit is always from the top, where the fluid is in a vapor.

To the bottom of the U-shaped tube, a metering hole is drilled so that liquid and oil accumulated at the bottom can be metered back to the compressor.

For all low temperature applications, the suction accumulator is recommended by most compressor manufacturers and adopted by system designers. Also, in some cases, to improve the liquid evaporation process, a means of heating is added to the container either by electric resistance or even by the system hot gas [53].

This component does not affect the energy efficiency of the system; its function is rather operational safety. That is why it is not part of the thermodynamic system analysis.

2.2.5.2 Oil Separators

Oil mixes with refrigerant and circulates in the system. Oil circulating in the system tends to reduce the heat transfer in the heat exchangers. To minimize the amount of oil leaving the compressor, an oil separation device is connected to the discharge port of the compressor. The oil separator is basically designed as a canister that has an inlet and outlet ports to its top. As the refrigerant enters, the heavy oil droplets fall to the bottom of the canister, and the refrigerant leaves the exit port. When the oil level collected at the bottom reaches a certain level, a float mechanism opens a port for oil to return to the compressor.

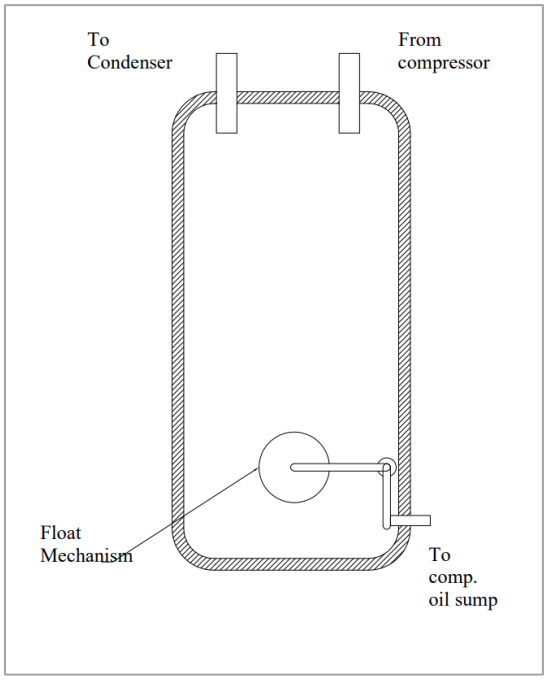

Figure 2.9: Schematic for oil separator [54], [55].

A study by Li et al. investigated the effect of the circulating oil ratio on the heating performance of a heat pump. By recording the heating capacity and power consumption for the system at different mass flow rates of oil, their study showed the decline of both capacity and COP with the increase of circulating oil [56].

On the other hand, compressor manufacturers consider the oil separator a requirement for low ambient applications. That is to minimize the risk of compressor failure due to loss of lubrication [24].

2.2.5.3 Air Moving Devices

To benefit from the higher heat transfer rates of forced convection as compared to natural convection, the condenser and evaporator of the system often utilize an air moving device like a fan or a blower. Depending on the application, the required airflow, and static pressure, the type of air moving device could be selected [57], [58] [59].

There are 3 fan laws that define the relationship between horsepower, static pressure, and flowrate that are helpful in the design aspects of airflow control [3].

i. Airflow is directly proportional to the fan's rotational speed.

$$\frac{Q}{N} = constant \tag{2.1}$$

ii. Static pressure is directly proportional to the square of the flowrate.

$$\frac{p}{Q^2} = constant \tag{2.2}$$

iii. Horsepower is directly proportional to the cube of flowrate.

$$\frac{P}{Q^3} = constant \tag{2.3}$$

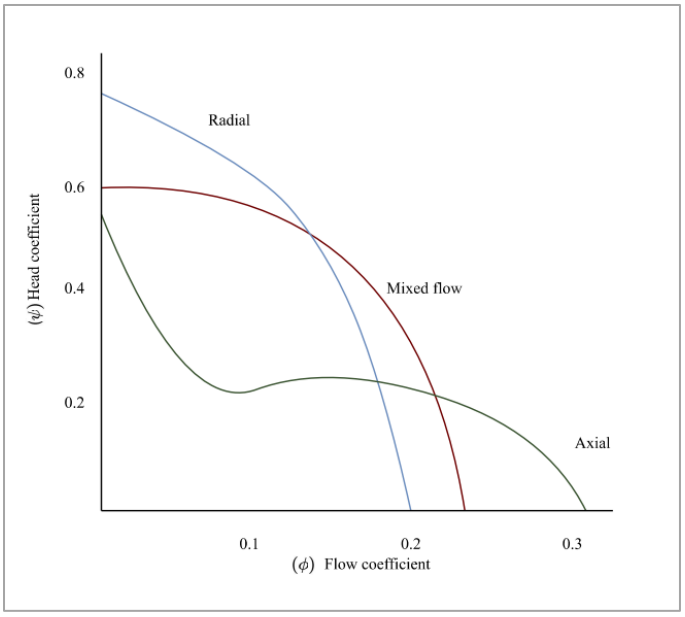

Figure 2.10: Characteristic curves of the various fan designs [3].

The pressure coefficient of a fan, ψ, is defined as:

$$\psi = \frac{\Delta p}{\rho \cdot \frac{U^2}{2}} \tag{2.4}$$

The flow coefficient, ϕ, is defined as:

$$\phi = \frac{V}{\pi/4 D^2 U} \tag{2.5}$$

Fan manufacturers test their fans per ASHRAE/AMCA 51 standard and publish the fan performance curves [60].

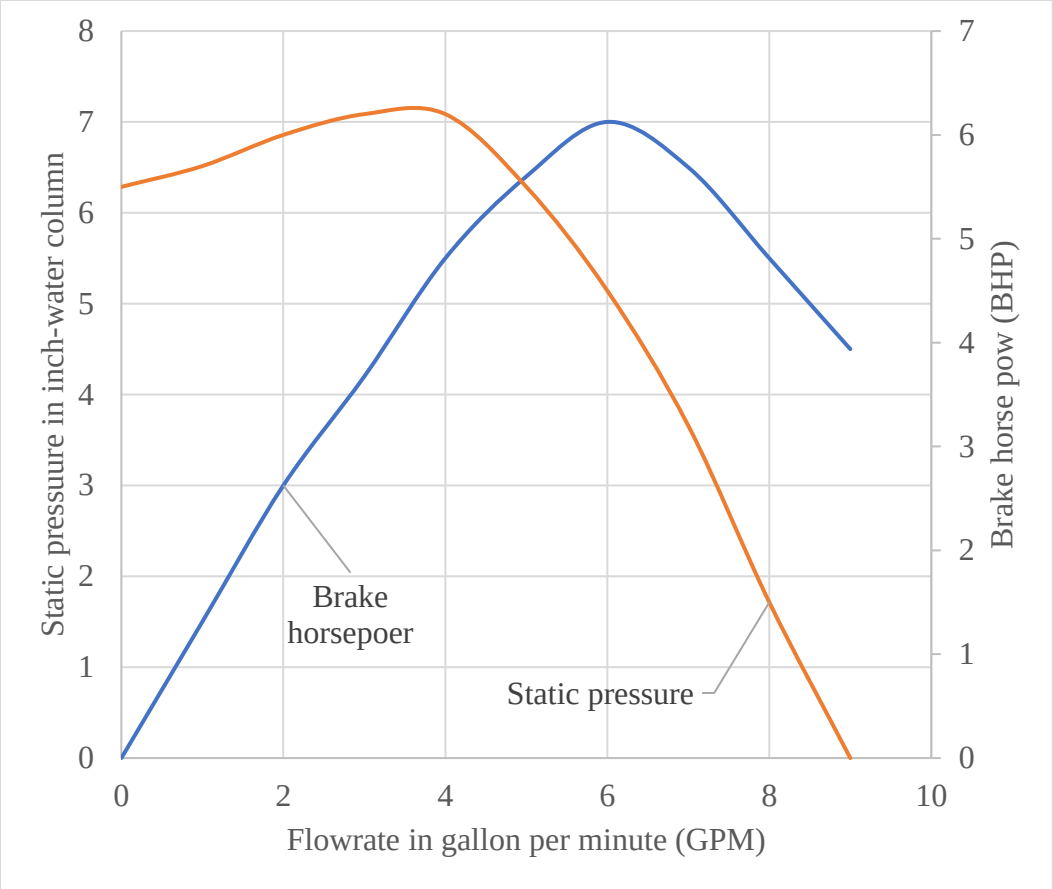

Figure 2.11: Typical fan performance curve [3].

Axial fans are fans where the airflow is parallel to the axis of rotation of the fan. They provide economical means of the air movement of higher air flowrates at lower static pressure requirements. That is why they are usually selected as air movers for outdoor heat exchangers [61].

Centrifugal fans, or radial fans, more commonly referred to as blowers, are the type of fans where the air moves in a radial direction to their axis of rotation. Depending on the fan blade's design, they are subdivided into 1) backward curved, 2) forward curved, and 3) radial blades. Centrifugal fans/blowers can achieve higher static pressures as compared to axial fans. In residential heating and cooling ducted applications, they are the choice as air movers for the indoor coil [61].

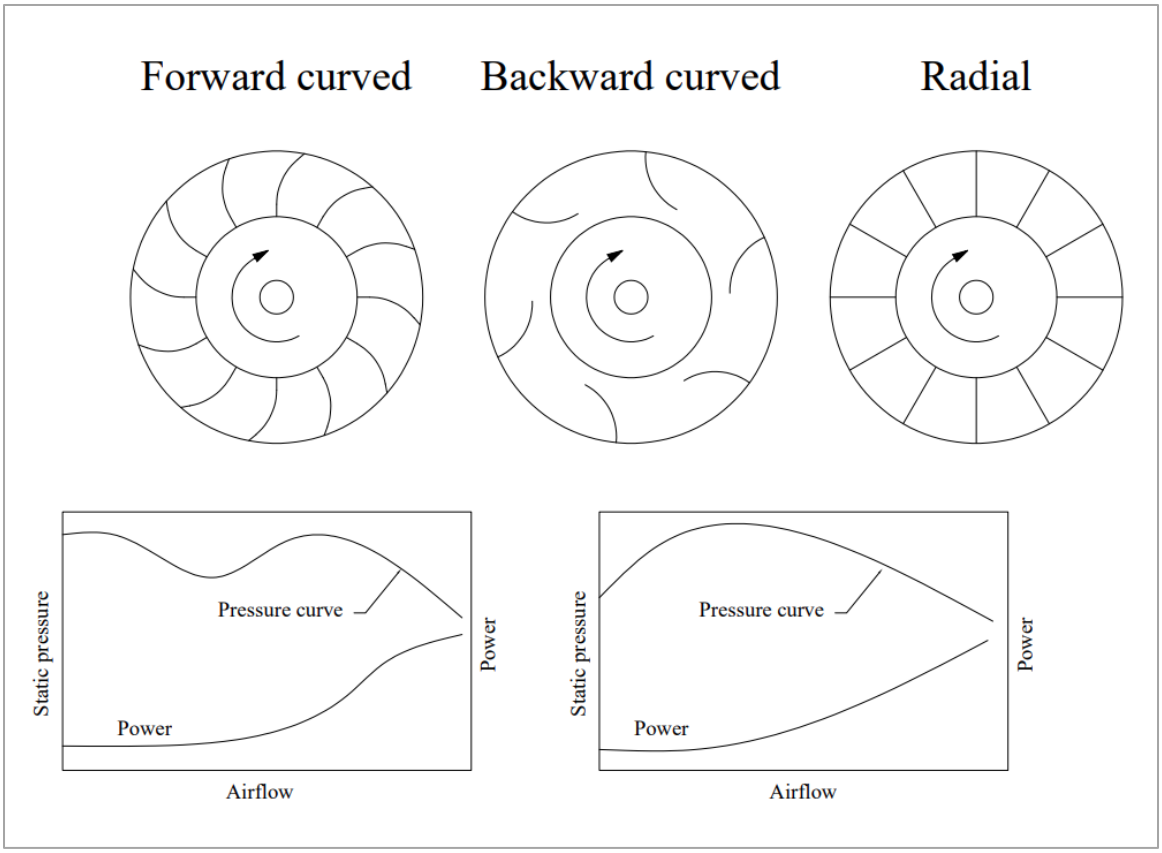

Figure 2.12: Blower performance curves for different types of radial flow blades [3].

2.2.5.4 Motors

Motors, in air conditioning and heat pump applications are used to drive fans. Induction type motors are the most used type. The speed of the AC motor is dependent solely on the frequency of the supply power and the number of pairs of magnet poles of which the motor is wound. The theoretical speed of the motor, referred to as the synchronous speed, is calculated from the following equation:

$$RPM = \frac{60 \times Frequency}{No.\,of\ pair\ of\ magnet\ poles} \tag{2.6}$$

Synchronous speed is the theoretical one if there are no losses. However, by applying load to the motor shaft, the actual speed tends to be a bit lower than the synchronous speed. This difference, at the motor's full load, is defined as the slip.

$$Slip\ \% = \frac{Synchronus\ speed - Full\ load\ rated\ speed}{Synchronous\ speed} \times 100 \qquad (2.7)$$

One of the most important aspects of the AC motor is the power factor. The power factor represents how much of the electric power supplied to the motor is used to create the motion of the motor.

To be able to calculate the PF, three kinds of power must be identified: 1) apparent power, 2) reactive power, and 3) active power.

1) Apparent power: is the product of voltage and current in volt-ampere (VA).
2) Reactive power: is the portion of power that is not utilized in volt-ampere reactive (var)
3) Active power: is the power that is utilized in watts (W).

The power factor (PF) is defined as:

$$PF = \frac{Active\ Power\ (kW)}{Aparent\ Power\ (kVA)} \qquad (2.8)$$

The value of PF is always less than one for an inductive load like the AC motor. The performance curves for motors are published by the manufacturers, see Figure 2.13 [62], [63].

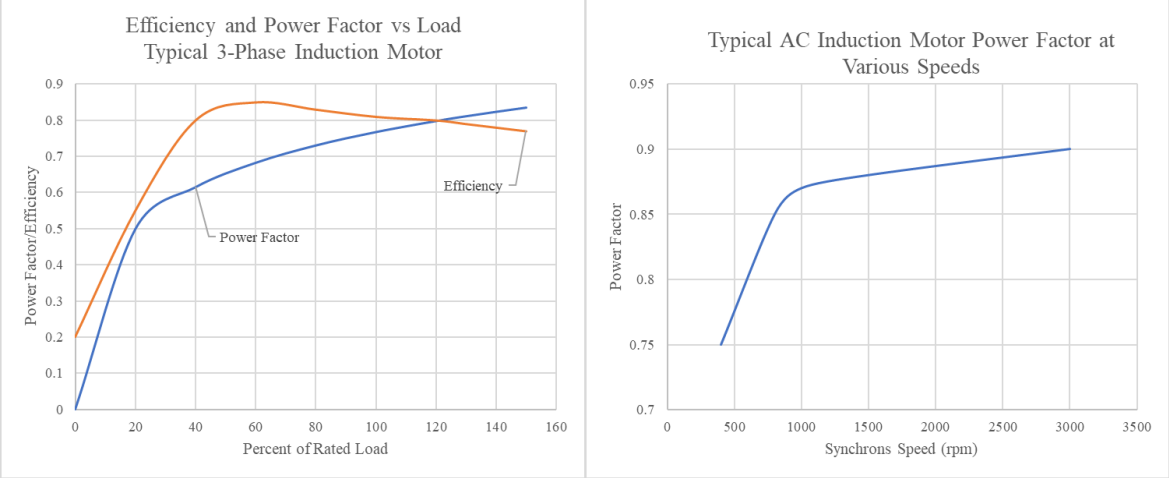

Figure 2.13: Induction motor characteristic curves [62], [63].

Single phase motors need means to start rotation; they do not simply rotate by applying power to them. The most common ways of starting are: 1) split phase, 2) start capacitor, and 3) start and run capacitors. Figure 2.11 illustrates the wiring diagram of each method [17].

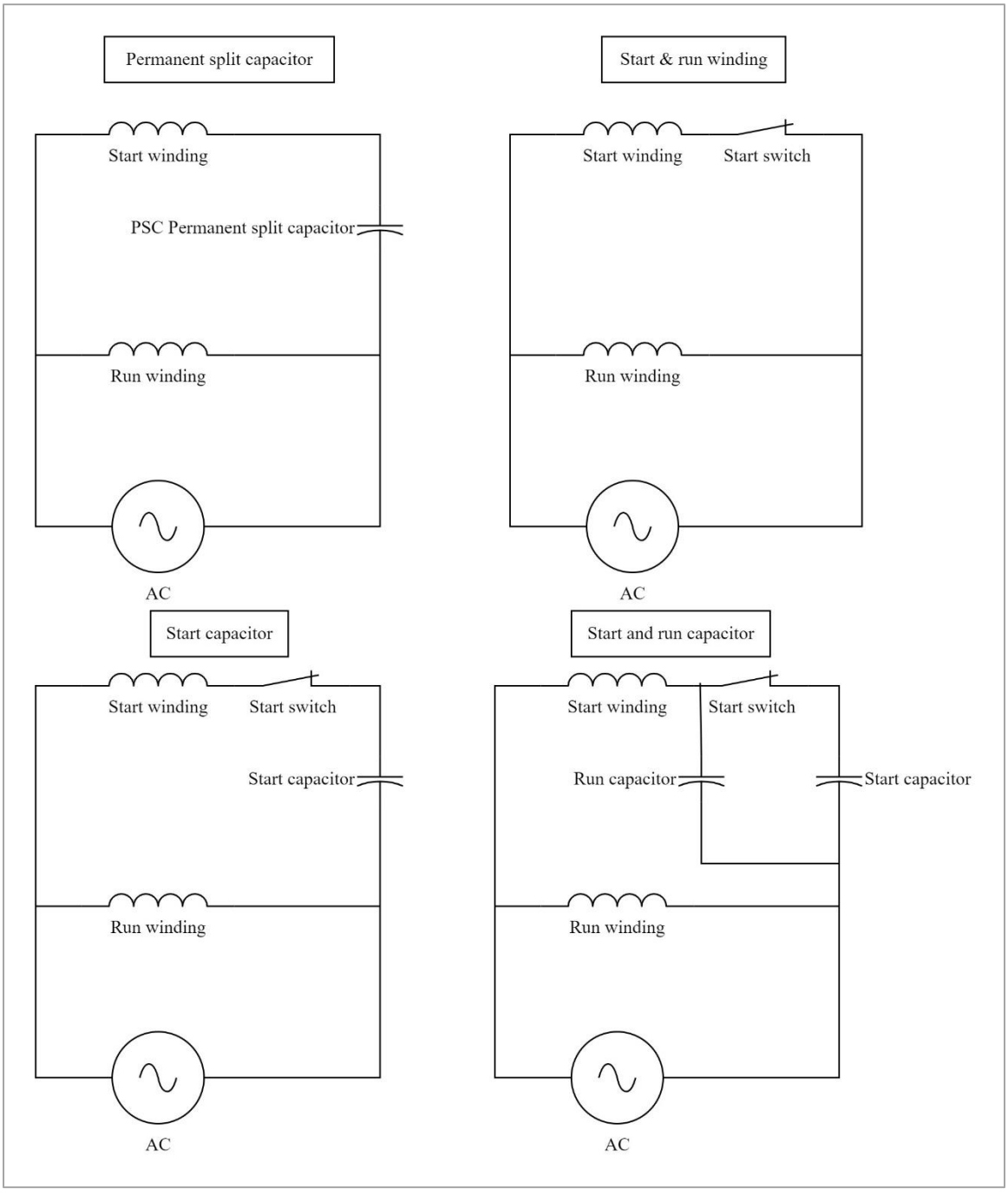

Figure 2.14: Single phase motor starting methods, wiring diagrams [62], [63], [17].

2.3 Defrosting

The process of defrosting is essential to air source heat pumps that work in low ambient temperatures. When the temperature of the outdoor heat exchanger is below the freezing point of water, frost starts to build up on the heat exchanger. After some time, the frost build-up restricts, or even blocks, the airflow, which results in a deterioration of the heat exchange process. That is why some sort of defrost technique must be applied to get rid of the frost once that build up reaches an undesirable level. The following defrosting methods exist:

- Electric Heater Defrost

In this method, electric heater elements are embedded in the heat exchanger during the manufacturing process. By switching off the compressor and turning on the electric heaters, the heat energy of the heaters allows the frost to thaw. Systems usually need longer times to defrost if compared to the other methods of defrost mentioned here.

- Reverse Cycle Defrost

The system runs in reverse mode, cooling mode. The evaporator becomes a condenser. The hot gas delivered by the compressor rejects its heat energy to the surface of the heat exchanger and thus clears the frost. Although the defrost period is shorter than the electric defrost, the disadvantage of this method is that it absorbs heat from the heated space. This is the method commonly used in residential heat pumps [64].

- Hot Gas Bypass Defrost

Some of the compressor's hot gas is directed to the evaporator to defrost it. This is usually done in bigger systems with multiple evaporators, and there is enough hot gas in the system to defrost the evaporator [65].

One of the more common methods of controlling defrosts is to initiate a defrost cycle periodically at predetermined intervals. More sophisticated methods are also implemented to initiate the defrost based on demand. A method to terminate defrost is always provided. Termination could be time based, temperature based or a combination of both [1].

There is so much research targeting the defrost methods and their improvement in heat pump applications. Wang et al. published a field study of defrost in air source heat pumps and showed that a mal-defrost could result in a 17% to 24% loss of capacity and COP, respectively [66]. This is significant for the proper operation of this kind of heat pump, especially in a cold climate.

Minglu et al. published a study about improving thermal comfort during defrosting. The technique they used was to force a defrost cycle right after the end of each heating cycle. That is, instead of the periodic defrost methods implemented commonly in ccASHP systems. Their study shows that their method improved comfort levels as compared to the periodic method [64].

A novel conceptual study by Fan et al. [67] utilized the heat exhausted by the ventilation heat recovery system to defrost the heat pump heat exchanger without the need to. This eliminates the need for additional power consumption to achieve the defrost function. They were able to thaw the frost on the coil in about 4 minutes. The idea is just a concept and needs more research to validate its feasibility on a commercial level.

Therefore, a proper method of defrosting must be implemented in the design of any ccASHP. The proposed design by this thesis should be capable of performing the defrost function. However, the optimization of defrost is beyond the scope of this thesis.

2.4 Cold Climate Air Source Heat Pumps (ccASHP)

According to Northeast Energy Efficiency Partnerships (NEEP), a cold climate Air Source Heat Pump (ccASHP) must meet a coefficient of performance greater than or equal to 1.75 when operating at an ambient temperature of 5 °F (-15 °C). This must be at the maximum capacity operation [68].

To be able to achieve high performance at lower ambient temperatures, which means higher compression ratios, the system must apply some multi-stage or cascade techniques.

2.4.1 Multi-Stage Systems

Multi-stage systems comprise more than one compressor connected in series to achieve the overall compression ratio. The compressors used in such a system are either totally separate compressors or internally divided into multi-stages that are run by the same motor. A

method of refrigerant cooling is provided between the discharge of the lower stage compressor to the suction of the higher stage one. This allows operation at higher pressure ratios, as discussed in Sections 1.1.2 and 1.1.3, which enhances the performance of heat pump applications at lower ambient temperatures. This is the basic principle of operation for cold climate air source heat pumps. They are implemented by manufacturers in different ways to achieve the performance requirements at an economical cost. In his book, Heat Pumps for Cold Climate Heating, Hui Huang divides these systems into three categories: 1) Two-stage vapor injection system with flash tank, 2) Two-stage vapor-injection system with economizer and de-superheater, and 3) Two-stage system with flash tank [69].

2.4.1.1 Two-Stage Vapor Injection System with Flash Tank

In this type of system, shown in Figure 2.15, the liquid refrigerant coming out of the condenser passes through an expansion valve to a medium pressure between the condenser pressure and the evaporator pressure. The output from the expansion valve is a liquid-vapor mixture. It is sent to a tank, a flash tank. The vapor refrigerant from the top of the tank is passed to the compressor at an intermediate stage. In the case of a Scroll type compressor, that would be in one of the middle Scroll pockets explained earlier. The liquid refrigerant sitting at the bottom of the flash tank is then passed to another expansion valve. Then the refrigerant makes its way to the evaporator, and the cycle continues [70].

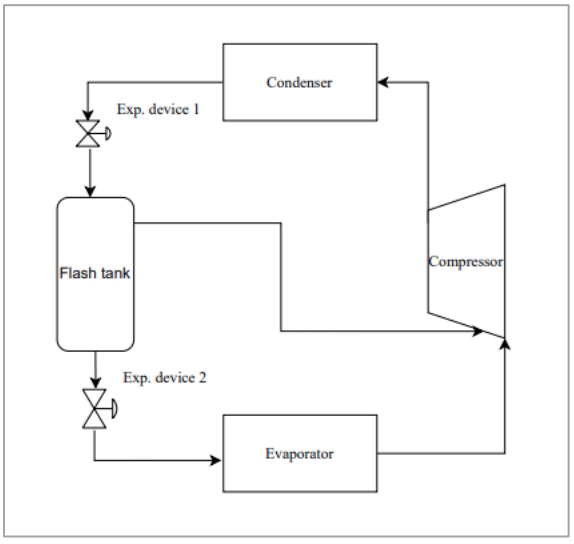

Figure 2.15: Two-stage vapor injection system with flash tank [69].

GREE, one of the major manufacturers of cold climate air source heat pumps, implements this concept in their equipment.

Research by Qiao et al. showed modeling methodology for the flash tank vapor injection system, which was validated by experimental data [71], [72]. Another paper was published by Winkler et al. for the simulation of such a system [73].

2.4.1.2 Two-Stage Vapor Injection System with Economizer and Desuperheater

Shown in Figure 2.16, this system is different from the one described in Section 2.4.1.1 in that instead of a flash tank. It utilizes an intermediate heat exchanger. Some of the liquid refrigerant coming out of the condenser is directed to an expansion valve. The vapor-liquid mixture then exchanges heat with the rest of the liquid coming out of the condenser inside a separate heat exchanger. The vapor-liquid mixture picks up heat from the liquid to totally evaporate and is injected into the medium stage of the compressor. The liquid is further subcooled to flow to another expansion valve and then to the evaporator [74].

Apparently, with more components and design complexity, this system is more expensive as compared to the flash tank method explained in Section 2.4.1.1. However, the performance is slightly better. Ma and Zhao compared the performance of both the flash tank and heat exchanger and found that both systems achieved a lower temperature -25 °C at improved COP and heating capacity than a single-stage system [75]

Another study by Wang et al. confirmed the improvement in performance for both vapor injection systems as compared to a single-stage system at lower ambient temperatures. Although the study did not find a significant difference between the 2 systems compared, the heat exchanger system provided more flexibility in controlling the compressor superheat, which can result in a steadier performance [76].

These studies, however, do not investigate temperatures below -25 °C.

Both Mitsubishi and LG implemented this method in their residential cold climate air source heat pumps [77].

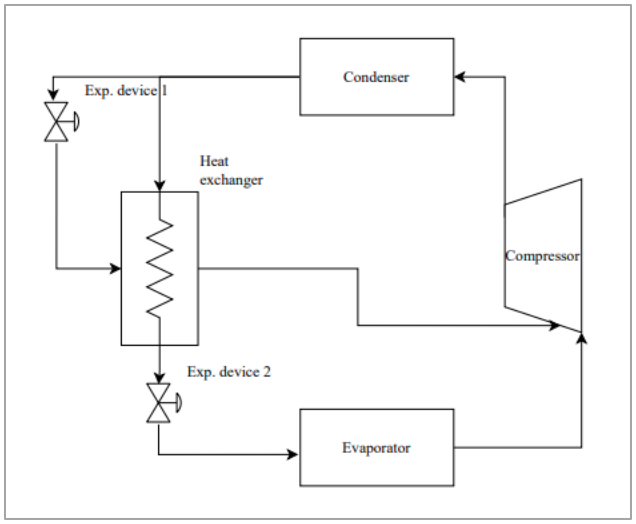

Figure 2.16: Two-stage, vapor injection system with economizer and desuperheater [69], [78].

2.4.1.3 Two Stage System with Flash Tank

In this system, shown in Figure 2.17, the compression process is divided into two steps. The whole liquid refrigerant leaving the condenser is throttled to an intermediate pressure to get mixed, in a flash tank, with all the hot gas coming from the low-pressure compressor. The saturated vapor from the top of the flash tank enters the high-pressure compressor. While the liquid refrigerant from the bottom of the tank expands in a second throttling device to e the system evaporator.

The system is like the cascade system 44urrenbed in Section 2.4.1, except for the flash tank in lieu of the closed intermediate heat exchanger.

Mancuhan published a paper studying the performance of this system with different refrigerants. An improvement in performance is reported for ambient from -40 to -20° C. The system was not investigated from ambient below -40 °C. For higher ambient temperatures, the system performance is degraded. The system also cannot reverse operation to work in cooling mode [79].

No44urrentt manufacturer was identified using this system for residential air source heat pump applications. Apparently, the system is applicable for low temperature applications but not for high or medium temperatures.

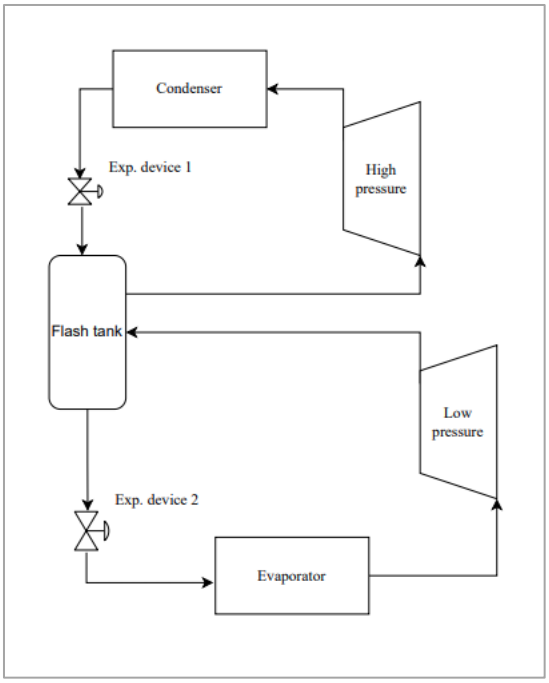

Figure 2.17: Two stage system with flash tank [69].

2.4.2 Cascade Systems

2.4.2.1 Closed Cascade System

The system comprises two or more separate systems. Each system can use a different type of refrigerant adequate to the temperature range. The systems are thermally connected through an intermediate heat exchanger. It acts as the evaporator of the higher-pressure system and the condenser of the lower-pressure system. This arrangement allows each compressor to take a share of the overall compression ratio. Also, it allows the use of a low temperature refrigerant with a high vapor density at lower temperatures [8]. A schematic for this system is shown in Figure 1.6.

The system is primarily developed for ultra-low freezing applications. Bansal and Jain [68] provided a brief history of the system, an explanation, and the potential of future applications. CO2 systems show potential for use in low temperature systems. However, the system pressure at higher temperatures is excessively high. This could hinder their application in residential applications as they require much more stringent safety measures[80] [81].

However, some relatively recent research has been done to utilize this kind of system for heat pump applications. Song et al. published research regarding the use of cascade heat pumps for space heating utilizing R134a and CO2 as refrigerants. The study shows improvement in heating performance for the cascade system at lower temperatures from -10 to -20. Whereas between 0 and -10 its performance is lower. The system also did not operate at high ambient temperatures. The cooling mode was not available in the system[82].

Yang et al. studied the cascade system applied to residential heating in northern China. Their research showed an improvement in COP for the cascade system as compared to the single-stage system from -35 °C to -2.5 °C saturation suction temperature. Above this temperature, the single-stage system has better performance. The research focused on heating but did not address working in cooling mode [83].

Another research by Shen et al. compared a cascade system to a single-stage system for a range of ambient temperatures between -12 °C and +12 °C. Their study showed improvement in COP and capacity of the cascade mode at up to 0 °C ambient. [78].

Roh and Kim studied the effect of the vapor injection technique to cascade heat pump systems. They tried different variations of the vapor injection to the low-pressure system and the high-pressure system with different injection percentages. The study showed an increase in heating capacity, however, the system COP decreased. The research stopped short of presenting a decisive recommendation as to where to apply the vapor-injection technique, whether to the low-pressure system or the high-pressure system [84].

Research reviewed in this area showed that the cascade system is efficient in targeting low temperature applications with high compression ratios. However, they underperform their single-stage counterpart when it comes to higher temperature applications with lower compression ratios. Applying vapor-injection technique to a cascade system showed it can lead to a slightly improved performance given a high compression ratio, however, this technique will lead to a lower COP if applied at lower compression ratios.

2.4.2.2 Auto-Cascade System

In the auto-cascade systems, vapor-liquid separation and expansion processes occur for multiple refrigerants. This happens in multiple stages resulting in cooling at very low temperatures. By selecting the proper refrigerant mixtures and the design of counter flow heat exchangers, this kind of system can achieve -60 °C. The system offers lower compression ratios and higher volumetric efficiency; however, the system chemistry and the heat exchanger system design are challenging [8], [85], [86].

Tan et al. studied an auto-cascade system with R-32 and R-236fa. Their system achieved a lower refrigerant temperature of -30 °C. by applying ejector refrigeration to their system, and they aimed at lowering the operating temperature of their proposed system as compared to a regular auto-cascade. The system was not designed to work in cooling mode [87].

He et al. published a theoretical study for a two-stage auto cascade system. System performances were presented for a range between -60 °C and -35 °C. Multiple combinations of refrigerants were studied and compared. Their study showed the capability of operation under lower ambient conditions. However, the system cannot perform in higher ambient or cooling modes [85].

Another study by Cui et al. investigated the auto-cascade system combined with the two-stage compression and compared it to the flash tank injection system and the internal heat exchanger injection system [88]. The study showed an improvement in COP between 1.8% to 9%. However, being an experimental model, the system design did not factor in the cooling mode operation capability. Also, it did not provide any means for defrosting.

Zuev et al. simulated the performance of R32/R134a/R365mfc auto-cascade system and R410A/R134a cascade heat pumps in a cold climate. They compared the COP at different ambient temperatures. The COP of the auto-cascade system outperformed its cascade counterpart by 7% to 2% at temperatures of -40 °C and -20 °C, respectively. Above -20 °C, the cascade heat pump had a higher COP. They concluded that above -10 °C, both systems would be outperformed by a single-stage system which makes the operation of either kind of cascade unnecessary, inefficient, and impractical [89]. The research did not address the means of operation at higher ambient temperatures above -15 °C, in cooling mode, or defrost.

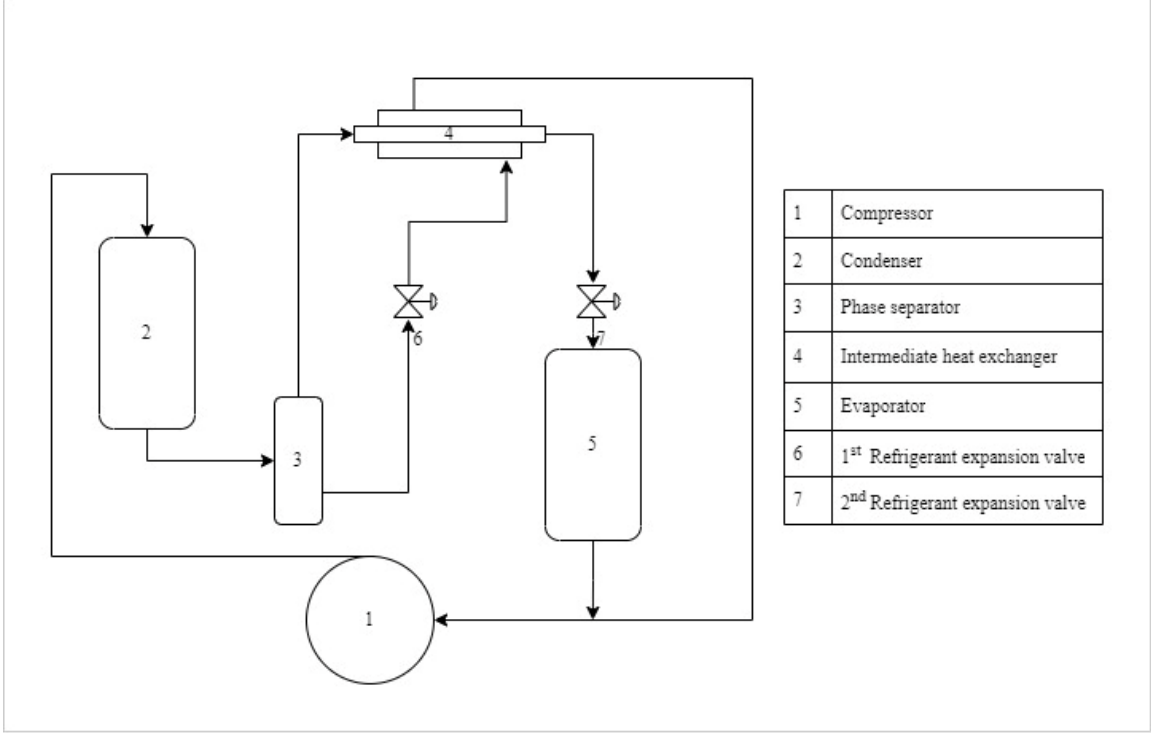

Figure 2.18: Schematic for simple auto-cascade system [8].

Auto-cascade systems are originally developed for cryogenic storage applications. The method allows for reaching lower evaporation temperatures with improved overall efficiency. Research in applying this method for space heating is still in the preliminary phase. The system lacks the flexibility to operate in both heating and cooling modes which are required for residential applications. In addition, the system design cannot perform a reverse cycle defrost, which adds more challenges to applying this system for air source heat pump applications.

2.4.3 Multi-Function Heat Pumps

Multi-function refers to heat pumps that can switch between modes of operation depending on the operating conditions[90]. There is no actual heat pump in the market that can perform multi-function. However, some limited research could be found that addresses this area.

A simulation study by Yang et al. experimented with two heating modes of operation, cascade mode and single-stage mode. They presented results for operation between -35 °C

and 20 °C evaporator temperature. They were able to improve the COP and heating capacity at lower temperatures by switching to cascade mode [91].

A similar conclusion could be found in the research by Shen et al. They experimented with dual modes of operation, cascade and single-stage [92].

Johnson presented a field trial with a multi-mode of operation for a 4 tonne heating capacity heat pump system that switches between cascade, single-stage modes along with electric heaters. The unit was built by Hallowell International, which went out of business due to some economic difficulties. The experiment took place in New Haven, CT and lasted for two winters, 2009/2010 and 2010/2011. The system maintained a promising SCOP of 2.78 in the first year and 2.83 in the second year. However, some operational reliability issues have been reported [93].

Multi-function heat pump application is in its very early research and development stages. Systems become more complicated and thus more expensive to build, install and maintain. This was noted by the users of the equipment in the Johnson report [93], which could have made it less desirable for investors and consumers. However, the improved performance is evident on both theoretical and empirical levels. With more emphasis in the last decade on improved energy efficiencies and global warming issues, there is an ongoing focus on improving heat pump technologies in operation in cold weather. The author anticipates that the multi-function heat pump shows the potential to provide a solution, and it will gain momentum in the coming few years.

2.4.4 Market Survey for ccASHP

A residential air source heat pump is identified by its capacity being less than 65,000 Btu/h (19 kW) [94]. The standard practice in the market is to offer equipment sizes from 1.5-ton refrigeration to 5-ton refrigeration with 0.5-ton increments. Table 2.6 shows the standard sizes and their equivalent capacity [95], [37].

On their website, NEEP allows manufacturers to list their ccASHP products and publish their performance ratings. A full list of all listings has been downloaded and shown in Appendix D [96].

Table 2.6: Standard sizes of residential air source air conditioners and heat pumps.

Size	Capacity	
ton refrigeration	Btu/h	kW
1.5	18000	5.3
2	24000	7.0
2.5	30000	8.8
3	36000	10.6
3.5	42000	12.3
4	48000	14.1
4.5	54000	15.8
5	60000	17.6

The takeaways from this survey are as follows:

- Less than 100 systems are listed on NEEP and identified as ccASHP. Out of which, a mere 80 are different heat pump outdoor units, while the rest are just a combination of the same heat pump unit with a different furnace or indoor air handling units.
- All ccASHP in the market utilize a variable speed compressor technology, addressed earlier in Section 2.2.1.3
- All systems implement the multistage concepts described in Section 2.3.
- Maximum COP at 5 °F (-15 °C) outdoor temperature is 2.29 achieved by MRCOOL system listed at AHRI# 208960636 at a rated capacity of 24000 Btu/h and can deliver a maximum of 18100 Btu/h at 5 °F outdoor temperature.
- COP at 5 °F (-15 °C) outdoor temperature ranges between 1.77 and 2.29. Two-thirds of the systems fall below 2.0.
- System capacity at 5 °F (-15 °C) ranges between 75% and 100% of the rated capacity at 47 °F (8.3 °C).
- The minimum operating temperature is -30 °C. That is for just a handful of systems. MRCOOL system mentioned above is the one with the highest COP at

this temperature, 1.47. However, the capacity at -30 °C falls to 40% of the system's rated capacity.

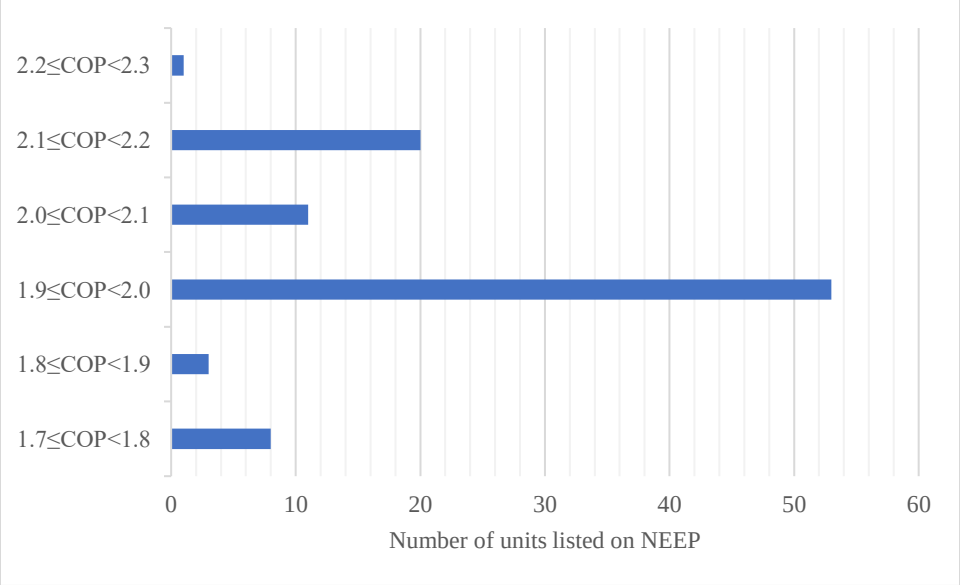

Figure 2.19: Number of units listed on NEEP categorized by a range of heating COP at 5 °F, compiled from the table available in Appendix D [96].

The above analysis considered the systems from a statistical point of view. It is noteworthy to mention that the full list discussed here represents the most efficient heat pump systems available in the market. The difference in system performance is minimal. So, to study a system's performance in depth, one system could be selected as a representative of the whole list. Therefore, the system with the highest performance numbers is selected and analyzed.

The criterion for selection is as follows:

1- The system with the highest COP at 5 °F. MRCOOL, AHRI Cert #: 208960636. COP at 5 °F = 2.29

2- The system with the highest HSPF. BLUERIDGE, AHRI Cert #: 208101243. HSPF region IV = 12

Accordingly, the performance data for the two systems mentioned above are compiled, and the system performance curves as shown in Figures 2-20 and 2-21.

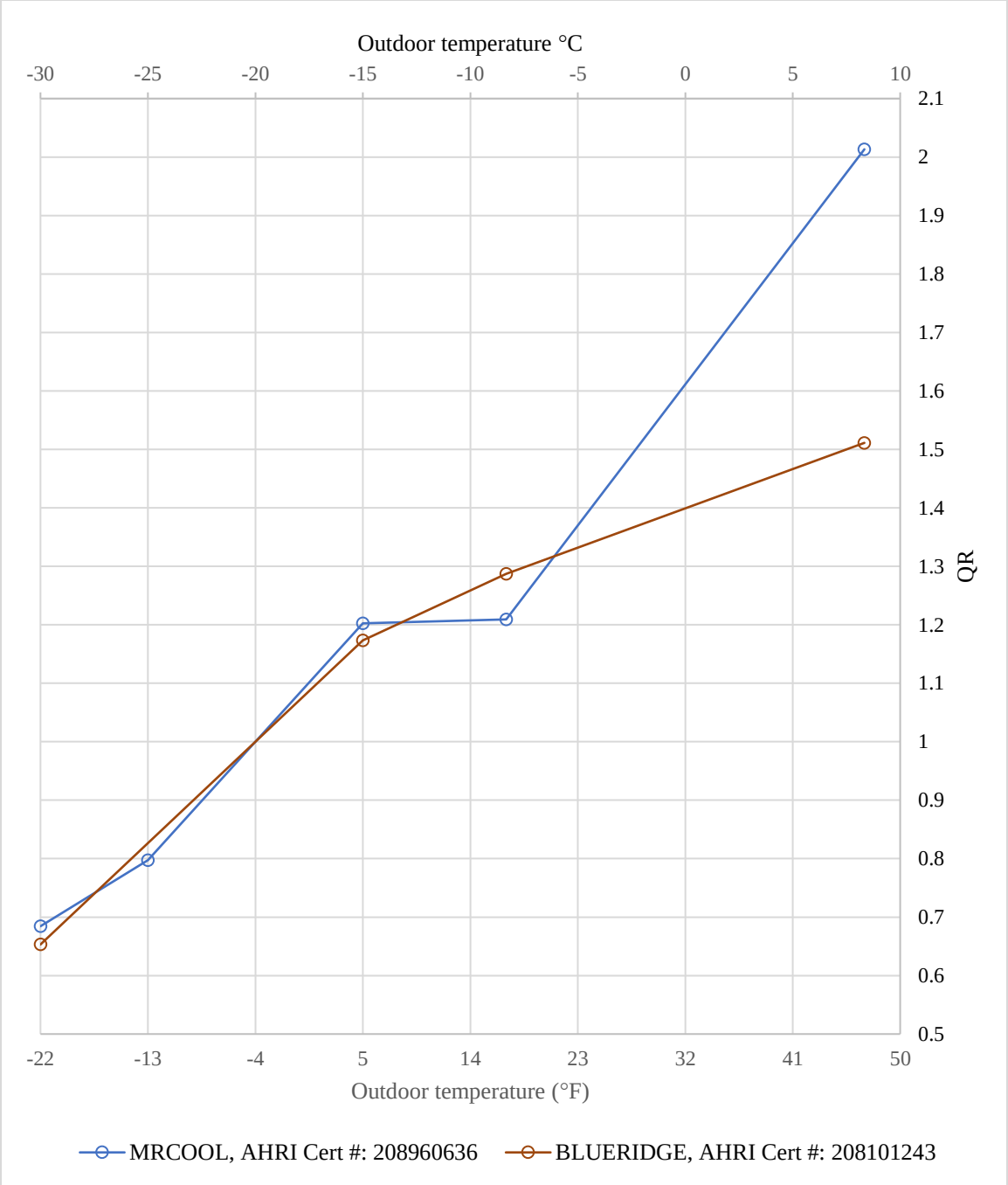

Figure 2.20: Capacity ratio (QR) for MRCOOL, AHRI Cert #: 208960636 and BLUERIDGE, AHRI Cert #: 208101243 ccASHP systems at various outdoor temperatures.

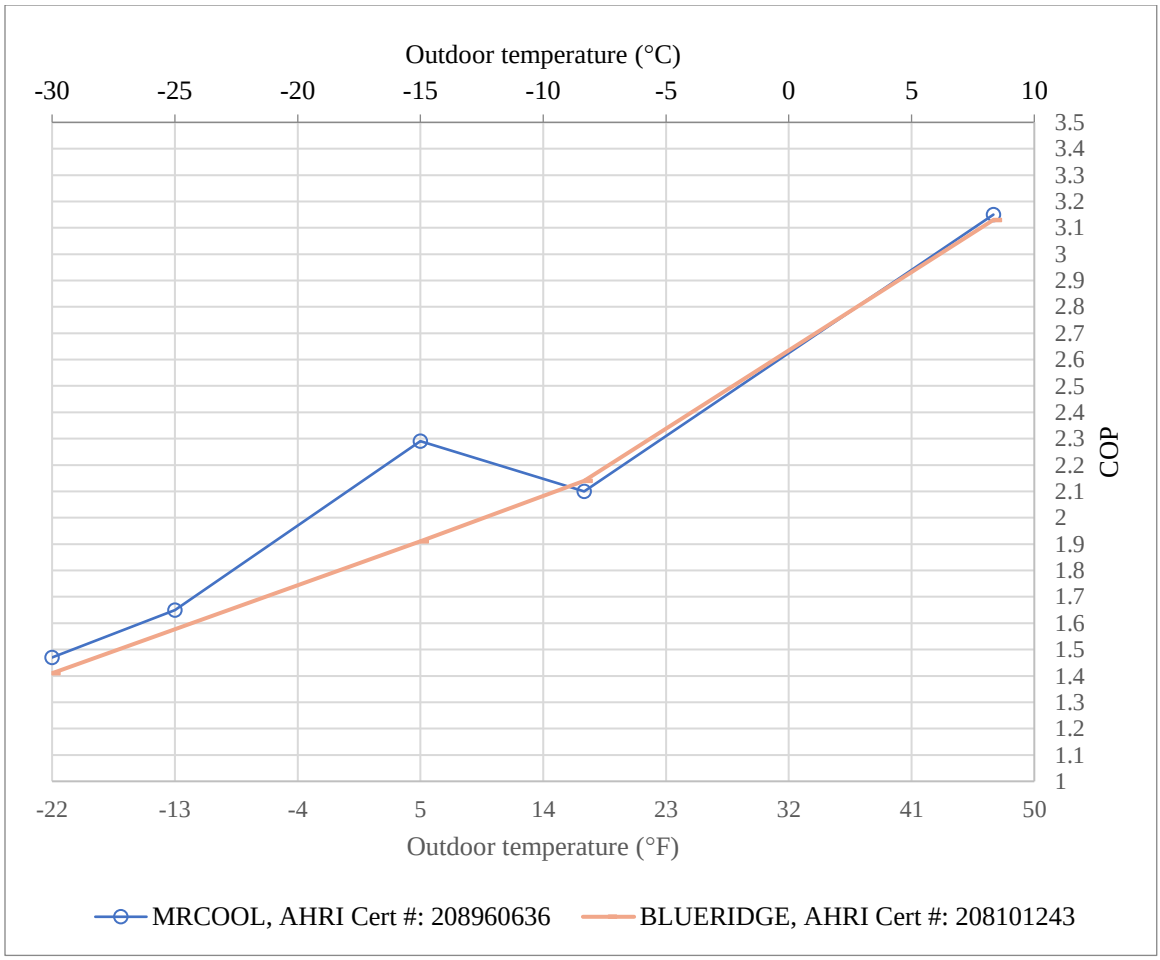

Figure 2.21: COP for MRCOOL, AHRI Cert #: 208960636 and BLUERIDGE, AHRI Cert #: 208101243 ccASHP systems at various outdoor temperatures.

Operating range:

Both systems can operate down to -30 °C ambient temperature. This is the minimum ambient temperature that any system available in the market and listed on AHRI or NEEP can operate.

Coefficient of Performance (COP):

The COP curves follow the same trend explained earlier in Chapter 1. The COP decline with the decrease in ambient temperature. The effect of reduced volumetric and isentropic efficiencies explained in Section 1.1.2 can explain why the COP drastically declines at lower ambient temperatures.

At 47 °F the COP is at an appealing value of around 3.2, making the operation very efficient.

At 5 °F, the COP drops to less than 2.0. Then at -22 °F the COP is a mere 1.4. The COP line between 47 °F and 5 °F has a higher slope than the range from 5 down to -22 °F. That is due to applying the vapor-injection technique discussed earlier. If the system follows the slope of the line between 47 and 5 °F, the COP at -22 °F would have reached a value below 1. That shows how the vapor-injection technique helped improve the COP of this system at the lower ambient temperature.

Heating capacity:

The capacity curve follows the same trend explained earlier in Chapter 1. As expected, generally, the capacity decline as the ambient temperature decrease

At the minimum operating temperature, -30 °C, system capacity plummets to around 60% of the capacity at -20 °C and 50% of its value at -10 °C. If compared to the capacity at 47 °F, it is only 40%.

For the system to attain the COP values discussed above, it is seen that the system capacity must be reduced at a higher rate at lower temperatures. It is clear that the capacity decline rate is higher in the +5 to -22 range than that in the +47 to +5 °F range.

HSPF Region IV:

This represents the overall performance of the system when operating for a full heating season in Region IV area. The BLUERIDGE system at 12 HSPF is better than the 10 HSPF of MRCOOL system.

This could be explained by examining both Figures 2-20 and 2-21. The BLURIDGE system designers opted to maintain a higher capacity throughout the whole operating range from 47 °F to -22 °F. This is achieved by running the compressor at a higher speed. It is seen that the capacity line of MRCOOL system falls below that of BLUERIDE. But it is the other way around on the COP lines, Figure 2.21. The COP line of MRCOOL system is above that of BLUERIDGE. By

gaining more heating capacity by sacrificing COP, the BLUERIDGE system designers managed to gain a better overall seasonal system performance that is reflected in their higher HSPF number.

It is worth mentioning that Region IV is not representative of the coldest regions. The analysis in this section focuses on the published performance numbers. Later in this thesis, the study in colder regions will be conducted.

Finally, the 2 systems have a comparable performance only within 5% difference. They are a representation of the performance of the most efficient system that is currently available for sale in the market.

2.4.4.1 Summary of the Survey

The lowest ambient temperature that any system can run at is -30 °C. No system in the market can run below this temperature.

The decline in heating capacity at -30 °C prevents the heat pumps from being the main source or the only source of space heating. An auxiliary heating system must be installed to satisfy the heating demand at low ambient temperatures.

Assuming the same technology is used to cover the performance below -30 °C. If the performance curves of the systems are extended below -30 °C following the same line trends of Figures 2-20 and 2-21, The value of the COP will drop to 0.7, and the capacity ratio will drop below 15% at -50 °C. Apparently, operating with these numbers is impractical. This means that a different approach must be taken to address the performance below -30 and as low as -50 °C.

2.4.4.2 Industry Future Challenges for ccASHP

In its endeavour to reduce the carbon footprint of cold climate heating solutions, the US Department of Energy (DOE) partnered with leading industry manufacturers to boost the efforts of improving the efficiency and affordability of ccASHP. The DOE started a ccASHP technology challenge program. Six of the main players in this industry have already participated in this challenge: Carrier, Daikin, Johnson Controls, Lennox, Mitsubishi, and Trane [97].

The challenge set forth the performance targets as follows [98]:

- HSPF2 (Region V) ≥ 8.5
- Heating Capacity at 5 °F ambient temperature = 100% Capacity at 47 °F
- Heating at -15 °F capability
- COP at 5 °F ≥ 2.4

The timeline for the challenge has been outlined in Figure 2.22 [99].

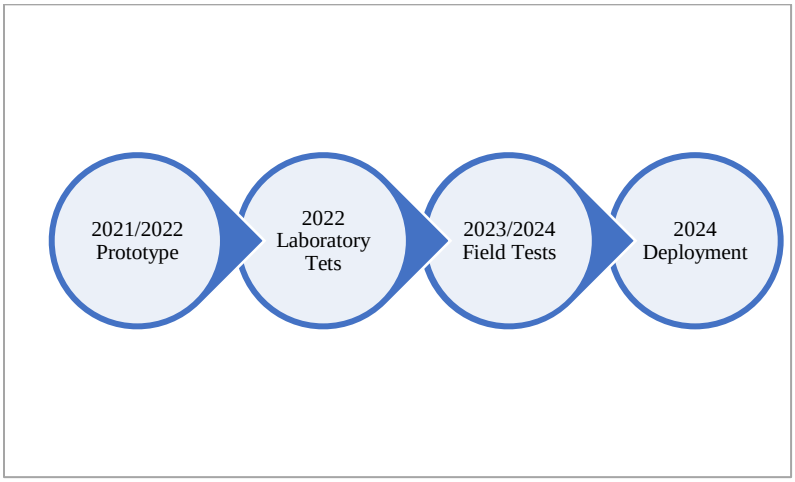

Figure 2.22: US DOE ccASHP Challenge, Timeline [99].

Some of the manufacturers participating in the challenge have already announced that they have done the prototype testing phase and will start on the field trials [100], [101]. Though manufacturers claim breakthroughs in the technology, it is not clear what is new in their development. Confidentiality is expected and could be understood as it is a proprietorship matter.

It is evident that the challenge raises the bar for the manufacturers to develop more efficient ccASHP. But, as the challenge is coming from the USA, the targets do not come close to the Canadian northern extremely cold regions. It has been mentioned earlier in Chapter 1 that region V cannot represent Northern Canada, where the temperature dips way below the -15 °F targeted by this challenge.

2.5 Gaps in the Literature

The literature review shows that there is a lot of research done on heat pumps for residential applications. Recently, research has been more focused on the application of air source heat pumps to cold climate regions. However, the studies target temperatures down to -30 °C. No heat pump is available in the market that can operate below -30 °C as seen on the NEEP list. Moreover, the operation at -30 °C for the current designs is inflicted by lower COP and heating capacity. This could be applied to so many cold climate regions, but there are some Canadian areas where the overnight temperatures go down to as low as -50 °C, which implies that air source heat pumps can only be used as secondary heating equipment. Auxiliary heating equipment must be installed to provide the full necessary heating load at a temperature between -30 °C and -50 °C.

No research could be found that covers the operation of an air source heat pump to as low as -50 °C and can work as an air conditioner to provide cooling in summer as well.

Such a system could be installed in extremely cold climates as the main source of heating and cooling without the need for an auxiliary heating or cooling system. That is the target of this research.

Chapter 3. Thermodynamic Analysis

3.1 Methodology

The system is thermodynamically modeled by establishing the performance equations for each component, then combining them all together based on the refrigeration cycle equations to calculate the overall system performance. The EES software is used to facilitate modeling and simulation study. Each system is studied in both heating and cooling modes, and the performance is simulated for ambient temperature ranging from -50 °C to +20 °C in heating mode and from +20 °C to +45 °C in cooling mode. The system component parameters are kept the same when calculating each mode of operation to simulate real-life scenarios. The main component that will drive the refrigerant flow is the compressor, which will be sized to deliver a certain heating effect at a standard outdoor temperature of 8.3 °C. The volume flowrate of the compressor will be determined and will be kept constant when modeling the performance at different outdoor conditions. Following the AHRI 210/240-2023 standard used in North America for rating residential air source air conditioners and heat pumps, the indoor temperature in cooling operation will be kept at 26.7 °C and 21.1 °C in heating operation [94].

As the study is mainly a comparative one, power consumption from common auxiliary components will not be considered as they are common in all systems. Examples of these include indoor air-blower motors, outdoor condenser fan-motor, etc. The exception will be when they can influence the performance comparison, and in that case, they will be appropriately modeled and simulated.

Table 3.1: Outdoor design dry bulb temperature for rating per AHRI 210/240.

	Indoor Temperature		Rated Capacity	
	°C	°F	°C	°F
Heating, winter operation	21.11	70	35.00	95
Cooling, summer operation	26.67	80	8.33	47

3.2 Modeling the Heat Exchangers, Condenser and Evaporator

The system under study is an air-to-air system, meaning the system exchanges energy between its heat exchangers and the space of interest when air passes over the heat exchangers. The heat exchangers of fin-and-tube utilize a variable speed fan to provide forced convection between the refrigerant and the air. The heat exchanger is sized to always maintain a temperature difference of 10 °C between the refrigerant and the air by varying the speed of rotation of the fan.

The equation for heat transfer through the heat exchanger is [57]:

$$\dot{Q} = U \cdot A \cdot \Delta T_{lm} \tag{3.1}$$

The heat transfer area of the heat exchanger (A) is a constant based on the physical size of the heat exchanger. If the logarithmic mean temperature difference (ΔT_{lm}) is to be kept constant, then Equation 3.1 shows that the rate of heat transfer $(\dot{Q})$ is directly proportional to the value of the overall coefficient of heat transfer (U). The main contributor to the value of (U) is air velocity. Therefore, by changing the air velocity by changing the fan speed, the desired value of $(\dot{Q})$ could be achieved.

In a different approach, where variable refrigerant flow is applied to gain better efficiency, the heat exchanger will be modeled in a way that both air and refrigerant temperatures can be varied to match the required amount of heat exchange. By maintaining the airflow constant, the logarithmic mean temperature can be determined for a certain heat transfer rate.

The logarithmic mean temperature difference (ΔT_{lm}) can be calculated by the following equation[57]:

$$\Delta T_{lm} = \frac{\Delta T_1 - \Delta T_2}{\ln(\Delta T_1 / \Delta T_2)} \tag{3.2}$$

Were, ΔT_1 and ΔT_2 are temperature differences between the fluids at the heat exchanger inlet and outlet.

For both heat exchangers, condensers and evaporators, the internal fluid is at constant pressure and temperature, undergoing either boiling or condensation processes. Only a

small portion of the heat exchanger is dedicated to superheating in the case of the evaporator or desuperheater, in the case of the condenser. In these portions of the heat exchanger, the temperature of the internal fluid, refrigerant, changes until it reaches the corresponding saturated temperature.

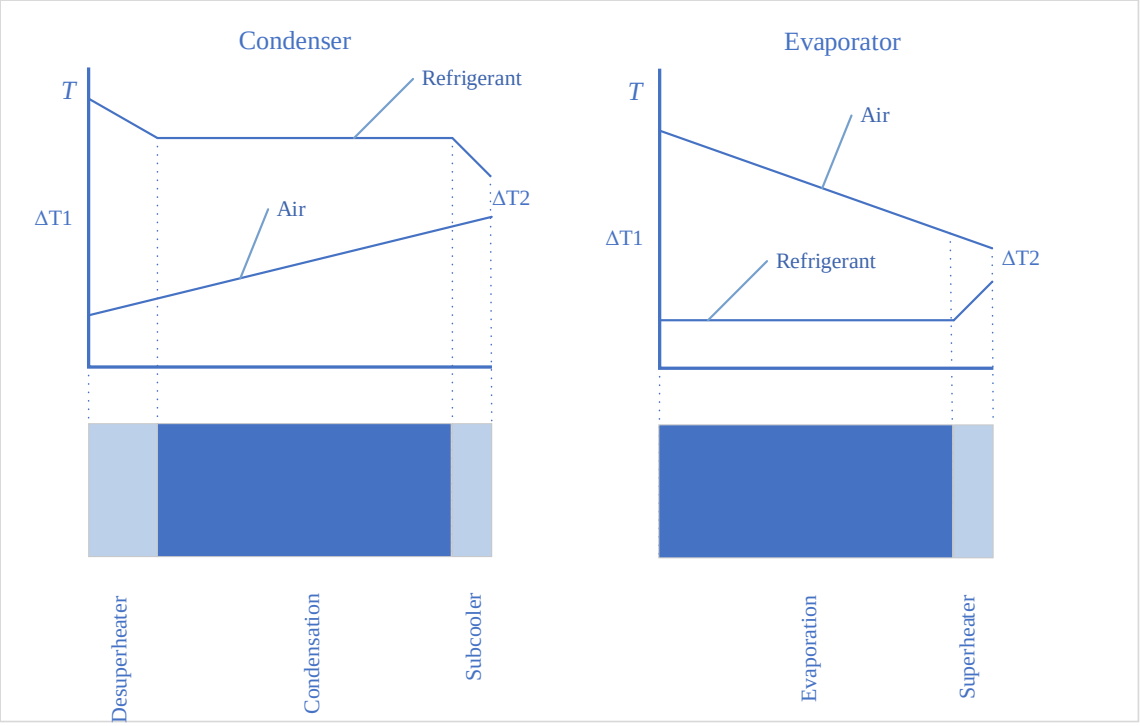

Figure 3.1: Variation of fluid temperatures in a heat exchanger.

It is assumed that only 10% of the initial design size of the heat exchanger will be used for the temperature changing portion, while the rest will be dedicated to the rest of the heat exchange process.

The initial design will be specific to given conditions and rates of heat transfer; therefore, a heat exchanger constant (K_{HE}) can be calculated by rearranging Equation 3.1 as:

$$K_{HE} = \frac{\dot{Q}}{\Delta T_{lm}} \tag{3.3}$$

Accordingly, the heat exchanger will be modeled using equation 3.2 as multiple condensers in series. For an evaporator, a main heat exchanger is followed by a superheater, and for a

condenser, a desuperheater, then a sub-cooler. This method has been reported by Byrne et al. [102].

Furthermore, the energy equation shall be applied to the air side of the heat exchanger, which shall equal the one calculated for the refrigerant side of the heat exchanger.

$$\dot{Q} = \dot{m_{air}} \cdot c_p \cdot \left(T_{air,out} - T_{air,in}\right) \tag{3.4}$$

$\dot{m_{air}}$ = air mass flowrate, c_p = specific heat of air at constant pressure, $T_{air,out}$ & $T_{air,in}$ = air temperature at the outlet and inlet of the heat exchanger

For the evaporator, the air temperature difference will be a negative value; thus, the resulting rate of energy exchanged is a negative value, which means that the energy moved from the refrigerant to the air. For the condenser, it is vice versa.

3.3 Modeling the Compressor

There is considerable literature on this topic. For example, Byrne et al. [30] summarized some methods that have been previously published for modeling scroll compressors[103]. In addition, Cuevas and Lebrun [31] addressed the same topic for variable speed scroll compressors[104]. Further, the AHRI Standard 540-2020, d ANSI/ASHRAE Standard 23.1-2019, ANSI/ASHRAE Standard 23.2-2014 describe how manufacturers test and publish the performance values for their compressors.

3.3.1 Single Speed Compressor

The compressor is first modeled in the ideal case where the compression process is isentropic. This will be the baseline to which any practical system cannot outperform. Then a more practical approach is considered by applying the manufacturer's published performance data for any selected compressor. All manufacturers publish the compressor performance data in the form of a 10-coefficient that can be applied to a standard quadratic equation with only two variables: the saturated suction temperature and the saturated discharge temperature [105], [106], [107].

The equation is of the form:

$$X = C_1 + C_2 \cdot t_S + C_3 \cdot t_D + C_4 \cdot t_S^2 + C_5 \cdot (t_S \cdot t_D) + C_6 \cdot t_D^2 + C_7 \cdot t_S^3 + C_9 \cdot (t_s \cdot t_D^2) + C_{10} \cdot t_D^3 \tag{3.5}$$

Where:

- X = Refrigeration capacity, Power input, or Refrigeration mass flow rate.
- t_D = Discharge saturation temperature in °C or °F
- t_S = Suction saturation temperature in °C or °F
- C_1 through C_{10} = Regression coefficients provided by the manufacturer.

Given the compressor performance based on the manufacturer's published data at standard conditions, Dabiri and Rice provided methods to calculate compressor mass flow rate and power consumption under any conditions [108]. This method is recommended by ASHRA and AHRI for system manufacturers and designers to adopt for their system evaluation [105].

$$\dot{m} = \dot{m}_{std}\left(1 + F\left(\frac{\rho}{\rho_{std}} - 1\right)\right) \tag{3.6}$$

Where F is a factor depending on the compressor volumetric efficiency, it can be considered 1 without noticeable error.

The compressor power ($\dot{W}$) can also be calculated as follows.

$$\dot{W} = \dot{W}_{std} \cdot \frac{\dot{m}}{\dot{m}_{std}} \cdot \frac{\Delta h_s}{\Delta h_{s,std}} \tag{3.7}$$

In Equations 3.6 and 3.7, std denotes standard conditions, and s denotes isentropic process. $\dot{m}, \rho, \Delta h$ refer to refrigerant mass flowrate, density, and enthalpy difference.

Table 3.2: Temperature ranges for refrigeration and air-conditioning applications [105].

Application	Evap. T. Range °C	
Air-conditioning (including heat pump)	-23.33	12.78
High temperature	-6.67	10.00
Medium temperature	-23.33	0.00
Low temperature	-40.00	-12.22
Extended medium temperature	-31.11	-3.89

Application ranges are defined for the refrigeration and air-conditioning industry. Manufacturers tend to designate a specific application when they develop their components, like compressors, expansion devices, and heat exchangers [105].

3.3.2 Variable Speed Compressor

For modeling the variable speed compressor, the same concepts of the single speed ones will be applied in addition to some more considerations.

In the air conditioning industry, the term compressor refers to a compressor-motor combination inside a single shell. Once a compressor is selected, its internal volume is fixed throughout its operation. One way to vary the refrigerant flowrate of the compressor is by changing the rotational speed of its motor. The rotational speed of the induction motor is dependent only on the frequency of the power supplied to it [109].

$$RPM = \frac{60 \times Frequency}{No.\,of\ pair\ of\ magnet\ poles} \tag{3.8}$$

By adding a variable frequency drive to the system, the compressor rotational speed can then be controlled.

The compressor manufacturers publish the performance data for their variable speed compressors in two ways:

1) A 20-coefficient formula with the variables saturation suction temperature, saturation discharge temperature and the compressor rotational speed.

$$\begin{aligned} X = \ & C_1 + C_2 \cdot t_S + C_3 \cdot t_D + C_4 \cdot N + C_5 \cdot t_S \cdot t_D + C_6 \cdot t_S \cdot N \\ & + C_7 \cdot t_D \cdot N + C_8 \cdot t_S^2 + C_9 \cdot t_D^2 + C_{10} \cdot N^2 + C_{11} \cdot t_S \cdot t_D \cdot N \\ & + C_{12} \cdot t_S^2 \cdot t_D + C_{13} \cdot t_S^2 \cdot N + C_{14} \cdot t_S^3 + C_{15} \cdot t_S \cdot t_D^2 \\ & + C_{16} \cdot t_D^2 \cdot N + C_{17} \cdot t_D^3 + C_{18} \cdot t_S \cdot t_R^2 + C_{19} \cdot t_D \cdot N^2 \\ & + C_{20} \cdot N^3 \end{aligned} \tag{3.9}$$

Where:

$$N = Compressor\ rotational\ speed\ in\ revolution\ per\ minute$$

In this case, the compressor performance will be modeled directly through this equation.

2) They publish the 10-coefficients like the single speed compressors at discrete frequencies [110].

Interpolation will be done to calculate performance points between the range of each 2 discrete frequencies.

3.4 Modeling the Expansion Valve

The expansion device is to be an electronic expansion valve. The valve controls the refrigerant flow rate by varying the diameter of its throttling orifice to maintain a constant refrigerant superheat at the system's evaporator exit. As the heat loss through the expansion process is negligible, the expansion process will be assumed to be adiabatic.

There is as much research on modeling electronic expansion valves, however, the modeling addresses the question of how the valve will react in response to the control algorithm. Basically, it is all about how to achieve the desired superheat [111]. However, this is beyond the scope of this thesis. Here it will be assumed that the superheat value is achieved by the expansion device.

3.5 Modeling Single-Stage System

The single-stage system comprises the four main components of a refrigeration system, 1) compressor, 2) condenser, 3) evaporator, and 4) expansion device, as shown in Figure 1.2 in Chapter 1.

3.5.1 Ideal Single-Stage System

The equations given in Section 1.1.1.2 are applied to the EES software. The system is designed to deliver 5.86 kW of heating at an ambient of 8.3 °C. The system performance in terms of heating capacity, cooling capacity, and coefficient of performance in both heating and cooling modes of operation. The results are shown at various outdoor temperatures and for multiple refrigerants.

3.5.2 Practical Single-Stage System

As explained earlier, a more practical system will consider the actual performance of the compressor based on the manufacturer's published performance values. In addition to that, the following is considered:

- Refrigerant pressure-drop across vapor pipelines is 1 °C.
- Refrigerant pressure-drop across the liquid line is 1 °C.
- All pipelines are well insulated, and the heat loss or gain across them is neglected.

The above assumptions are based on the ASHRAE guidelines for pipeline designs, so it is expected that any properly designed system will be within these values. The pressure-drop value is given in terms of the drop in saturation temperature corresponding to the evaporator or condenser saturation pressure [20].

This researcher could not find a compressor that can cover the whole range of saturation suction temperature from -50 °C to +20 °C from the so-called air-conditioning or heat pump compressors. Compressors designated for residential air conditioning applications are limited to a minimum of -23.3 °C saturated suction temperature. However, other compressor families designed for deep freezing applications only cover saturated suction temperatures from -40 °C to -12 C, which still falls short of the required. All these compressors do not work with R410A; instead, they can run with refrigerants designed specifically for low-temperature applications like R404A, and R507. Therefore, ZP24K6E-PFV was selected from Copeland, a Scroll compressor that represents an air-conditioning and heat pump family of compressors that run with R410A refrigerant.

3.6 Modeling 2-Stage Vapor- injection System with Sub-cooler

In this system, as shown in Figure 3.2, part of the liquid refrigerant exiting the condenser is flashed through an expansion device and then exchanged heat with the discharge of the first stage compressor to cool it down to a saturated-vapor state before it enters the second stage compressor [23].

The thermodynamic calculations for this system are as follows:

$$\dot{Q_H} = \dot{m} \cdot (h_2 - h_3) \tag{3.10}$$

$$\dot{W_{Hp}} = \dot{m} \cdot (h_2 - h_{1'}) \tag{3.11}$$

$$\dot{W}_{Lp} = (\dot{m} - \dot{m}_{inj}) \cdot (h_{2'} - h_1) \tag{3.12}$$

$$\dot{m}_{inj} \cdot (h_{1''} - h_{4'}) = (\dot{m} - \dot{m}_{inj}) \cdot (h_3 - h_{3'}) \tag{3.13}$$

$$\dot{m}_{inj} \cdot h_{1''} + \left(\dot{m} - \dot{m}_{inj}\right) \cdot h_{2'} = \dot{m} \cdot h_{1'} \tag{3.14}$$

$$COP = \frac{\dot{Q}_H}{\dot{W}_{Hp} + \dot{W}_{Lp}} \tag{3.15}$$

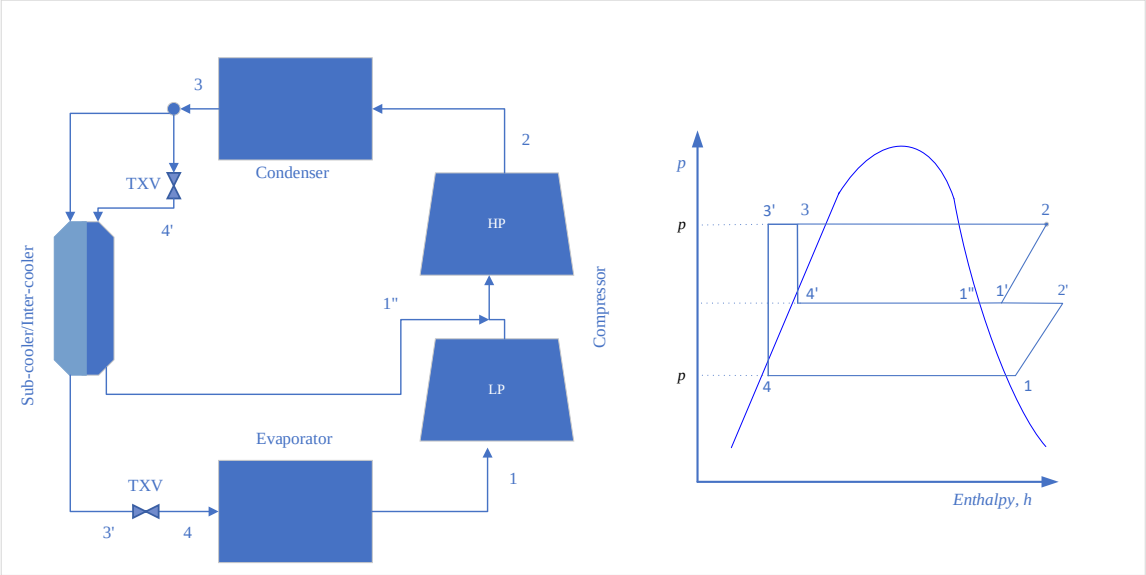

Figure 3.2: Two stage system with vapor injection and sub-cooler.

3.7 Modeling Cascade System

The cascade system comprises two vapor refrigeration systems with an intermediate heat exchanger. Figure 1.6 shows the system design and the corresponding T-s diagram, and the concept has been explained in Sections 1.1.3 and 2.4.2. One of the most important parameters when designing such a system is the selection of the intermediate pressure. The theoretical optimum intermediate pressure for a single refrigerant system is considered the geometric mean of the high and low pressures of the system [81]. Many empirical studies have been published that address this topic, and depending on the application and the refrigerants used, the optimum intermediate pressure could be found [112].

A study by Park et al. [112] established an empirical formula for the optimum intermediate pressure for an R134a/R410A cascade system. For this analysis, the intermediate pressure will be selected as per the minimum condensing temperatures allowed by the compressor manufacturer. The lower condensing temperatures, below the traditional 21 °C, have high benefits for system performance and for the long-term reliability of the compressor [24].

By standardizing the intermediate pressure, a valid comparison can be conducted. However, optimizing the intermediate pressure is outside of the scope of this thesis.

The temperature difference between the fluids at the intermediate heat exchanger will be selected between 2.5 °C to 5 °C. Previous studies showed that this is acceptable from a design from an economic standpoint [80].

To model the system, the compressors were selected from Copeland, one of the most prominent compressor manufacturers in the industry. Their compressors are the basis for so many air conditioner manufacturers across North America and around the globe. Air conditioner and heat pump manufacturers like Goodman and York, among many, utilize Copeland's compressors for their products [95], [37]. This compressor family is identified as ZP**K6E-PFV where the ** is a two-digit number that represents the capacity of the compressor in terms of volume flowrate. The operating range is between -23.3 °C [-10 °F] and 12.78 °C [55 °F] for the saturated suction temperature and 26.67 °C [80 °F] to 62.78 °C [145 °F] for the saturated discharge temperature [21]. Therefore, the ZP**K6E-PFV family of compressors can only work as the high-pressure one and cannot satisfy the operating conditions of the low-pressure compressor. Therefore, a different family of compressors designed for freezing applications, ZF series of compressors, will be employed. This family of compressors can operate down to -40 °C saturated suction temperature and up to 7 °C, and at lower saturation discharge temperatures as -10 °C they can operate safely [113].

The compressors will be sized so that the heat rejected from the low-pressure system condenser meets the heat absorbed by the high-pressure system evaporator at the design conditions and the initial intermediate temperature selection as described earlier. The intermediate operating pressure will then be determined based on the heat rejection/heat absorption balance. Applying this concept, and with the aid of the manufacturer selection software, compressors can be selected to establish the system design constants [114].

The compressor coefficients of all the compressors used in this study can be found in Appendix B.

By applying Equation 3.15 to the values of Table 3.1, the heating COP of this system is 2.42.

Running the equations for the system on EES, the performance of the system along the various outdoor temperatures can be modeled. The concept of maintaining a constant temperature difference across the heat exchangers that were addressed in Section 3.1 is applied.

Table 3.3: Cascade system compressor selection & operating parameters at design conditions.

	Low-pressure system	High-pressure system
Compressor Model	ZF15K4E-TF5	ZP24K6E-PFV
Refrigerant	404A	410A
Min. Cond. (°C)	15.0	26.7
Max. Cond. (°C)	140.0	62.8
Min. Evap. (°C)	-40.0	-23.3
Max. Evap. (°C)	45.0	12.8
Saturated suction Temperature, °C	-40.0	-2.5
Saturated discharge temperature, °C	2.5	31.7
Condenser heat rejection, W	6,354.0	7,671.0
Evaporator heat absorption, W	4,750.0	6,190.0
Power absorbed by the compressor, W	1,765.0	1,400.0

Another approach will be tried as well. The speed of the low-pressure compressor will be controlled to match the heat rejection of the low-pressure system to the demand of the evaporator of the high-pressure system. This will bring a more practical intermediate pressure. An intermediate pressure representing the arithmetic mean of the outdoor and indoor temperatures will be used. As mentioned earlier, the optimum intermediate pressure is outside the scope of this thesis.

As a result, two assumptions will be applied for the compressor operates at a given condition:

1) The refrigerant mass flow rate is directly proportional to the compressor rotational speed. The compressor rotational speed can be controlled with a variable frequency drive, as described earlier.
2) The compressor's isentropic efficiency is constant at all rotational speeds.

The manufacturer of the compressor, Copeland, allows for the above assumptions for a range of motor rotation speed between as low as 40% of the full speed [22].

3.8 System Seasonal Performance

In calculating the seasonal coefficient of performance (SCOP), the bin method for modeling energy usage explained in the ASHRAE Fundamentals Handbook will be used. Grouping the temperatures into 2 °C bins and using the medium bin temperature as a basis to calculate the equipment performance and then multiplying by the hourly duration of this temperature bin usually yields acceptable results [38]. This is the same method adopted by the DOE and the AHRI standard 210/240 used for rating the seasonal performance of residential air conditioners and heat pumps.

The building's heating load can be modeled in so many ways. Many Simulation software applications are available for complex calculations that can estimate the energy usage of buildings based on various modes of operation. The US Department of Energy has an open-source building energy modeling software [115]. However, for the purpose of this research, the simplest way that models the building heating load as directly proportional to the outdoor temperature is applied. Two points of operation are established to define the equation or the slope & interception of the straight line. The first one is at the outdoor design temperature, and the second one is the point of balance where heat gain equals heat loss, and there is no heat energy required to maintain the indoor temperature. See Figure 3.3. This is the same approach taken by ASHRAE standard 116 and AHRI 210/240 and the US DOE in calculating the seasonal performance of heating and cooling equipment [94], [9], [116].

$$BL = a_1 t_{OD} + b_1 \tag{3.16}$$

$$where, a_1 = \frac{BL(t_{OD,design})}{\left(t_{OD,design} - t_{OD,balance}\right)} \tag{3.17}$$

$$and, b_1 = \frac{t_{OD,balance} \cdot BL(t_{OD,design})}{(t_{OD,balance} - t_{OD,design})} \quad (3.18)$$

BL = Building load, t_{OD} = Outdoor dry-bulb temperature,

Heating hours (HH) for each temperature bin for a given location can be calculated from the fractional bin hours $(\frac{n_j}{N})$ and the total heating hours (HLH) as follows:

$$HH = \frac{n_j}{N} HLH \quad (3.19)$$

Normally, there will be an auxiliary source of heat, like a furnace or an electric heater element. As with the proposed system, it can run for the whole heating season. Therefore, there will be no auxiliary heat. The heat pump capacity will be sized to match the building load at minimum outdoor temperature. The capacity and COP of the heat pump at each outdoor bin temperature can be obtained directly from the modeled values.

The total system capacity at each bin temperature for a given location is obtained by adding the heat pump capacity plus the auxiliary heat capacity. The auxiliary heat will be substituted for by zero in the proposed system. At the same time, the heat pump will be running only within its operating range.

$$Q_t = Q_{HP} + Q_{aux} \quad (3.20)$$

Q_t= total energy, Q_{HP}= heat pump energy, Q_{aux}= auxiliary heat energy

System run time (τ) at each bin temperature for a given location can be calculated as follows:

$$\tau = \frac{HH \times BL}{Q_t} \quad (3.21)$$

Then heat energy can be calculated,

$$H = Q_t \times \tau \quad (3.22)$$

Power input to the heat pump at a steady state can be calculated as follow:

$$P'_{HP} = \frac{Q_{HP}}{COP_{HP}} \quad (3.23)$$

Equation 3.28 calculates the power input to the heat pump while running in a steady state. It does not consider the ramp-up time when the unit starts and stops. AHRI 210/240 standard establishes a method to account for the part load in terms of a partial load factor (PLF) which will be applied here.

$$PLF = \frac{P'_{HP}}{P_{HP}} \tag{3.24}$$

And,

$$PLF = 1 - C_D\left(1 - \frac{BL}{Q_{HP}}\right) \; for \; Q_{HP} > BL, else \; PLF = 1 \tag{3.25}$$

Where the degradation coefficient C_D is given a default empirical value of 0.25 as per the same standard.

Then the total power input is the sum of the heat pump power input plus the power input of the auxiliary heat, which again will be zero in the proposed system.

$$P = P_{HP} + P_{aux} \tag{3.26}$$

P =total power, P_{HP}= heat pump power, P_{aux}= auxiliary power

Therefore, the total energy input can be calculated.

$$E = P \times \tau \tag{3.27}$$

Eventually, the seasonal coefficient of performance ($SCOP$) can be calculated as the ratio between the sum of heat energy for each temperature bin to the energy input for each temperature bin.

$$SCOP = \frac{\sum_{j=1}^{n} H(t_j)}{\sum_{j=1}^{n} E(t_j)} \tag{3.28}$$

Calculations for SCOP for the modeled systems as applied to northern Canadian cities can be found in Appendix D.

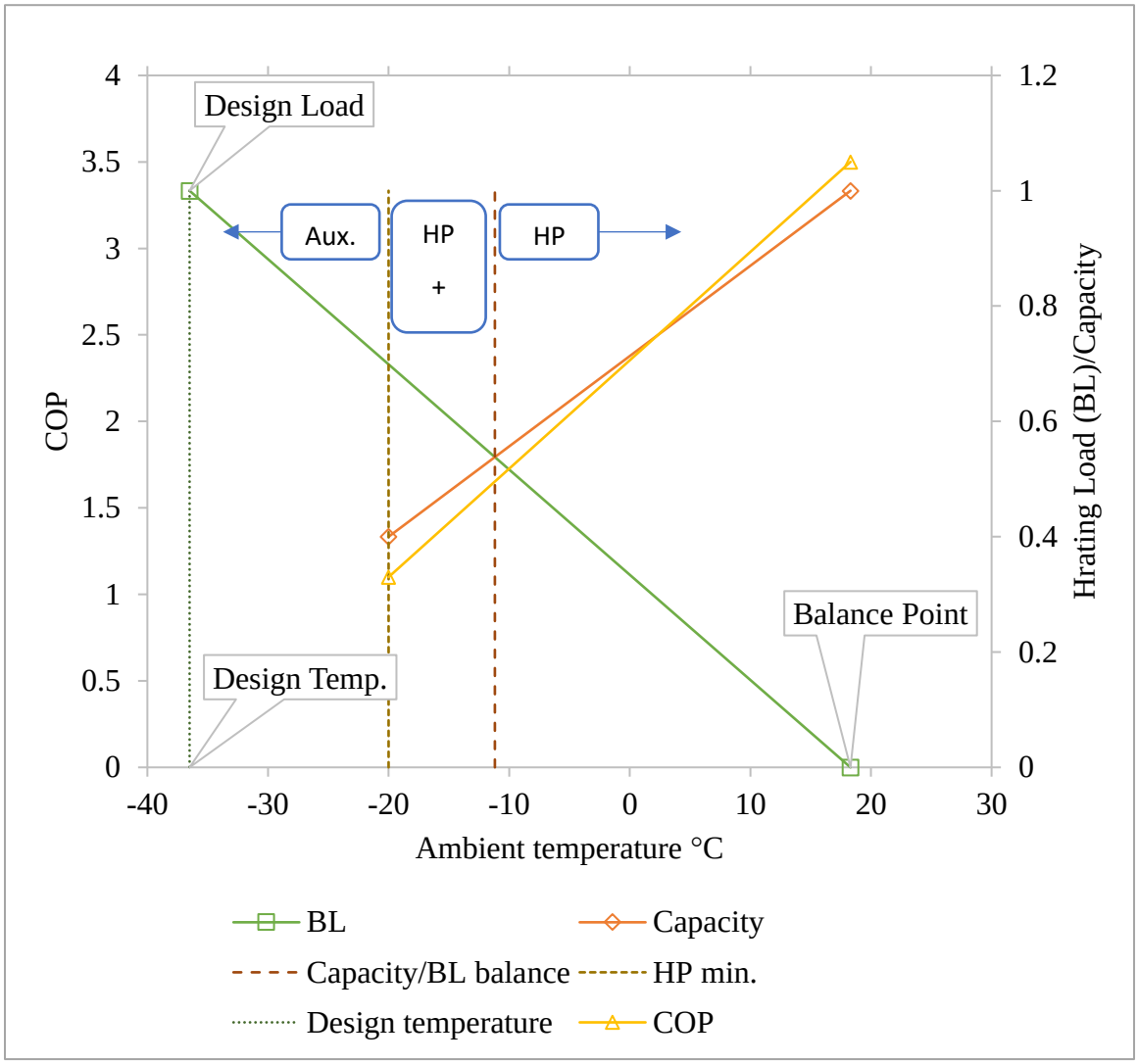

Figure 3.3: Building heating load (BL), capacity and COP at various outdoor temperatures showing ranges of operation of HP only, HP + auxiliary heat and auxiliary heat only.

3.9 Proposed System Design

The system utilizes a 4-way reversing valve, two 3-way valves, and a solenoid valve to control the flow of refrigerant so that the system can operate in the desired mode of operation. Figure 3.4 is a schematic of the system, while Table 3.4 illustrates the state of each valve during each mode of operation.

The low-pressure compressor is a variable speed one that is controlled by a variable frequency drive that controls its rotational speed, and thus its capacity depending on the

outdoor temperature and the heat capacity demand of the intermediate heat exchanger. The flow of this compressor is controlled via expansion valves that maintain constant superheat.

i. Cooling mode.

The 4-way reversing valve is energized. The flow of the hot gas coming out of the high-pressure compressor is directed to the outdoor heat exchanger that acts as a condenser, and the heat energy is rejected to the atmosphere. The two 3-way valves are de-energized so that the condensed liquid refrigerant coming out of the outdoor heat exchanger is directed towards the expansion device and the indoor heat exchanger that acts as an evaporator. After evaporation, the vapor refrigerant is directed back to the suction port of the high-pressure compressor. In this mode of operation, the low-pressure system components stay idle. Figure 3.5.

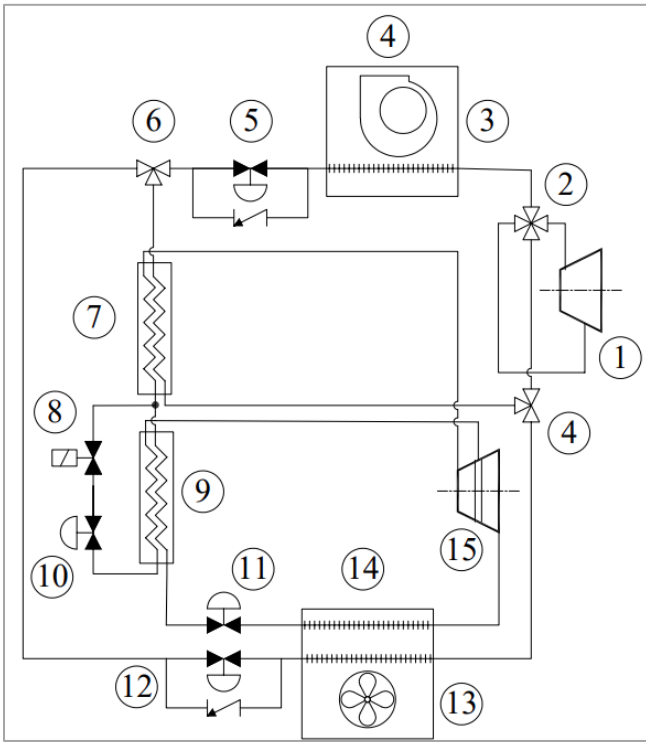

Item	Description
1	High-pressure compressor
2	4-way reversing valve
3	Indoor heat exchanger
4	Indoor air blower
5, 11	Expansion valve with built-in check valve
6,4	6 3-way valve
7	Intermediate heat exchanger
8	Vapor injection solenoid valve
9	De-superheater/Sub-cooler heat exchanger
10	Vapor injection expansion valve
11	Expansion valve
13	Outdoor heat exchanger
14	Outdoor heat exchhanger fan

Figure 3.4: Proposed system schematic.

Table 3.4: Status of system components for each mode of operation.

	Compressor, Lop-p	Compressor, High-p	Reversing valve	3-Way valve 1	3-Way valve 2	Injection solenoid valve	Outdoor Min (°C)	Outdoor Max (°C)
Cooling mode	○	●	●	○	○	○	20	45
Heating mode 1	○	●	○	○	○	○	-5	20
Heating mode 2	●	●	○	●	●	○	-30	-5
Heating mode 3	●	●	○	●	●	●	-50	-30
Defrost mode	○	●		○	○	○	-50	20

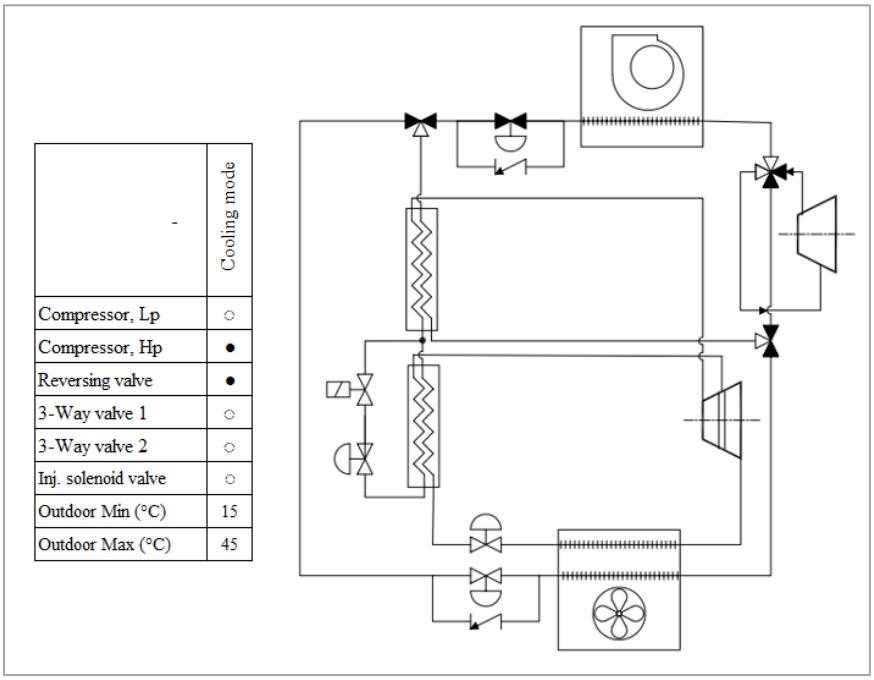

Figure 3.5: System in cooling mode.

ii. Heating mode 1, single-stage.

The 4-way reversing valve is de-energized. The flow of the refrigerant discharged from the high-pressure compressor goes to the indoor heat exchanger to reject heat energy to the

heating space. The condensed liquid coming out of the indoor heat exchanger is directed to the expansion device and the first bank of tubes of the outdoor heat exchanger. Then, the vapor refrigerant makes its way to the suction port of the high-pressure compressor. Like the cooling mode, the low-pressure system components are kept off.

iii. Heating mode 2, cascade with no vapor injection.

Like heating mode 1, the 4-way reversing valve is de-energized to direct the flow of the hot gas discharged from the high-pressure compressor towards the indoor heat exchanger. The two 3-way valves are energized, so the liquid flow from the outdoor heat exchanger goes to the expansion device and intermediate heat exchanger, then to the suction port of the high-pressure compressor. The Low-pressure compressor is running to circulate the low-pressure cycle refrigerant to the intermediate heat exchanger, where it rejects heat energy to the high-pressure cycle refrigerant. The low-pressure cycle liquid refrigerant coming out of the intermediate heat exchanger flows to the expansion device and the second back of tubes of the outdoor heat exchanger. The vapor refrigerant coming out of the outdoor heat exchanger then goes to the suction port of the low-pressure heat exchanger. The injection solenoid valve is de-energized.

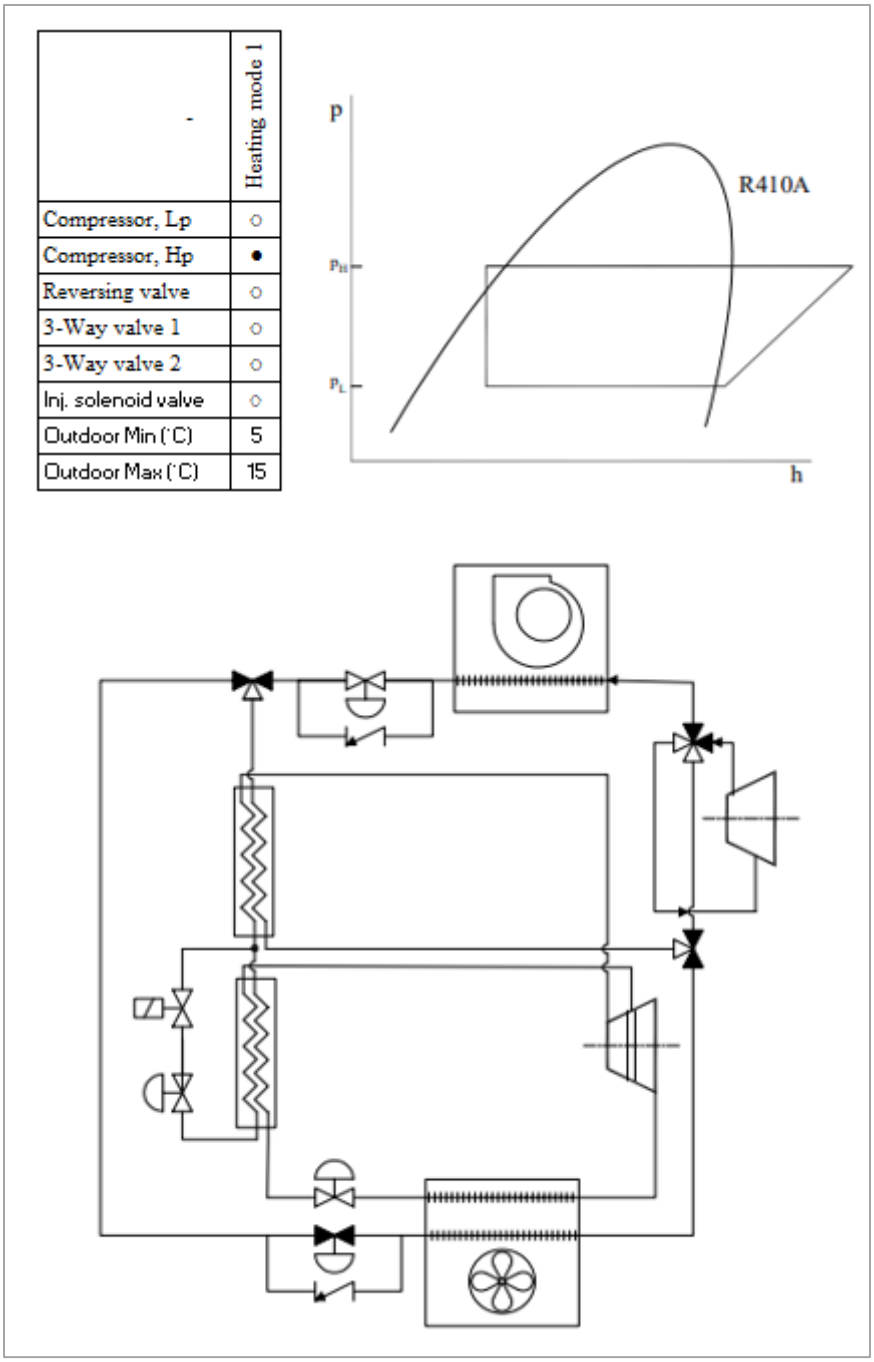

Figure 3.6: System in heating mode 1.

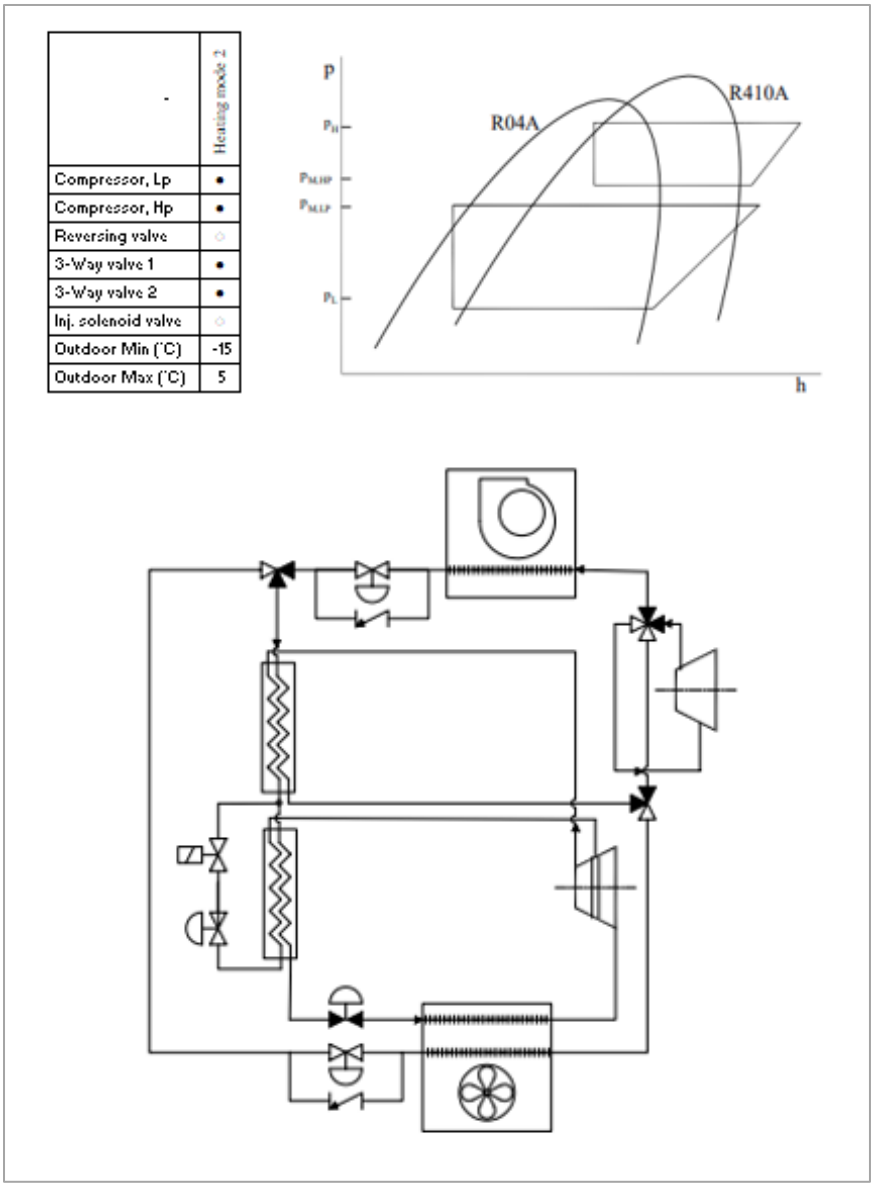

Figure 3.7: System in heating mode 2.

iv. Heating mode 3, cascade with 2-stage vapor injection and sub-cooler.

In this mode, the system runs like heating mode 2, but the injection solenoid valve is energized to provide vapor injection and liquid subcooling, as explained earlier in section 2.4.1.

i. Defrost mode.

The system runs like the cooling mode, just to provide heat to the outdoor heat exchanger to defrost it. In this case, the indoor coil will be running as the evaporator, so there are no

worries about low ambient temperatures influencing the evaporator pressure/temperature. The outdoor heat exchanger will act as the condenser and reject heat to the cold atmosphere. That is why in this mode, the system can run safely at any outdoor temperature.

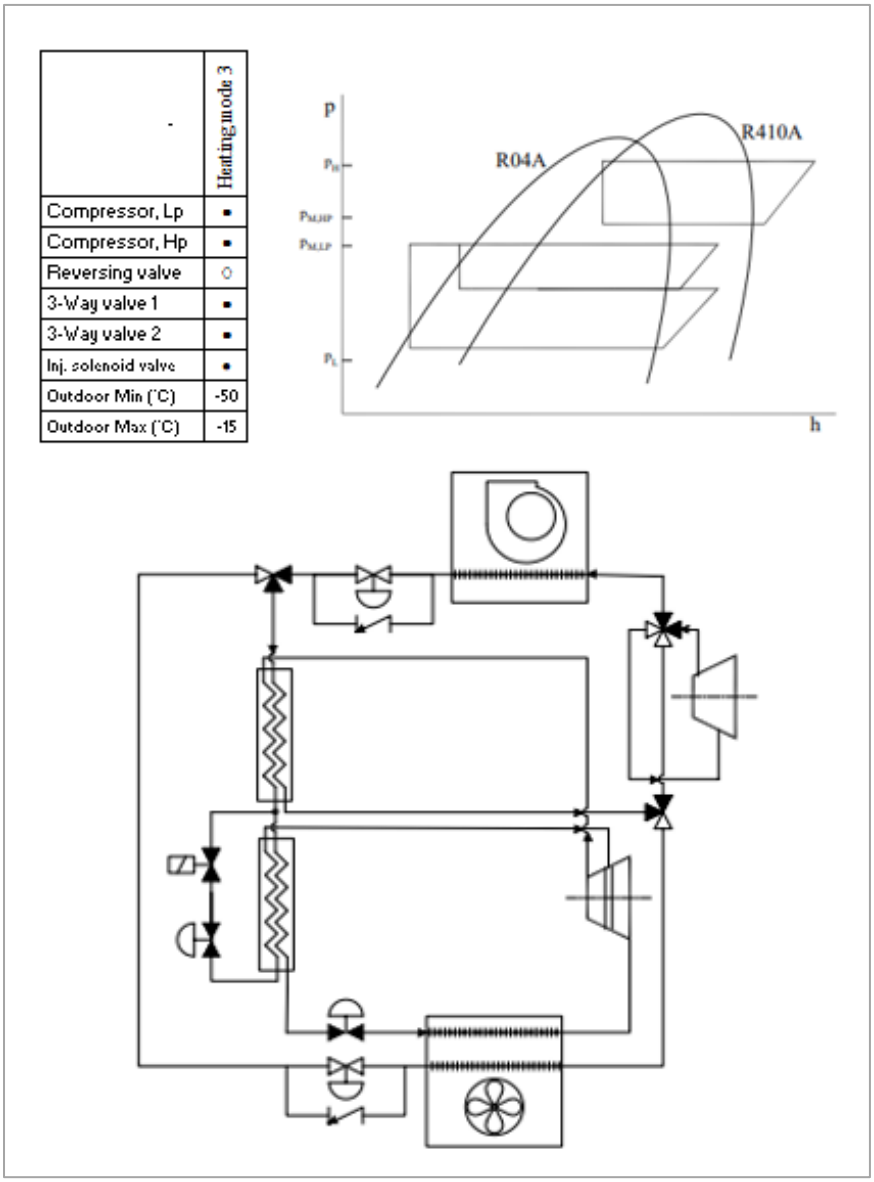

Figure 3.8: System in heating mode 3.

Chapter 4. Results and Discussion

This chapter provides discussions of the results obtained from the analysis. The EES software was used for the system modeling. The calculation tables for the SCOP can also be found in Appendix C.

4.1 Single-stage System

4.1.1 Ideal Single-Stage System performance

Figures 4-1 and 4-2 show the performance of an ideal single-stage system in both heating and cooling modes, respectively. It is clear that both the heating capacity and coefficient of performance decrease as the ambient temperature decreases. As discussed earlier in Sections 1.1.2 and 1.1.3, both volumetric efficiency and isentropic efficiency decline with the higher-pressure ratios. Therefore, it is expected that with lower ambient temperature, the system's overall efficiency declines. Also, with lower ambient temperature, the evaporation process occurs at lower pressure resulting in a decline in the refrigerant density at the compressor suction port. Accordingly, the refrigerant mass flowrate decreases, and thus the heating capacity.

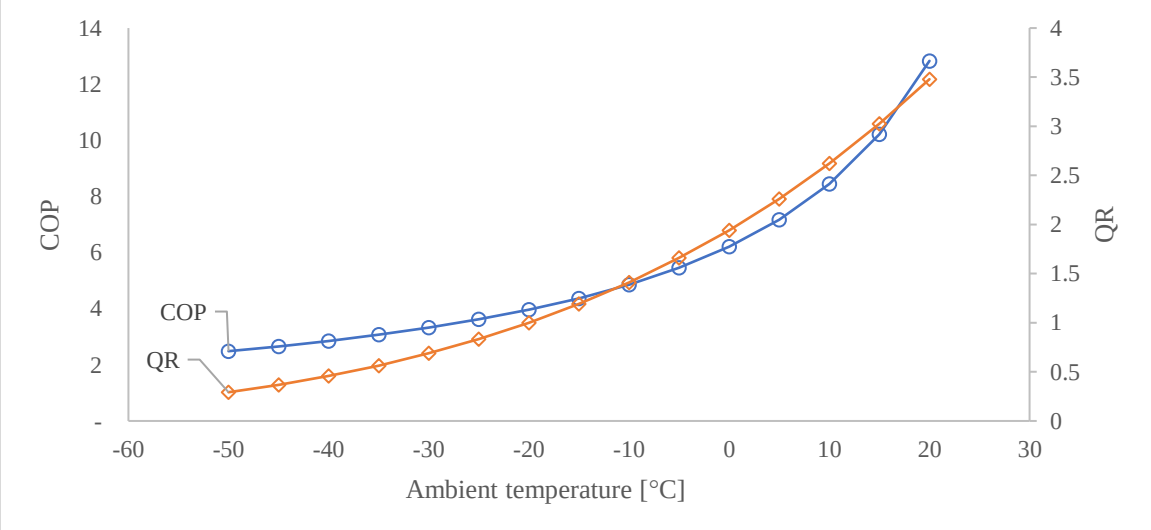

Figure 4.1: Heating coefficient of performance (COP) and heating capacity ratio (Q/QR) for an ideal single-stage heat pump system in heating mode.

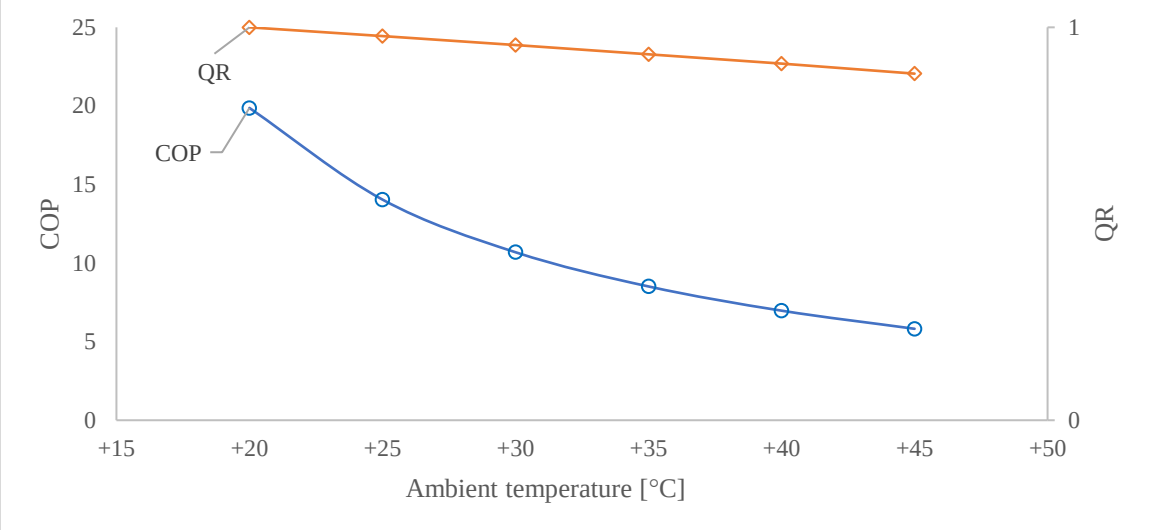

Figure 4.2: Cooling coefficient of performance (COP) and cooling capacity ratio (Q/QR) for an ideal heat pump system in cooling mode.

Furthermore, the modeling did not show changes in trends when using different refrigerants. The trend was the same for R410A, which is the main player in the residential air conditioning industry, R32, R454B, which are the most promising low GWP (Global Warming Potential) candidates to replace R410A [117], [118]. Obviously, as both R32 and R-454B are developed to replace R-410A, they have similar physical properties to R-410A. Only they have lower GWP. Therefore, in this study, just one refrigerant will be studied, and it would be expected that alternative refrigerants will follow suit.

4.1.2 Practical Single-Stage System performance

Figure 4.3 shows the performance of a practical single-stage system. The trend of both the COP and heating capacity follows the ideal cycle. However, the rate of decline of COP values is higher at lower temperatures. Again, this is explained by the decrease in isentropic and volumetric efficiencies as the compression ratio increases. The line labeled Min in the Figure is the minimum operating limit of this compressor.

It is also seen in Figure 4.4 that the compressor isentropic efficiency decline rate increase with lower ambient temperatures. As the discharge pressure is kept constant, the main factor here is the compression ratio. These results are consistent with what was presented in Sections 1.1.2 and 1.1.3. Cuevas and Lebrun conducted a study for testing and modeling

a variable speed scroll compressor. Their research has come to the same conclusion, and a similar plot to Figure 4.4 is shown in their published paper [104].

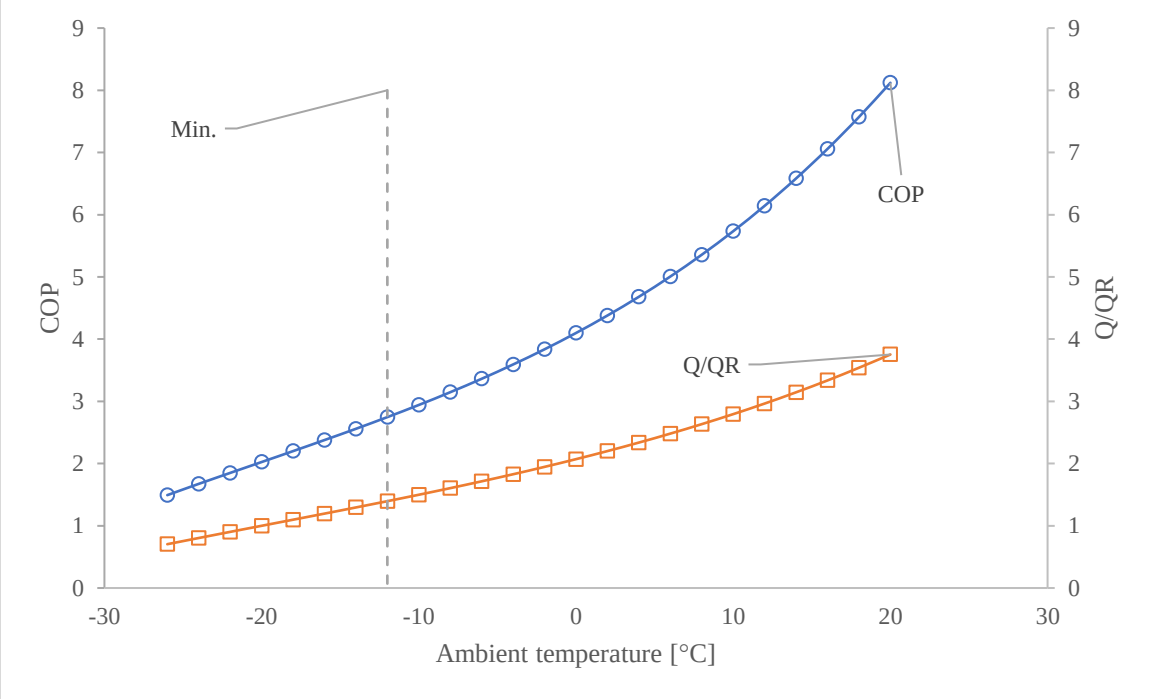

Figure 4.3: Actual single-stage heat pump system performance with minimum operating ambient temperature. Left vertical axis is the coefficient performance (COP), and the right vertical axis is the heating capacity (Q/QR). Vertical dash line (Min) is the minimum compressor working temperature.

In cooling mode, it can be seen that the system performance still follows the ideal pattern, with a drop to almost half, as shown in Figure 4.5. That is expected as in the actual system, the system losses as well as the compressor efficiency, are accounted for.

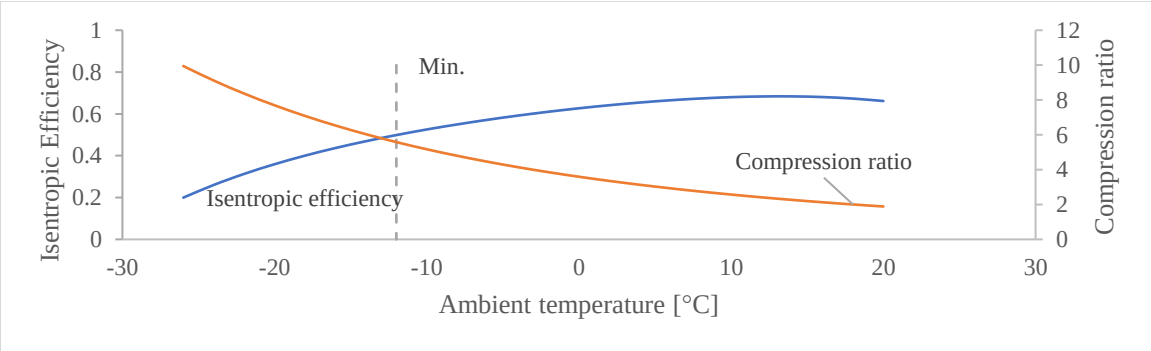

Figure 4.4: Compressor isentropic efficiency and compression ratio at different ambient temperatures and the minimum operating temperature of the compressor.

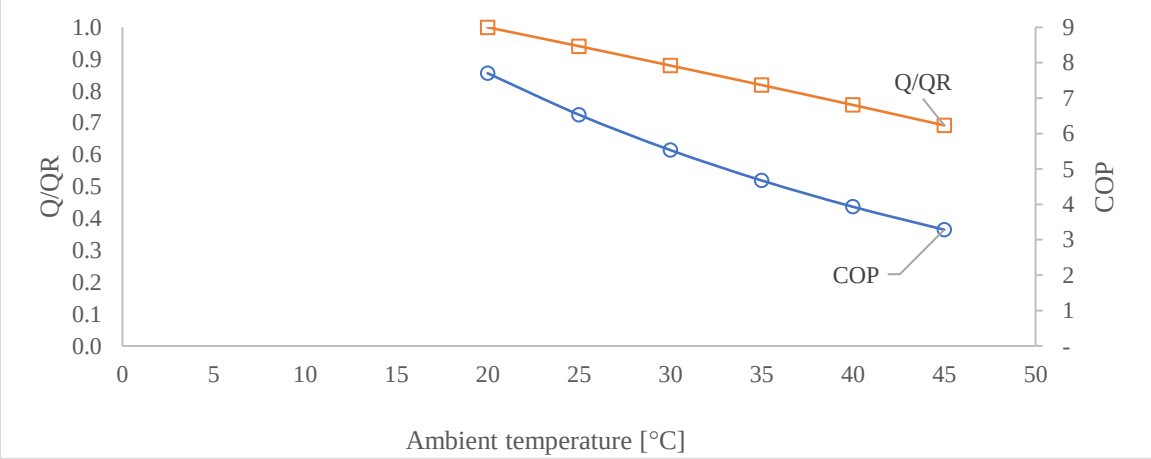

Figure 4.5: Actual heat pump system performance in cooling mode.

To validate the simulation method, simulated values are compared to a laboratory tested unit that employs the same simulated compressors. The comparison is made for two operating points as can be found in the table below.

Table 4.1: Comparison between simulation and laboratory results for a heat that employed the same compressor, as the one simulated in this study.

Operating parameter	Unit	Point 1	Point 2
Outdoor temperature	°C	8.33	-8.33
Indoor temperature	°C	21.11	21.11
Saturated suction temperature	°C	0.82	-13.86
Saturated discharge temperature	°C	36.44	31.89
Compressor superheat	°C	8.97	9.33
Condenser sub-cool	°C	5.00	5.71
Measured heat capacity	W	7844.87	5124.52
Measured compressor power	W	1559.40	1465.60
Measured COP		5.03	3.50
Simulated heat capacity	W	8400.00	5496.00
Simulated compressor power	W	1601.00	1508.00
Simulated COP		5.25	3.64

4.2 Two-Stage Vapor-Injection with Sub-Cooler System Performance

Figure 4.6 is the performance curve for the two-stage vapor-injection system with a sub-cooler, where both the COP and the heating capacity are plotted against the ambient temperature.

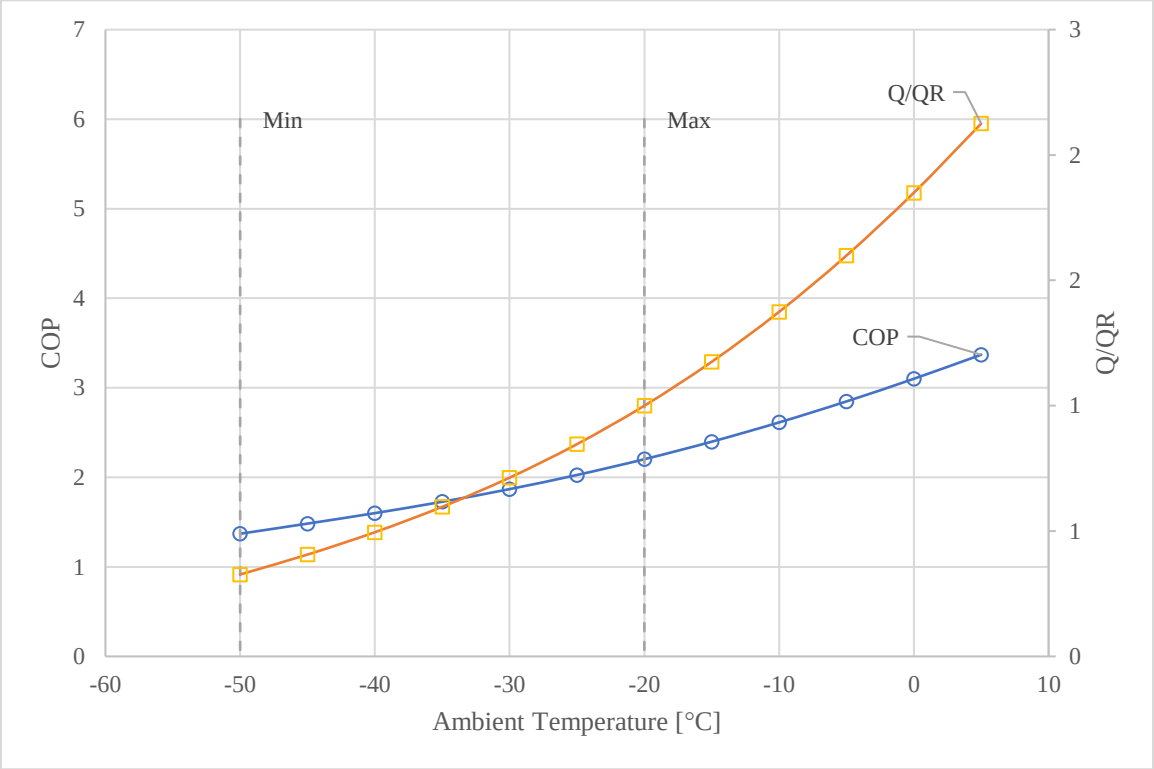

Figure 4.6: Performance curves for a two-stage vapor-injection system with a sub-cooler. Vertical dash lines represent the minimum and maximum operating limits.

The shortcoming of this kind of system is that it is designed for deep freezer applications only. Its operating range, as recommended by the compressor manufacturers, is in the range of -70 °C to -20 °C saturated suction temperatures. Its operation is also limited to a handful of refrigerants that are designated only for low temperature applications like R404A and R507 [23]. As seen in Figure 4.6, the maximum operating ambient temperature is -20 °C. Therefore, the cooling conditions in the summertime are totally outside the operating range of this compressor. That is why the cooling performance was not studied here, only the heating performance was analyzed.

4.3 Cascade System Performance

4.3.1 Cascade System with Fixed Speed Compressors

The performance curves of the cascade system with fixed speed compressors are shown in Figure 4.7.

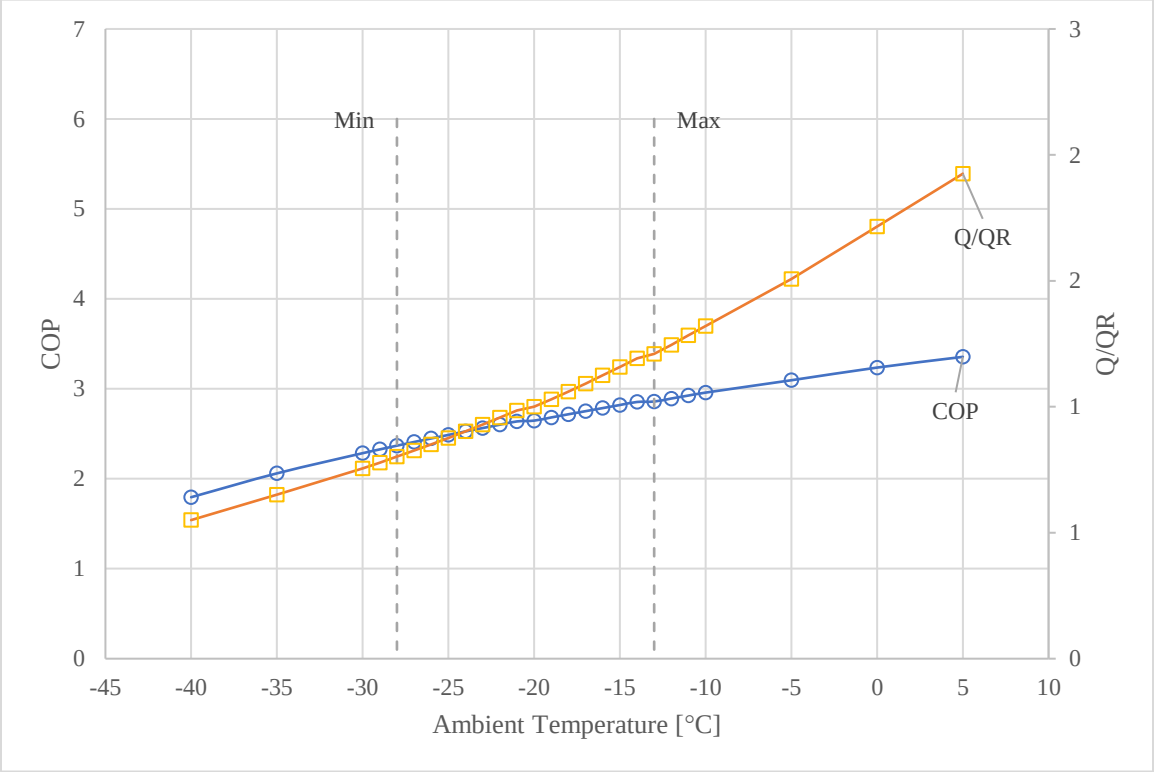

Figure 4.7: Performance curves of a cascade system with fixed speed compressors. Vertical dash lines represent the minimum and maximum operating limits.

It was noticed that the intermediate pressure kept increasing as the ambient temperature increased. Eventually, the maximum operating range got limited to just about -14 °C. As stated earlier, this is not good for summer cooling. To overcome this problem, the other approach of a variable speed low-pressure compressor is applied and discussed in the next section.

4.3.2 Cascade System with Variable Speed Low-Pressure Compressor

Figure 4.8 shows the performance of the cascade system with variable speed low-pressure compressor. It can be seen that the limiting maximum temperature mentioned in Figure 4.7 does not exist here. The system could operate to as high as 5 °C ambient temperature.

Comparing the COP in Figure 4.8 with that in Figure 4.7, it can be observed that there is a slight improvement in favor of the variable speed system. However, most importantly, the Max operating limit has been removed, and the system can run at ambient temperatures as high as 5 °C.

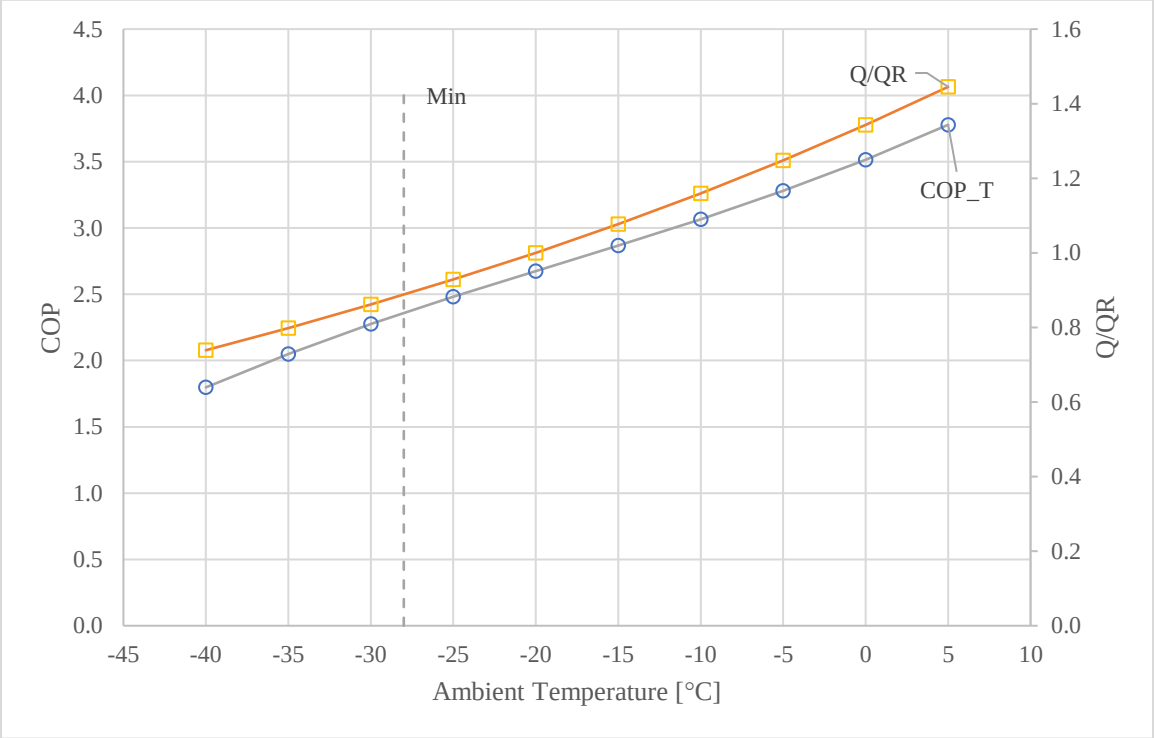

Figure 4.8: Performance curves for cascade system with variable speed low-pressure compressor. Vertical dash line is the minimum operating ambient temperature.

The variable speed operation of the compressor is limited by the manufacturer to 40% to 120% of its rated speed. These criteria have been examined and presented in Figure 4.9, and the compressor is safely within the manufacturer approved range of operation.

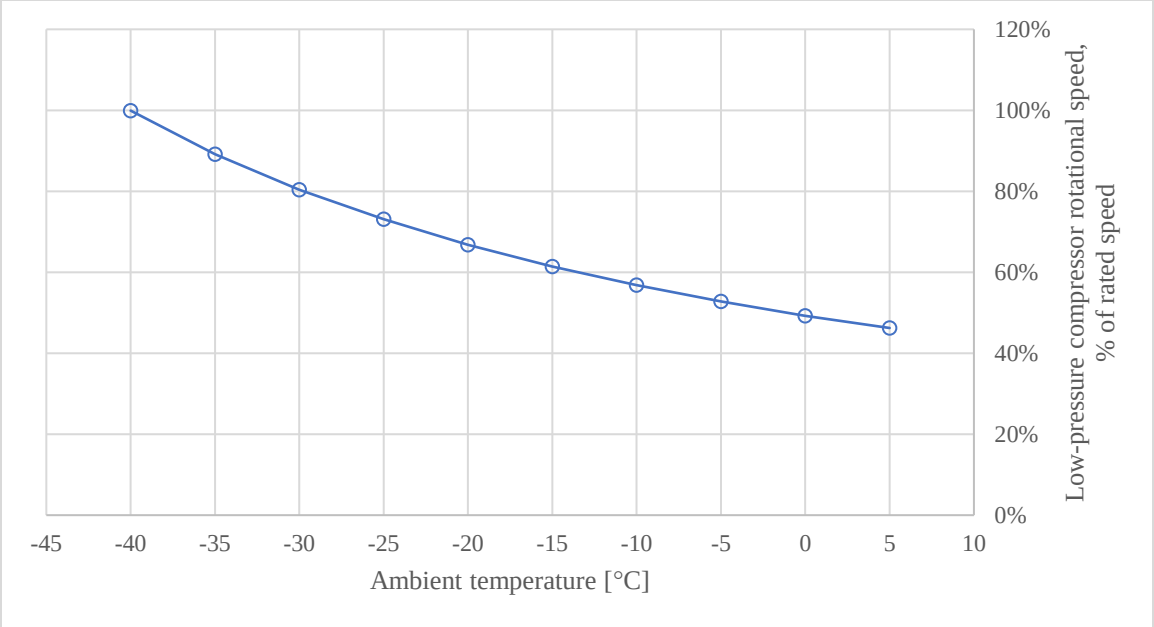

Figure 4.9: Rotation speed of the low-pressure compressor of the cascade system as a percentage of its rated speed at various outdoor temperatures.

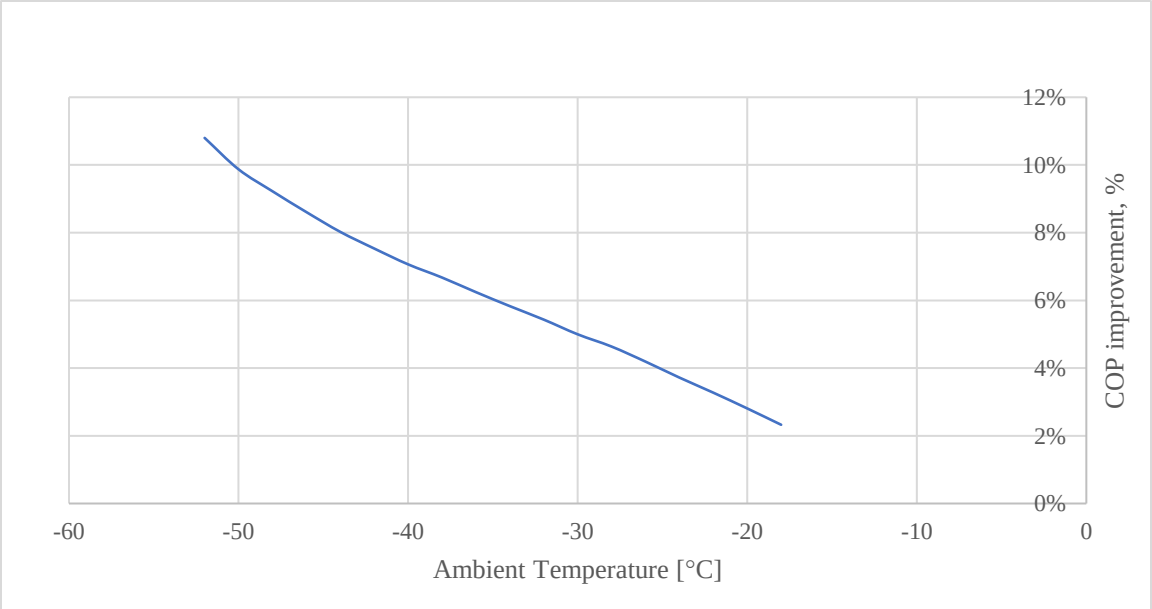

Figure 4.10: Percent improvement in COP value of the cascade with vapor injection and sub-cooler system is used instead of the vapor-injection with sub-cooler system.

4.4 Summary of Systems Modeling Results

The thermodynamic analysis conducted has shed light on each system's applicable operational ranges and the performance within these ranges. It showed that there is no

single system that can offer the best solution for the wide outdoor temperature range targeted. That is why it was concluded that such a system must utilize each and all of these techniques in a multi-mode operation manner that can adapt to the performance based on the outdoor temperature.

The observation from the comparison in Figure 4.11 can be summarized as follows:

- For the temperature range from -52 °C to -30 °C, the cascade with the 2-stage vapor injection and sub-cooler system and the 2-stage vapor injection and sub-cooler system (without a cascade) are the only options available. There is only a slight difference in their performances. Figure 4.10 shows the percent increase in COP if the cascade with vapor injection and sub-cooler system is used rather than the vapor-injection with sub-cooler system. The COP is better by around 3% to 11%, depending on the ambient temperature. The improvement is greater at lower ambient temperatures.
- For the temperature range from -28 °C to -6 °C, the cascade mode provides the highest COP.
- Also, for the temperature range from -4 °C to 20 °C, the single-stage mode outperforms all other options and becomes the only choice.

For the cooling mode, the single-stage mode is always better, but this study does not focus on the cooling operation mode.

Likewise, the heating capacity for the different modeled systems is shown in Figure 4.12.

The modeling of the various systems showed that there is no single compressor that can handle the wide range of target ambient temperatures. In fact, all manufactured compressors are designed for a definite application, freezers, refrigerators, air-conditioners, etc. The operating range for each application can be found in Table 3.2. From a practical standpoint, and by scanning all manufacturers in the market, there is no compressor that can operate from -60 °C suction temperature to +20 °C that will be required for a cold climate application location like Whitehorse, YT, which was mentioned earlier.

Similarly, refrigerants are designed to operate by targeting one or more applications. R4040A for freezing applications, R410A for air conditioning applications, R134a can go

to higher saturated discharge pressure, and R717 is suitable for ultra-low temperatures. That is why if the system can utilize two or more refrigerants for each outdoor temperature segment, it is expected to: 1) improve overall performance and 2) reach higher temperatures that might not be attainable with a single refrigerant.

Therefore, to handle this wide range of outdoor temperatures, the system must utilize a multi-compressor, multi-refrigerant, and multi-mode operation design. It must switch modes of operation depending on the ambient temperature so each compressor can run within its manufacturer's operation limits and with the better refrigerant that would optimize performance.

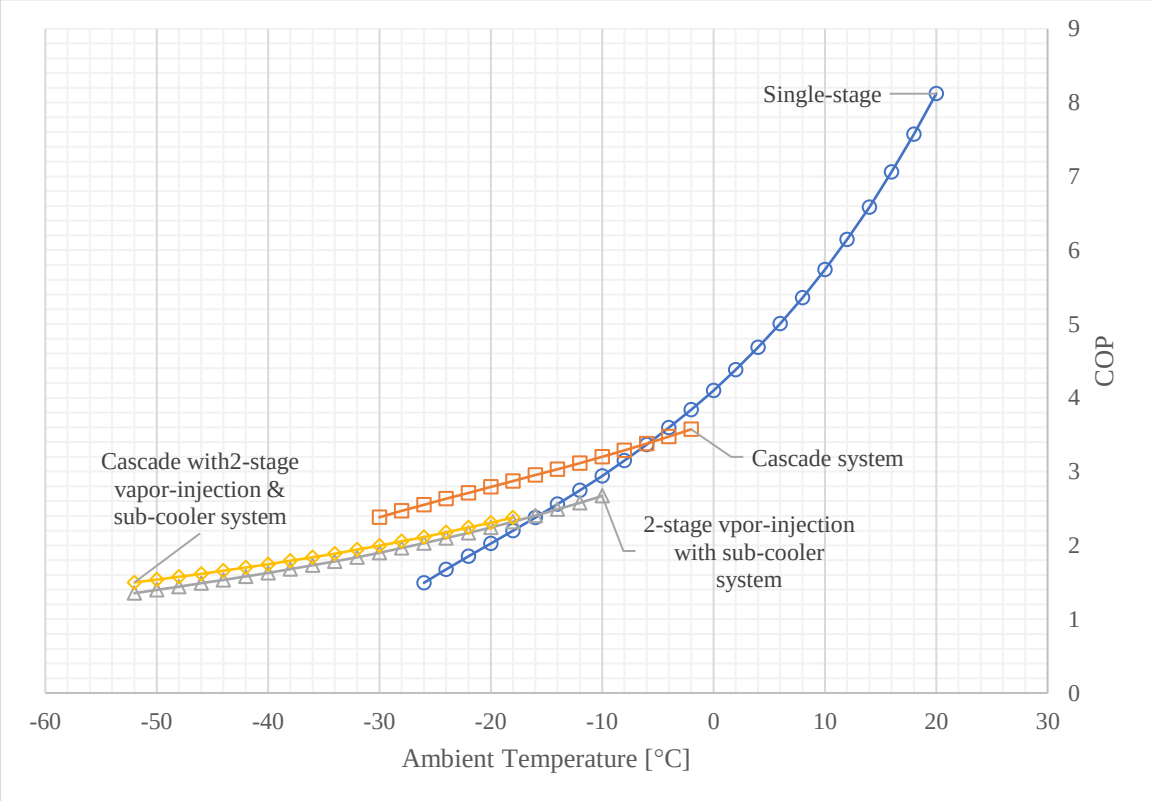

Figure 4.11: Performance comparison of COP of the different systems with the ambient temperature.

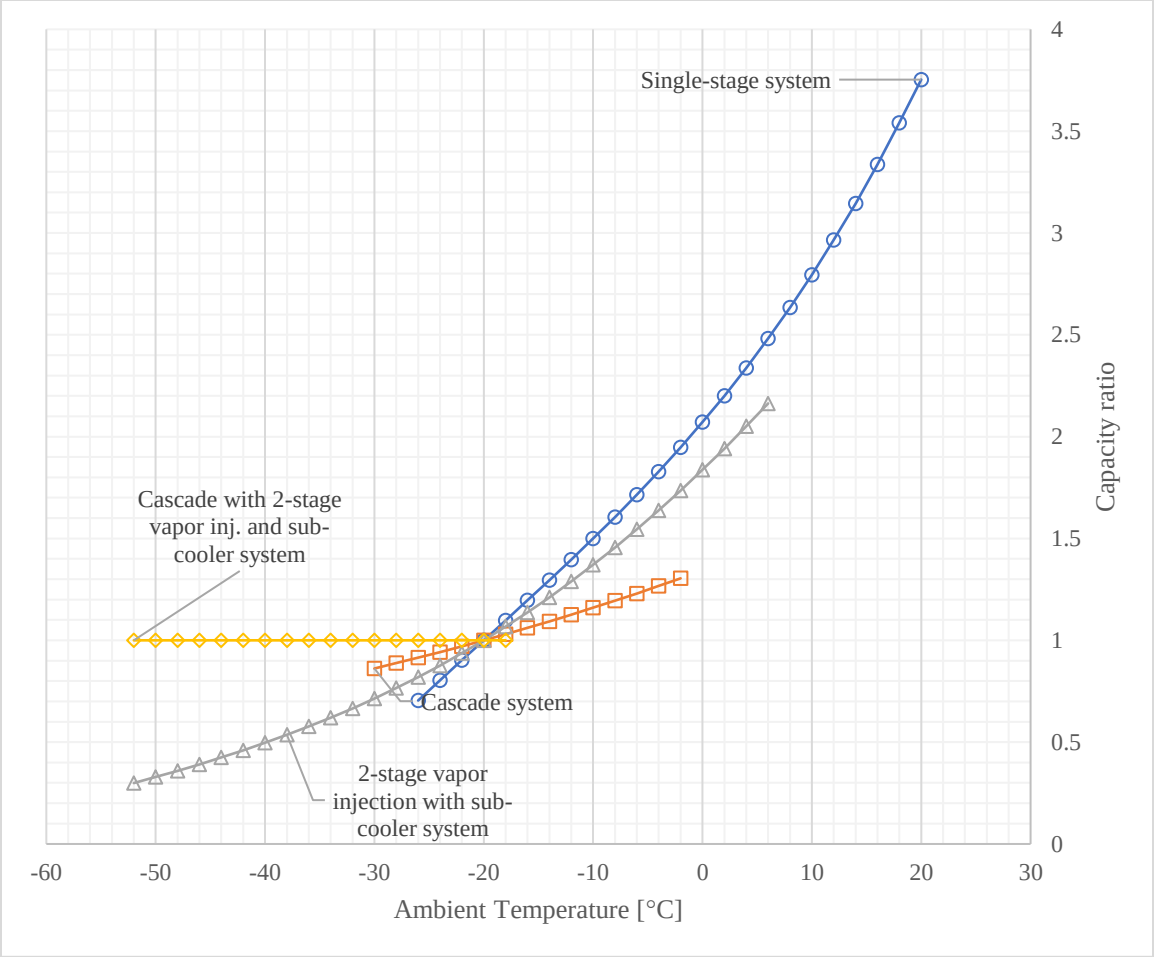

Figure 4.12: Capacity ratio for single-stage, cascade, 2-stage vapor injection with sub-cooler, and cascade with 2-stage vapor injection and sub-cooler systems at various ambient temperatures.

4.5 Proposed System Performance

As stated earlier, the focus of this study is on heat pumps for applications in extremely cold climates; therefore, cooling is not given any importance here.

4.5.1 Heating Mode Performance

The heating cycle is divided into three modes of operation based on the outdoor temperature. Figure 4.13 shows the performance curves, COP, and capacity. As the size of the system is not considered, the capacity is stated with reference to the capacity at a certain ambient temperature. Any ambient temperature can serve the purpose as long as it is normalized through the study. An ambient temperature of -20 °C is chosen as the standard reference point throughout this study. The temperature range of each mode of operation is

decided based on the modeled data shown in Figure 4.11 and 4-12, where the mode of operation is selected based on: 1) compressor operation limits and 2) better COP.

As shown in Table 3.4 and Figure 4.13, the operating heating modes can be grouped as follows:

- From +20 to -5 °C ambient temperature, the system operates in single-stage mode.
- From -5 to -30 °C ambient temperature, the system operates in cascade mode. It is noticeable that the slope of both COP and capacity ratio is decreased. That is to slow down the decline of both COP and capacity with the decrease in ambient.
- From -30 to -50 °C ambient temperature, the system operates in cascade with vapor injection with sub-cooler mode. It is clear that the capacity ratio was kept constant no matter how low the ambient temperature is. The COP, although, kept decreasing with a decrease in ambient temperature but still at a slower rate.

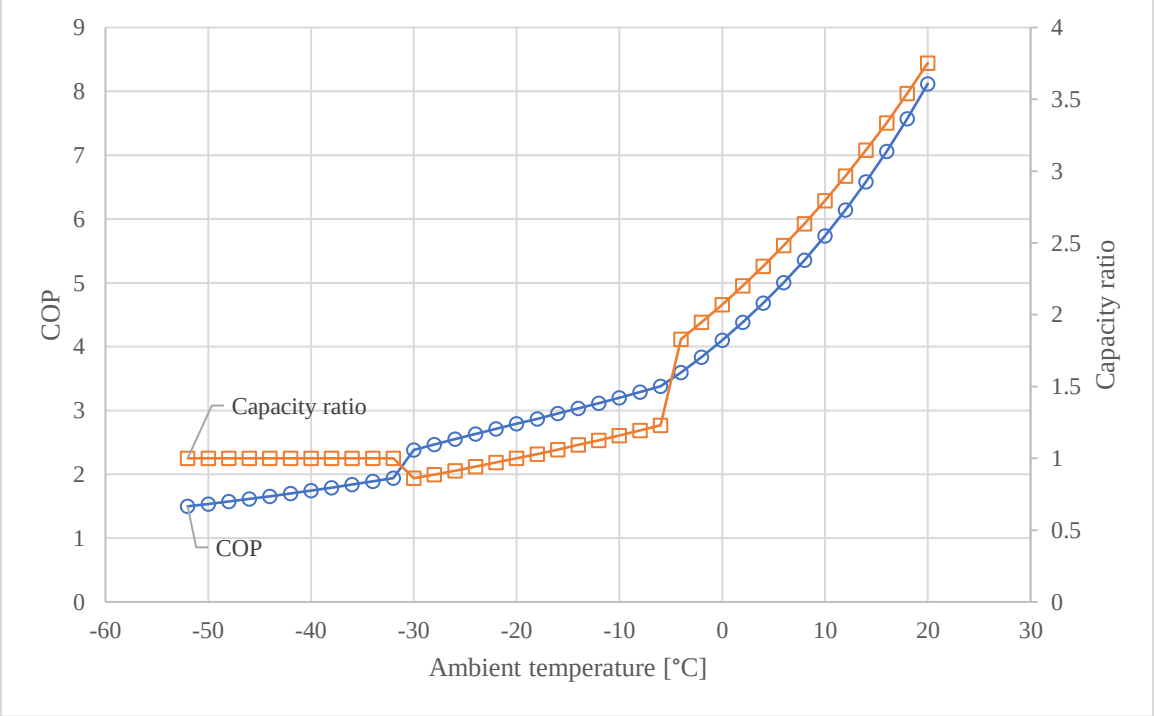

Figure 4.13: Performance curves of the proposed system.

4.5.2 Seasonal Performance in Northern Canadian Cities.

Whitehorse, YT and Sudbury, ON, are chosen as a representative for the extremely cold areas in Canada and in similar countries like Norway, Russia, Sweden, and Finland.

The full calculation of the SCOP can be found in Appendix C.

Figure 4.14 shows a comparison between the SCOP for the proposed system vs. a regular single-stage heat pump plus an auxiliary electric heat element. This will give an indication of the feasibility of the proposed system.

Figure 4.14: SCOP comparison for proposed system vs. modeled single-stage heat pump system plus electric auxiliary heat.

4.6 Comparison to Market Available Systems

The modeling presented so far did not consider the power consumption of the air moving devices. As the results look promising, a more practical approach is to take into account the influence of air moving devices. Thus, a comparison with an existing system could be conducted.

Based on AHRI 210/240, systems must consider the power consumption of the fan at 365 W per 1000 CFM (1700 m^3/h) of airflow. According to the same standard, this will be a bonus to the system heat rejection, as the motor heat will be delivered to the heated space indoors. Similarly, it should be subtracted from the cooling effect in the cooling mode of operation [94].

The system performance is modeled considering the power consumption of the air moving devices, as discussed in Section 3.1. This provides an actual approach where the airflow is

constant depending on the installed fan design while the refrigerant temperatures fluctuate accordingly.

Figure 4.15 illustrates the proposed system performance with the fan power consumption being accounted for.

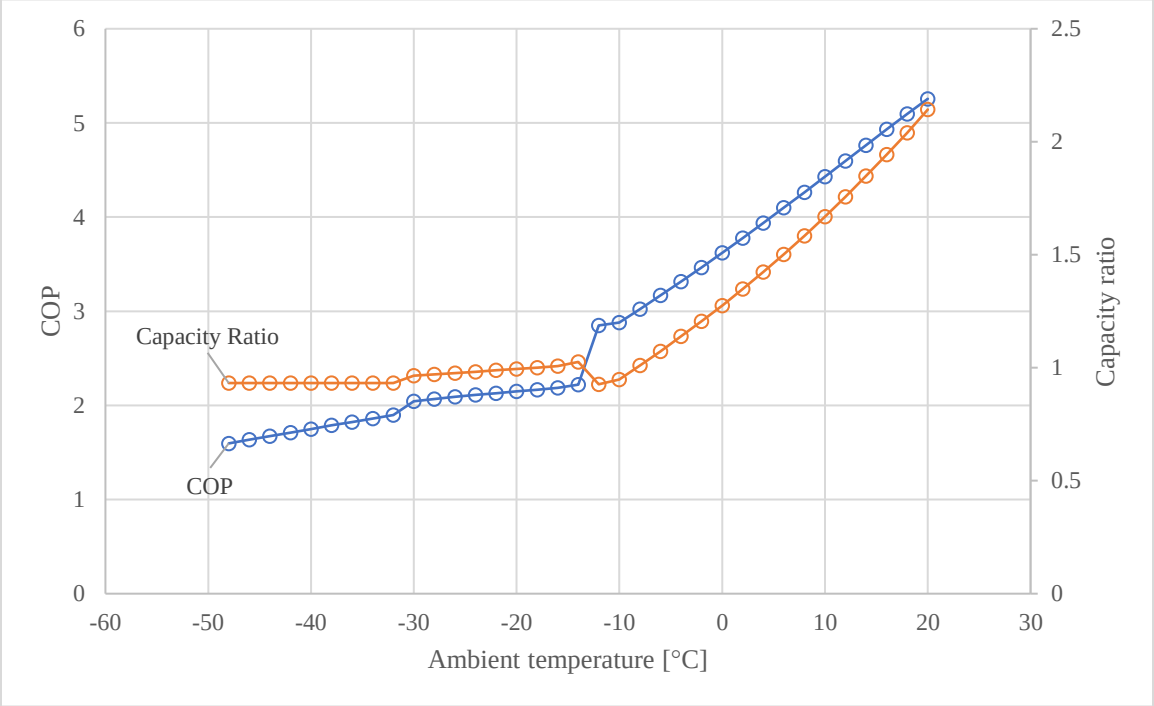

Figure 4.15: Performance curves of the proposed system with fan power consumption included.

A heat pump system manufactured by MRCOOL, one of the most prominent manufacturers of heat pumps, has been selected. The selection has been made from the NORTHEAST Energy Efficiency Partnership (NEEP) listing website. NEEP is specialized in listing cold climate air source heat pumps. The selected system is one of the highest heating performances in the market. The system carries the Energy Star label as well as the cold climate Air Source Heat Pump (ccASHP) designation. Table 4.1 lists the information related to this system [96].

Another system selected that does not have the ccASHP designation, however, is an efficient Energy Star single-stage system manufactured by Goodman. Table 4.2 shows the

data for this system [16]. Goodman published the operating points of their equipment on their website [95].

Table 4.2: MRCOOL ccASHP Energy Star unit information.

Brand	MRCOOL
Unit Model	CENTRAL-24-HP-C-23025
Indoor Model #	CENTRAL-24-HP-MUAH-23025
AHRI Certificate #	208960636
Cold Climate	Yes
Energy Star	Yes
Stages	Multi

The system performance of the ccASHP is listed on NEEP at discrete ambient temperature points. The data is compiled in Figures 4-16 and 4-17. Linear interpolation and extrapolation are used to estimate performance at any temperature within the manufacturer's operation limits [96].

Table 4.3: Goodman single-stage Energy Star heat pump system information.

Brand	GODMAN
Unit Model	GSZ160241B
Indoor Model #	ASPT29B14A
AHRI Certificate #	201667130
Cold Climate	No
Energy Star	Yes
Stages	Single

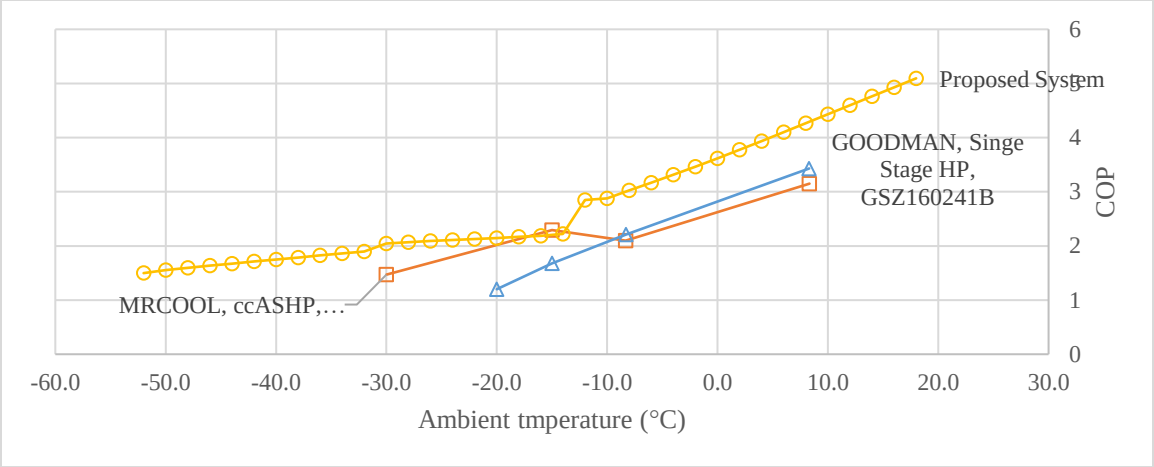

Figure 4.16: COP curves for 1) proposed system, 2) ccASHP, and 3) Single-stage heat pump.

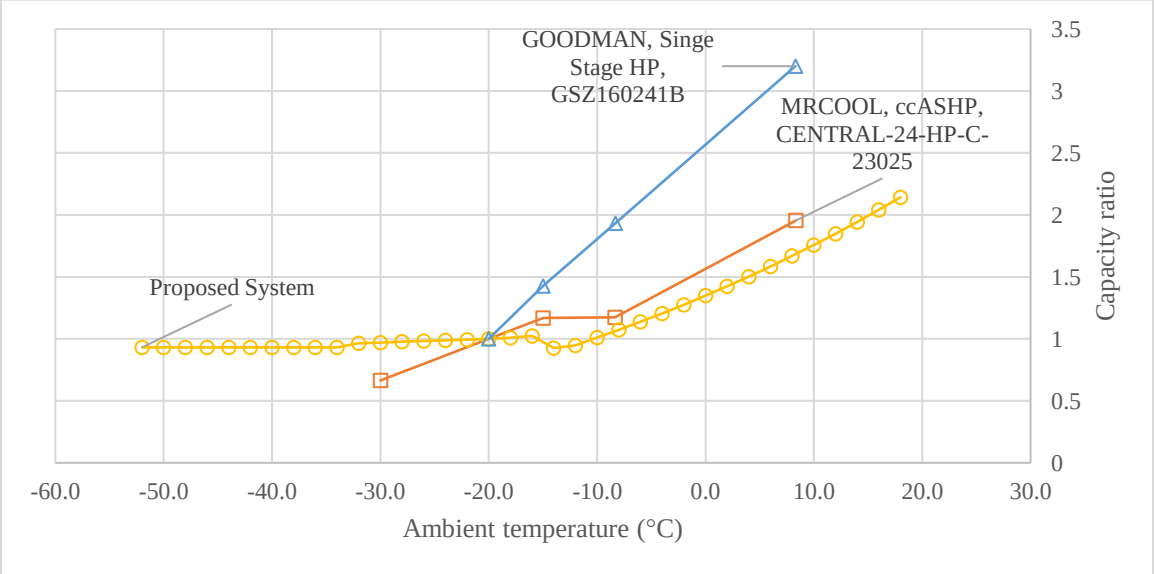

Figure 4.17: Capacity ratio of: 1) proposed system, 2) ccASHP COOL, CENTRAL-24-HP-C-23025, and 3) Goodman Single- stage heat pump GSZ16 at various ambient temperatures.

Figures 4-16 and 4-17 show the COP and capacity ratios at various outdoor temperatures for three systems: i) the proposed system, ii) the cold climate air source heat pump manufactured by MRCOOL with data in Table 4.1, and iii) a single-stage heat pump manufactured by Goodman with data in Table 4.2.

The observations can be summarized as follows:

- In moderate ambient temperatures, down to -8 °C
    - COP: The single-stage heat pump, which is not designed for cold climates, has a better COP than that of its cold-climate counterpart. The proposed system follows almost the same trendline as that of the single-stage system.
    - Capacity ratio: The capacity ratio line of the single-stage heat pump is too steep, indicating that the capacity of the system declines drastically as the outdoor temperature declines. The ccASHP has a less steep line. The proposed system has almost the same trendline as the ccASHP.
- In the low temperature ambient between -10 and -30 °C
    - COP: The cold climate heat pump can operate down to -30 °C, while the single-stage is limited to -20 °C. The cold climate heat pump also has a better COP. The slope of the COP line of the ccASHP is improved in this region, whereas the single-stage shows a steeper degradation in the COP single-stage compared to the ccASHP. The proposed system has a very low slope in this region and outperforms the other systems.
    - Capacity ratio: Both the ccASHP and single-stage heat pumps keep following their trend. The proposed system stays steady at the design capacity as indicated by the horizontal line.
- In the extremely low temperature ambient down to -52 °C
    - COP: Even the ccASHP cannot operate. The only option is the proposed system. The proposed system COP line still follows an almost horizontal straight line that slows down the degradation of the COP with the decrease in the ambient temperature.
    - Capacity ratio: Only the proposed system can operate in this zone with a constant capacity ratio independent of ambient temperature.

Eventually, to validate the overall system performance when operating in an extremely cold weather location, the SCOP for the three systems has been calculated for both Sudbury, ON and Whitehorse, YT. The comparison is shown in Figure 4.18.

Figure 4.18: SCOP comparison for systems running in Whitehorse, YT and Sudbury, ON: 1) proposed system, fan power included, 2) ccASHP unit plus auxiliary electric heating, and 3) Energy Star single-stage system plus auxiliary electric heating.

4.7 Summary of the Results

It has been clearly shown that there are no such vapor injection refrigeration systems that can work in a wide range of ambient from -50 to 20 °C. Each of the systems that have been modeled was developed for a certain application. In addition, it has been shown that a system that can run this wide range of temperatures better be a multimode system to benefit from the advantages of each system within its intended operating limits.

The proposed design showed that it could be used in extremely low climate regions as the only source of heating. The result is a seasonal performance coefficient that is around 35% better than other systems when used in extremely cold weather. Whitehorse, YT and Sudbury, ON, are taken as representative examples.

The comparison was made first with the proposed system vs. a modeled single-stage system with identical compressors with their performance based on the manufacturer's published data. In general, all criteria were applied similarly for both systems. The results show a better SCOP in favor of the proposed system.

The proposed system was then modeled, factoring in the influence of the system fans, and the performance resembled an actual unit running in different ambient temperatures. Thus, the modeled performance of the proposed system can be compared to an actual system already existing in the market. One of the most efficient units was selected and compared to the proposed system, and still, the proposed system outperformed it by 25 to 30% (Figure 4.18).

It is worth mentioning that the fan power consumption for the proposed system was calculated based on the worst-case scenario as identified by AHRI. This represents the least efficient fan motor used in the industry. This method is dictated by AHRI when manufacturers test their units without specifying the fan blower used. However, the MRCOOL unit selected here utilizes an efficient fan motor that helped improve its efficiency. It is clear that when the proposed system is paired with an efficient blower fan, its performance numbers will be further improved.

It should also be clear that with any available system in the market, an auxiliary heater must be added. This heater must be sized to the maximum building heating load, no matter how efficient the heat pump is and the capacity. Because currently, there is no heat pump available to operate in ambient temperatures below -30 °C. For places where the design temperature is below -30 °C, like Whitehorse, YT, the heat pump must stop running at its cutoff operating limit (-30°C), and another heating device must provide the full heat load needed. This is not the case with the proposed system, as it can operate down to -50 °C ambient and deliver the full heating load required. Thus, there is no need for any other auxiliary heating equipment to be installed. This is one of the greatest benefits of the proposed design. It also implies that they can completely replace furnaces. Therefore, it is a means to completely decouple space heating from fossil fuels in regions where electricity is from green sources.

Chapter 5. Conclusion and Recommendations

5.1 Conclusion

In this thesis, an innovative design is proposed that can switch operating modes to allow efficient heating operation in an ambient temperature range of -50 °C to +20 °C, which is typical in northern Canada. Almost all studies regarding cold climate air source heat pumps do not address operations below -15 °F (-26 °C). As overnight temperatures in northern Canadian winters can go lower than -15 °F, it is important to study the application of air source heat pump technology to temperatures below this value. Moreover, there is no such system in the market that can cover this low temperature range and therefore the proposed system could form the basis for the development of such equipment.

The proposed design is modeled and analyzed in detail using published performance specifications of actual compressors from current manufacturers, and the performance of each component is simulated for various operating conditions. Finally, thermodynamic simulations were conducted on the full system performance under various outdoor temperatures using the EES software. The simulation took into careful consideration the operating limits of the compressors as stated by the manufacturers. All of these made the simulation realistic.

The results show the advantages and disadvantages of each system type. Single-stage systems showed superior performance in higher outdoor temperatures. However, the slope of both the capacity and COP lines are much higher than the other systems. The capacity and COP eventually decrease with the ambient temperature to the point where they become undesirable. For example, at an ambient temperature of -30 °C, the system ceases to work within the manufacture's approved operating limits. However, the cascade system with 2-stage vapor-injection system with sub-cooler shows valid operation from this point down to -50 °C ambient temperature without violating the compressor manufacturer's limits of operation and still maintains a reasonable COP and capacity.

On the other hand, the proposed system's performance curves show a robust performance from -50 °C to +20 °C. It can also operate all year round, even within this wide temperature swing. Remarkably, the system capacity stays almost constant for the outdoor temperature

range from -10 to -50 °C. Thus, solving one of the biggest problems with this kind of system (i.e., air-source heat pumps). Also, the COP remains above 2 even for temperatures as low as -30 °C ambient, and for a temperature as low as -50 °C, the COP remains above 1.5.

Calculating the SCOP of the proposed system in the northern Canadian climate and comparing it to the specifications of the most efficient equipment available in the market showed that it outperforms the most efficient ccASHP by around 30%. To put in context the significance of the results, the most efficient ccASHP, specifically optimized for cold climate operation, outperforms a regular single-stage heat pump by only 10%. From an operational standpoint, the proposed system can also perform cooling and defrost functions. Therefore, it is not missing any function necessary for a practical installation.

The proposed system can be installed in a northern Canadian climate without the need for auxiliary heating, as is the case of current systems in the market. Thus, eliminating the challenge of supplying fossil fuels, like natural gas, to these remote locations. Furthermore, the higher SCOP of 2.5 means only 40% of the electricity required for an electric heater element needs to be generated for the proposed heat pump system. This also implies lower electricity transmission equipment, like electric cables, transformers, etc.

5.2 Recommendations for Future Work

The thesis demonstrated through modeling and conceptually the potential functionality and higher efficiency of the proposed system. The following are recommended for future works:

- Build a prototype based on the proposed design and test its performance to validate the modeled results.
- Investigate the use of different types of refrigerants, especially the emerging lower GWP refrigerants like R-454B, to validate and optimize the performance.
- Develop a control algorithm that selects the optimum intermediate pressure at each outdoor temperature for optimum system performance.
- The system design comprises variable speed compressors for the low-pressure system only, which is essential for the system to operate. However, a variable speed

compressor technology, if applied to the high-pressure compressor as well, will lead to higher efficiencies. A study for synchronization of the two compressor speeds and the development of the control algorithm could open a window for a much improved performance.

- Optimize the outdoor heat exchanger design for handling defrost within this application range and develop optimized defrost control methods.
- Perform cost analysis, running cost and capital cost of the proposed system in comparison to other options like electric heater, gas furnace, etc. Also, the impact on the environment could be part of a future study.

REFERENCES

[1] "Unitary Air Conditioners and Unitary Heat Pumps," in *ASHRAE Handbook: 2000 HVAC Systems and Equipment*, SI Edition.Atlanta, GA : ASHRAE, pp. 45.1-45.13.

[2] M. J. Moran, H. N. Shapiro, B. R. Munson, and D. P. DeWitt, *Introduction to Thermal Systems Engineering: Thermodynamics, Fluid Mechanics, and Heat Transfer*. New York, NY: Wiley, 2003.

[3] S. L. Dixon and C. A. Hall, *Fluid Mechanics and Thermodynamics of Turbomachinery*, 7th ed. Waltham, MA: Butterworth-Heinemann, 2014.

[4] Copeland, *Compression Ratio as It Affects Compressor Reliability*. Application Engineering Bulletin, AE17-1268, 2010.

[5] H. P. Bloch and H. J. Hoefner, *Reciprocating Compressors: Operation and Maintenance*. Houston, TX: Butterworth-Heinemann, 1996.

[6] R. N. Brown, *Compressors: Selection and Sizing*, 3rd ed. Gulf Professional Publishing, 2005.

[7] P. Grolier, "A Method to Estimate the Performance of Reciprocating Compressors," in *International Compressor Engineering Conference*, West Lafayette, IN: Perdue, 2002.

[8] *ASHRAE Handbook: 2002 Refrigeration*, SI Edition. Atlanta, GA: ASHRAE.

[9] "eCFR :: Appendix M1 to Subpart B of Part 430, Title 10 -- Uniform Test Method for Measuring the Energy Consumption of Central Air Conditioners and Heat Pumps." https://www.ecfr.gov/current/title-10/chapter-II/subchapter-D/part-430/subpart-B/appendix-Appendix%20M1%20to%20Subpart%20B%20of%20Part%20430 (accessed Jan. 30, 2023).

[10] "WHITEHORSE (719640)." https://weather.ashrae.org//#719640 (accessed Jan. 30, 2023).

[11] "Weather Data Viewer." https://weather.ashrae.org// (accessed Feb. 01, 2023).

[12] “Population Clock: World.” https://www.census.gov/popclock/world (accessed Apr. 01, 2023).

[13] Statistics Canada, “Households and the Environment: Energy Use 2011.” Accessed: Jan. 18, 2023. [Online]. Available: https://www150.statcan.gc.ca/n1/en/pub/11-526-s/11-526-s2013002-eng.pdf?st=3JXmR5Fx

[14] “Energy Use in Canada: Trends Publications | Natural Resources Canada.” https://oee.nrcan.gc.ca/publications/statistics/trends/2018/residential.cfm (accessed Jan. 18, 2023).

[15] “Paving the Road to 2030 and Beyond: Market transformation road map for energy efficient equipment in the building sector: Supporting the transition to a low-carbon economy,” in *Energy and Mines Minsters’ Conference*, Iqaluit, Nunavut, Aug. 2018.

[16] “AHRI Certification Directory.” https://www.ahridirectory.org/Search/SearchHome (accessed Jan. 18, 2023).

[17] B. Whitman, B. Johnson, J. Tomczyk, and E. Silberstein, *Refrigeration and Air Conditioning Technology*, 6th ed. Clifton Park, NY: Delmar, 2009.

[18] “Components for heat pumps – part 5: four-way reversing valves | Danfoss.” https://www.danfoss.com/en/service-and-support/case-stories/dcs/components-for-heat-pumps-part-5-four-way-reversing-valves/ (accessed Feb. 13, 2023).

[19] A. D. Althouse, C. H. Turnquist, and A. F. Bracciano, *Modern Refrigeration and Air Conditioning*, 9th ed. Tinley Park, IL: Goodheart-Willcox, 2004.

[20] Carrier, “Refrigerant Piping,” in *Handbook of Air Conditioning System Design, Part 3. Piping Design*, New York, NY: McGraw-Hill.

[21] Copeland, *1 to 5 Ton ZP*K6 R-410A Copeland Scroll™ Compressors*. Application Engineering Bulletin, AE4-1400 R2, 2015.

[22] Copeland, *Use of Variable Frequency Drives (VFDs) With Copeland Scroll ™ and Copeland Discus ™ Fixed Capacity Compressors in Refrigeration Applications*. Application Engineering Bulletin, AE21-1369 R5, 2021.

[23] Copeland, *Copelametic ® Two-Stage Compressors Application and Service Instructions*. Application Engineering Bulletin, AE19-1132 R8, 2010.

[24] Copeland, *Low Condensing Temperature Bulletin*. Application Engineering Bulletin, AE4-1334, 2010.

[25] P. W. Sunu, I. Made Rasta, D. S. Anakottapary, I. Made Suarta, and C. Santosa, "Capillary Tube and Thermostatic Expansion Valve Comparative Analysis in Water Chiller Air Conditioning," p. 12063, 2018, doi: 10.1088/1742-6596/953/1/012063.

[26] P. Blecich, "Experimental investigation of the effects of airflow nonuniformity on performance of a fin-and-tube heat exchanger," *International Journal of Refrigeration*, vol. 59, pp. 65–74, Nov. 2015, doi: 10.1016/J.IJREFRIG.2015.06.029.

[27] "Piston vs. TXV Metering Devices - HVAC School." https://hvacrschool.com/piston-vs-txv/ (accessed Mar. 20, 2023).

[28] *Thermostatic Expansion Valves, Theory of Operation, Application, and Selection*. Washington, MO: Parker Hannifin Corporation, Sporlan Division, 2011.

[29] Y. Xia and S. Deng, "The influences of the operating characteristics of an Electronic Expansion Valve (EEV) on the operational stability of an EEV controlled direct expansion air conditioning system," *International Journal of Refrigeration*, vol. 69, pp. 394–406, Sep. 2016, doi: 10.1016/J.IJREFRIG.2016.06.008.

[30] C. Park, H. Cho, Y. Lee, and Y. Kim, "Mass flow characteristics and empirical modeling of R22 and R410A flowing through electronic expansion valves," *International Journal of Refrigeration*, vol. 30, no. 8, pp. 1401–1407, Dec. 2007, doi: 10.1016/J.IJREFRIG.2007.03.011.

[31] A. Sadeghianjahromi and C. C. Wang, "Heat transfer enhancement in fin-and-tube heat exchangers – A review on different mechanisms," *Renewable and Sustainable Energy Reviews*, vol. 137. 2021. doi: 10.1016/j.rser.2020.110470.

[32] "Products | Friga-Bohn." https://friga-bohn.lennoxemea.com/en/products/ (accessed Feb. 13, 2023).

[33] L. L. Shao, L. Yang, and C. L. Zhang, “Comparison of heat pump performance using fin-and-tube and microchannel heat exchangers under frost conditions,” *Appl Energy*, vol. 87, no. 4, 2010, doi: 10.1016/j.apenergy.2009.08.021.

[34] J. Zhou, J. Wang, Z. Yan, and Q. Gao, “Development and application of a microchannel heat exchanger for the heat pump,” *International Journal of Energy for a Clean Environment*, vol. 19, no. 1–4, 2018, doi: 10.1615/INTERJENERCLEANENV.2018020983.

[35] S. S. Bhosale and A. R. Acharya, “Review On Applications of Micro Channel Heat Exchanger,” *International Research Journal of Engineering and Technology*, no. October, 2020.

[36] “MCHE for A/C | Microchannel heat exchanger | Danfoss.” https://www.danfoss.com/en/products/dcs/heat-exchangers/micro-channel-heat-exchangers/#tab-overview (accessed Mar. 20, 2023).

[37] “Home Heating And Cooling | HVAC Systems | YORK®.” https://www.york.com/residential-equipment/heating-and-cooling (accessed Feb. 02, 2023).

[38] *ASHRAE Handbook: 2001 Fundamentals.*, SI Edition. Atlanta, GA: ASHRAE.

[39] *Standard for Refrigeration Systems and Designation and Safety Classification of Refrigerants*. ASHRAE 15, 2022.

[40] *Safety Standard for Refrigeration Systems in Residential Applications*. ASHRAE 15.2, 2022.

[41] “Refrigeration handbook - SWEP.” https://www.swep.net/refrigerant-handbook/refrigerant-handbook/ (accessed Feb. 15, 2023).

[42] O. Hodnebrog, K. Shine, and T. Wallington, “Halocarbons: What Are They and Why Are They Important?,” *Eos (Washington DC)*, vol. 101, Sep. 2020, doi: 10.1029/2020EO149045.

[43] *SNAP Rule 23 - Protection of Stratospheric Ozone: New Listings for the Significant New Alternatives Policy Program in the Refrigeration & Air Conditioning Sector and Revised Listing in the Fire Suppression and Explosion Protection Sector*. Environment Protection Agency (EPA), USA: https://www.epa.gov/, 2021.

[44] *Federal Offset Protocol: Reducing Greenhouse Gas Emissions from Refrigeration Systems*. Gatineau, QC, Canada: Environment and Climate Change Canada, 2023.

[45] *Regulation (EU) No 517/2014 of the European Parliament and of the Council*. EU.

[46] M. O. McLinden, A. F. Kazakov, J. Steven Brown, and P. A. Domanski, "A thermodynamic analysis of refrigerants: Possibilities and tradeoffs for Low-GWP refrigerants," *International Journal of Refrigeration*, vol. 38, no. 1, pp. 80–92, Feb. 2014, doi: 10.1016/J.IJREFRIG.2013.09.032.

[47] B. Gil and J. Kasperski, "Efficiency evaluation of the ejector cooling cycle using a new generation of HFO/HCFO refrigerant as a R134a replacement," *Energies (Basel)*, vol. 11, no. 8, Aug. 2018, doi: 10.3390/EN11082136.

[48] V. Oruç, A. G. Devecioğlu, and S. Ender, "Improvement of energy parameters using R442A and R453A in a refrigeration system operating with R404A," *Appl Therm Eng*, vol. 129, pp. 243–249, 2018, doi: 10.1016/J.APPLTHERMALENG.2017.10.035.

[49] *Household and Similar Appliances -Safety - Part 2-40 Requirements of Electric Heat Pumps, Air Conditioners and Dehumidifiers*. UL 60335-2-40, 2022.

[50] "High-GWP Refrigerants | California Air Resources Board." https://ww2.arb.ca.gov/resources/documents/high-gwp-refrigerants (accessed Feb. 13, 2023).

[51] A. Mota-Babiloni, A. Fernández-Moreno, P. Giménez-Prades, C.-M. Udroiu, and J. Navarro-Esbrí, "Ternary refrigerant blends for Ultra-Low Temperature Refrigeration," *International Journal of Refrigeration*, Jan. 2023, doi: 10.1016/J.IJREFRIG.2023.01.006.

[52] "Freon^{TM} Refrigerants for Very Low Temperature Refrigeration." https://www.freon.com/en/industries/refrigeration/vlt-refrigeration (accessed Mar. 18, 2023).

[53] Copeland, *Suction Accumulators*. Application Engineering Bulletin, AE11-1147 R6, 2010.

[54] "Selecting, Installing Oil Separators | ACHR News." https://www.achrnews.com/articles/91004-selecting-installing-oil-separators (accessed Mar. 20, 2023).

[55] "Oil separator, type OUB; Oil separator, type OUB." [Online]. Available: www.products.danfoss.com

[56] K. Li *et al.*, "An experimental investigation of oil circulation ratio influence on heating performance in an air condition heat pump system for electrical vehicles," *International Journal of Refrigeration*, vol. 122, pp. 220–231, Feb. 2021, doi: 10.1016/J.IJREFRIG.2020.11.007.

[57] T. L. Bergman, A. S. Lavine, F. P. Incropera, and D. P. Dewitt, "Heat Exchangers," in *Fundamentals of Heat and Mass Transfer*, 7th ed. New York, NY: Wiley, 2011, pp. 705–767.

[58] Y. A. Cengel, *Heat and MassTransfer: A Practical Approach*, 3rd ed. New York, NY: McGraw-Hill, 2006.

[59] J. Mately, *Fluid Movers: Pumps, Compressors, Fans and Blowers*. New York, NY: McGraw-Hill, 1979.

[60] *Laboratory Methods of Testing Fans for Aerodynamic Performance Rating*. ASHRAE/AMCA 51, 2016.

[61] R. C. Monroe, "Fans and Blowers," in *Kirk-Othmer Encyclopedia of Chemical Technology*, 3rd ed. New York, NY: Wiley, 1993.

[62] *Electric Motors*. Bureau of Energy Efficiency. Accessed: Apr. 05, 2023. [Online]. Available: https://www.yumpu.com/en/document/read/48385958/2-electric-motors-bureau-of-energy-efficiency

[63] "Fact Sheet: DETERMINING ELECTRIC MOTOR LOAD AND EFFICIENCY," *Motor Challenge, a Program of the USA Department of Energy*.

[64] Q. Minglu, X. Liang, S. Deng, and J. Yiqiang, "Improved indoor thermal comfort during defrost with a novel reverse-cycle defrosting method for air source heat pumps," *Build Environ*, vol. 45, no. 11, 2010, doi: 10.1016/j.buildenv.2010.04.006.

[65] J. Kim, H. J. Choi, and K. C. Kim, "A combined Dual Hot-Gas Bypass Defrosting method with accumulator heater for an air-to-air heat pump in cold region," *Appl Energy*, vol. 147, 2015, doi: 10.1016/j.apenergy.2015.02.074.

[66] W. Wang, J. Xiao, Q. C. Guo, W. P. Lu, and Y. C. Feng, "Field test investigation of the characteristics for the air source heat pump under two typical mal-defrost phenomena," *Appl Energy*, vol. 88, no. 12, pp. 4470–4480, Dec. 2011, doi: 10.1016/J.APENERGY.2011.05.047.

[67] Y. Fan *et al.*, "A proof-of-concept study of a novel ventilation heat recovery vapour injection air source heat pump," *Energy Convers Manag*, vol. 256, p. 115404, Mar. 2022, doi: 10.1016/J.ENCONMAN.2022.115404.

[68] "Northeast Energy Efficiency Partnership (NEEP): Cold Climate Air Source Heat Pump Specification (V. 4.0)," Jan. 2023.

[69] H. Huang, *Heat Pumps for Cold Climate Heating: Variable Volume Ratio Two-stage Vapor Compression Air Source Heat Pump Technology and Application*. Boca Raton, FL: CRC, 2020.

[70] S. Jain, G. Jain, and C. W. Bullard, "Vapor Injection in Scroll Compressors," in *International Compressor Engineering Conference*, West Lafayette, IN: Perdue, Jul. 2004.

[71] H. Qiao, X. Xu, V. Aute, and R. Radermacher, "Transient modeling of a flash tank vapor injection heat pump system – Part II: Simulation results and experimental

validation," *International Journal of Refrigeration*, vol. 49, pp. 183–194, Jan. 2015, doi: 10.1016/J.IJREFRIG.2014.06.018.

[72] H. Qiao, V. Aute, and R. Radermacher, "Transient modeling of a flash tank vapor injection heat pump system – Part I: Model development," *International Journal of Refrigeration*, vol. 49, pp. 169–182, Jan. 2015, doi: 10.1016/J.IJREFRIG.2014.06.019.

[73] J. Winkler, X. Wang, V. Aute, R. Radermacher, and J. Winkler, "Purdue e-Pubs Simulation and Validation of a Two-Stage Flash Tank Cycle Using R410A as a Refrigerant Simulation and Validation of a Two-Stage Flash Tank Cycle using R410A as a Refrigerant", Accessed: Mar. 03, 2023. [Online]. Available: http://docs.lib.purdue.edu/iracc/899

[74] D. Zhang, J. Li, J. Nan, and L. Wang, "Thermal performance prediction and analysis on the economized vapor injection air-source heat pump in cold climate region of China", doi: 10.1016/j.seta.2016.10.008.

[75] G. Y. Ma and H. X. Zhao, "Experimental study of a heat pump system with flash-tank coupled with scroll compressor," *Energy Build*, vol. 40, no. 5, pp. 697–701, Jan. 2008, doi: 10.1016/J.ENBUILD.2007.05.003.

[76] X. Wang, Y. Hwang, and R. Radermacher, "Two-stage heat pump system with vapor-injected scroll compressor using R410A as a refrigerant," *International Journal of Refrigeration*, vol. 32, no. 6, pp. 1442–1451, Sep. 2009, doi: 10.1016/J.IJREFRIG.2009.03.004.

[77] M. E. Konrad, "Improving Cold Climate Performance of Heat Pumps Using Market-Available Systems," University of Ontario Institute of Technology, Oshawa, 2022.

[78] J. Shen, T. Guo, Y. Tian, and Z. Xing, "Design and experimental study of an air source heat pump for drying with dual modes of single-stage and cascade cycle," *Appl Therm Eng*, vol. 129, pp. 280–289, Jan. 2018, doi: 10.1016/J.APPLTHERMALENG.2017.10.047.

[79] E. Mancuhan, “Comparative evaluation of a two-stage refrigeration system with flash intercooling using different refrigerants,” *Thermal Science*, vol. 24, pp. 815–830, 2020, doi: 10.2298/TSCI180921011M.

[80] P. K. Bansal and S. Jain, “Cascade systems: past, present, and future,” *ASHRAE Trans*, vol. 113, no. 1, pp. 245–253, Jan. 2007.

[81] “Ultralow-Temperature Refrigeration,” in *ASHRAE Handbook: 2002 Refrigeration*, SI Edition.Atlanta, GA: ASHRAE, pp. 39.1-39.12.

[82] Y. Song, D. Li, D. Yang, L. Jin, F. Cao, and X. Wang, “Comparaison de performances entre une pompe à chaleur combinée au R134a/CO2 et une pompe à chaleur en cascade au R134a/CO2 pour chauffage de locaux,” *International Journal of Refrigeration*, vol. 74, pp. 590–603, Feb. 2017, doi: 10.1016/j.ijrefrig.2016.12.001.

[83] Y. Yang, R. Li, Y. Zhu, Z. Sun, and Z. Zhang, “Experimental and simulation study of air source heat pump for residential applications in northern China,” *Energy Build*, vol. 224, p. 110278, Oct. 2020, doi: 10.1016/J.ENBUILD.2020.110278.

[84] C. W. Roh and M. S. Kim, “Effect of vapor-injection technique on the performance of a cascade heat pump water heater,” *International Journal of Refrigeration*, vol. 38, no. 1, pp. 168–177, Feb. 2014, doi: 10.1016/J.IJREFRIG.2013.09.020.

[85] Y. Tan, L. Wang, and K. Liang, “Thermodynamic performance of an auto-cascade ejector refrigeration cycle with mixed refrigerant R32 + R236fa,” *Appl Therm Eng*, vol. 84, pp. 268–275, Jun. 2015, doi: 10.1016/J.APPLTHERMALENG.2015.03.047.

[86] Y. He *et al.*, “Theoretical performance comparison for two-stage auto-cascade refrigeration system using hydrocarbon refrigerants,” *International Journal of Refrigeration*, vol. 142, pp. 27–36, Oct. 2022, doi: 10.1016/J.IJREFRIG.2022.06.008.

[87] Y. Tan, L. Wang, and K. Liang, “Thermodynamic performance of an auto-cascade ejector refrigeration cycle with mixed refrigerant R32 þ R236fa,” 2015, doi: 10.1016/j.applthermaleng.2015.03.047.

[88] M. Cui, Z. Cheng, B. Wang, F. Wei, and W. Shi, “Experimental investigation on an auto-cascade quasi two-stage compression heat pump system,” *Appl Therm Eng*, vol. 219, p. 119498, Jan. 2023, doi: 10.1016/J.APPLTHERMALENG.2022.119498.

[89] O. A. Zuev, S. A. Garanov, E. V. Ivanova, and A. S. Karpukhin, “Investigation of the Efficiency of Autocascade and Cascade Heat Pumps in Cold Climate,” *Chemical and Petroleum Engineering*, vol. 56, no. 5–6, pp. 448–455, Sep. 2020, doi: 10.1007/S10556-020-00793-W.

[90] S. Jiang, “Air-source heat pump systems,” *Handbook of Energy Systems in Green Buildings*, pp. 349–391, May 2018, doi: 10.1007/978-3-662-49120-1_2.

[91] Y. Yang, R. Li, Y. Zhu, Z. Sun, and Z. Zhang, “Experimental and simulation study of air source heat pump for residential applications in northern China,” *Energy Build*, vol. 224, p. 110278, Oct. 2020, doi: 10.1016/J.ENBUILD.2020.110278.

[92] J. Shen, T. Guo, Y. Tian, and Z. Xing, “Design and experimental study of an air source heat pump for drying with dual modes of single-stage and cascade cycle,” *Appl Therm Eng*, vol. 129, pp. 280–289, Jan. 2018, doi: 10.1016/J.APPLTHERMALENG.2017.10.047.

[93] R. K. Johnson, “Measured Performance of a Low Temperature Air Source Heat Pump | Building America Solution Center,” Golden, CO, Sep. 2013. Accessed: Mar. 29, 2023. [Online]. Available: https://basc.pnnl.gov/library/measured-performance-low-temperature-air-source-heat-pump

[94] *Performance Rating of Unitary Air-conditioning & Air-source Heat Pump Equipment*. Arlington, VA: AHRI, 2020.

[95] “Air Conditioning and Heating Systems| HVAC | Goodman.” https://www.goodmanmfg.com/ (accessed Feb. 02, 2023).

[96] “Northeast Energy Efficiency Partnership | Northeast Energy Efficiency Partnerships.” https://neep.org/ (accessed Feb. 18, 2023).

[97] “United States : DOE to Partner with Heating Industry to Improve Performance and Energy-Efficiency of Cold Climate Heat Pumps - ProQuest.” https://www.proquest.com/docview/2592853521?accountid=14694&parentSessionId=vGH0FaTjdhQxfpqthQmMDlZRnlcdTbQ%2BLUqb%2Fbxn35s%3D&pq-origsite=primo (accessed Mar. 27, 2023).

[98] “CCHP Technology Challenge Specifications | Department of Energy.” https://www.energy.gov/eere/buildings/cchp-technology-challenge-specifications (accessed Mar. 27, 2023).

[99] “Residential Cold Climate Heat Pump Challenge | Department of Energy.” https://www.energy.gov/eere/buildings/residential-cold-climate-heat-pump-challenge (accessed Mar. 27, 2023).

[100] “Trane to Start Field Testing Cold Climate Heat Pump Prototypes - ProQuest.” https://www.proquest.com/docview/2755909209?accountid=14694&parentSessionId=JWq%2FqwpZgReHJXPgdPRXQ4C9b%2BDOqfg0m1RPA1294JM%3D&pq-origsite=primo (accessed Mar. 27, 2023).

[101] “US DOE partner develops ‘breakthrough’ in cold climate heat pump technology - ProQuest.” https://www.proquest.com/docview/2681282901/fulltext/6169AAC7BE344161PQ/1?accountid=14694 (accessed Mar. 27, 2023).

[102] P. Byrne, J. Miriel, and Y. Lénat, “Modelling and simulation of a heat pump for simultaneous heating and cooling,” *Build Simul*, vol. 5, no. 3, pp. 219–232, Sep. 2012, doi: 10.1007/s12273-012-0089-0.

[103] P. Byrne, R. Ghoubali, and J. Miriel, “Scroll compressor modelling for heat pumps using hydrocarbons as refrigerants,” 2013, doi: 10.1016/j.ijrefrig.2013.06.003.

[104] C. Cuevas and J. Lebrun, “Testing and modelling of a variable speed scroll compressor,” 2008, doi: 10.1016/j.applthermaleng.2008.03.016.

[105] *Performance Rating of Positive Displacement Refrigerant Compressors*. Arlington, VA: AHRI Standard 540, 2020.

[106] *Methods of Test for Rating the Performance of Positive Displacement Compressors that Operate at Supercritical Pressures of the Refrigerants*. ANSI/ASHRAE 23.2, 2019.

[107] *Methods for Performance Testing Positive Displacement Refrigerant Compressors and Condensing Units that Operate at Subcritical Pressures of the Refrigerant*. Atlanta, GA: ANSI/ASHRAE Standard 23.1-2019, 2019.

[108] D. A. E. Dabiri and C. K. Rice, "A Compressor Simulation Model with Corrections for the Level of Suction Gas Superheat," 2017, Accessed: Feb. 01, 2023. [Online]. Available: https://www.researchgate.net/publication/255075970

[109] A. M. Trzynadlowski, *Control of Induction Motors*. San Diego, CA: Academic Press, 2001.

[110] *Performance Rating of Modulating Positive Displacement Refrigerant Compressors*. Arlington, VA: AHRI Standard 545, 2017.

[111] H. Wan, T. Cao, Y. Hwang, and S. Oh, "An electronic expansion valve modeling framework development using artificial neural network: A case study on VRF systems," *International Journal of Refrigeration*, vol. 107, pp. 114–127, 2019, doi: 10.1016/j.ijrefrig.2019.08.018.

[112] H. Park, D. H. Kim, and M. S. Kim, "Thermodynamic analysis of optimal intermediate temperatures in R134a–R410A cascade refrigeration systems and its experimental verification," *Appl Therm Eng*, vol. 54, no. 1, pp. 319–327, May 2013, doi: 10.1016/J.APPLTHERMALENG.2013.01.005.

[113] Copeland, *Application Guidelines for Low Temperature ZF**KAE 1-2.5HP Copeland Scroll™ Refrigeration Compressors*. Application Engineering Bulletin, AE4-1425 R4, 2019.

[114] *Product Selection Software*. Emerson Climate Technologies. [Online]. Available: https://climate.emerson.com/en-us/tools-resources/product-selection-software

[115] *EnergyPlus*. U.S. Department of Energy. [Online]. Available: https://energyplus.net/

[116] *Methods of Testing for Rating Seasonal Efficiency of Unitary Air Conditioners and Heat Pumps*. ANSI/ASHRAE 116, 2005.

[117] H. Woerpel, "Configuring the Future of A2L Refrigerants," *Engineered Systems*, vol. 37, no. 10, p. 8, 2020.

[118] J. Turpin, "States Updating Codes to Allow Mildly Flammable Refrigerants," *Air Conditioning, Heating & Refrigeration News*, vol. 276, no. 1, pp. 10–11, 2022.

Appendix A. Weather Data

Weather data are collected using the ASHRA Weather Data Viewer 2021 software [11]

A 1. USA, Climate Regions, Heating Load Hours [94]

Distribution of Fractional Heating Hours in Temperature Bins, Heating Load Hours, and Outdoor Design Temperature for Different Climatic Regions in USA							
Region Number		I	II	III	IV	V	*VI
Heating Load Hours		493	857	1247	1701	2202	1842
Outdoor Design Temp.		37	27	17	5		30
Zero-Load Temp.		58	57	56	55	55	57
j tj (°F)	tj (°F)	Fractional Bin Hours, nj/N					
1	62	0	0	0	0	0	0
2	57	.239	0	0	0	0	0
3	52	.194	.163	.138	.103	.086	.215
4	47	.129	.143	.137	.093	.076	.204
5	42	.081	.112	.135	.100	.078	.141
6	37	.041	.088	.118	.109	.087	.076
7	32	.019	.056	.092	.126	.102	.034
8	27	.005	.024	.047	.087	.094	.008
9	22	.001	.008	.021	.055	.074	.003
10	17	0	.002	.009	.036	.055	0
11	12	0	0	.005	.026	.047	0
12	7	0	0	.002	.013	.038	0
13	2	0	0	.001	.006	.029	0
14	-3	0	0	0	.002	.018	0
15	-8	0	0	0	.001	.010	0
16	-13	0	0	0	0	.005	0
17	-18	0	0	0	0	.002	0
18	-23	0	0	0	0	.001	0

A 2. Weather Data for Whitehorse, YT, Canada

°C	hrs	°C	hrs	°C	hrs	°C	hrs	°C	hrs
-47.0	0.1153	-29.5	14.0683	-12.0	60.3511	5.5	116.3229	23.0	19.7593
-46.5	0.3459	-29.0	17.4510	-11.5	64.1183	6.0	126.8928	23.5	17.3760
-46.0	0.6150	-28.5	19.1040	-11.0	68.4239	6.5	126.7381	24.0	14.4928
-45.5	1.1531	-28.0	19.1809	-10.5	68.6547	7.0	134.6170	24.5	11.6100
-45.0	1.2684	-27.5	19.5652	-10.0	71.4992	7.5	140.3060	25.0	10.8798
-44.5	1.6144	-27.0	23.2170	-9.5	76.3809	8.0	135.4232	25.5	7.8806
-44.0	1.2684	-26.5	22.7940	-9.0	77.2276	8.5	143.9573	26.0	6.3046
-43.5	1.5375	-26.0	24.9466	-8.5	83.5698	9.0	151.5691	26.5	5.6127
-43.0	1.9603	-25.5	24.2165	-8.0	83.3783	9.5	142.4985	27.0	5.2666
-42.5	1.8450	-25.0	29.4826	-7.5	83.1481	10.0	149.4557	27.5	4.8436
-42.0	1.9219	-24.5	27.0225	-7.0	93.7970	10.5	142.4216	28.0	3.8057
-41.5	2.8828	-24.0	30.6743	-6.5	87.8008	11.0	141.1543	28.5	3.2674
-41.0	2.3062	-23.5	29.4059	-6.0	98.1032	11.5	136.3103	29.0	2.1526
-40.5	2.9212	-23.0	36.4786	-5.5	88.5699	12.0	129.2763	29.5	1.1149
-40.0	3.0750	-22.5	32.9425	-5.0	90.9920	12.5	120.1279	30.0	0.6919
-39.5	2.6137	-22.0	37.0934	-4.5	100.7179	13.0	126.2019	30.5	0.5382
-39.0	3.1519	-21.5	31.3278	-4.0	99.6810	13.5	107.4044	31.0	0.5382
-38.5	3.2287	-21.0	35.0566	-3.5	112.1762	14.0	109.5963	31.5	0.6919
-38.0	3.4978	-20.5	34.6339	-3.0	120.2871	14.5	100.7541	32.0	0.5382
-37.5	3.4594	-20.0	36.4022	-2.5	122.9780	15.0	95.2189	32.5	0.2691
-37.0	3.5747	-19.5	39.2851	-2.0	144.1224	15.5	88.4531	33.0	0.0384
-36.5	4.9200	-19.0	44.5897	-1.5	136.3570	16.0	84.3020		
-36.0	5.4197	-18.5	41.8604	-1.0	140.3942	16.5	80.8429		
-35.5	6.6881	-18.0	46.5886	-0.5	149.8895	17.0	68.2724		
-35.0	6.5344	-17.5	45.8198	0.0	151.6617	17.5	64.6978		
-34.5	7.5338	-17.0	51.2780	0.5	145.5501	18.0	61.5847		
-34.0	7.8797	-16.5	51.2785	1.0	149.6246	18.5	51.8593		
-33.5	8.4179	-16.0	55.8529	1.5	134.1322	19.0	49.0528		
-33.0	8.4179	-15.5	54.6996	2.0	134.3986	19.5	42.8634		
-32.5	9.3019	-15.0	64.3481	2.5	127.2862	20.0	38.2506		
-32.0	9.7631	-14.5	59.7738	3.0	121.1736	20.5	35.9437		
-31.5	9.9939	-14.0	62.0804	3.5	121.9795	21.0	30.3699		
-31.0	11.9157	-13.5	65.4639	4.0	120.2873	21.5	27.4479		
-30.5	13.8376	-13.0	63.4265	4.5	112.3667	22.0	25.1416		
-30.0	15.9903	-12.5	65.1558	5.0	125.3191	22.5	23.0659		

Station information

WMO: 719640
Name:
WHITEHORSE
State: YT

Country: CAN
Latitude: 60.7331°N
Longitude:
135.0978°W
Elevation: 706m
Month: Annual

Annual heating design dry bulb temperature

99.6%, -38.1 °C

99%, -33.5 °C

Annual cooling design dry bulb/wet bulb temperature

25.8/14.3 °C

A 3. Weather data for Sudbury, ON, Canada

℃	hrs.	℃	hrs.	℃	hrs.	℃	hrs.
-38.0	0.0384	-19.5	30.7115	-1.0	121.8574	17.5	127.2000
-37.5	0.0384	-19.0	32.8255	-0.5	140.2716	18.0	125.3934
-37.0	0.0384	-18.5	32.7487	0.0	161.8350	18.5	115.8225
-36.5	0.0769	-18.0	35.9392	0.5	137.3107	19.0	112.3632
-36.0	0.2306	-17.5	41.4357	1.0	134.0823	19.5	109.7489
-35.5	0.3075	-17.0	41.0899	1.5	127.4304	20.0	99.3316
-35.0	0.1922	-16.5	47.3553	2.0	121.5485	20.5	95.1031
-34.5	0.2691	-16.0	45.8948	2.5	116.4742	21.0	87.1079
-34.0	0.5766	-15.5	45.5105	3.0	106.0956	21.5	77.5740
-33.5	1.0762	-15.0	51.6220	3.5	111.1300	22.0	73.6151
-33.0	0.8072	-14.5	51.6993	4.0	107.9778	22.5	69.1557
-32.5	1.0762	-14.0	53.1214	4.5	102.6340	23.0	61.0450
-32.0	1.0762	-13.5	61.6546	5.0	102.2871	23.5	53.0876
-31.5	1.8065	-13.0	56.2733	5.5	95.2519	24.0	51.2042
-31.0	2.4215	-12.5	64.6917	6.0	104.2847	24.5	43.6313
-30.5	4.2281	-12.0	63.9233	6.5	91.8309	25.0	42.5164
-30.0	3.8822	-11.5	64.6537	7.0	97.4435	25.5	35.7125
-29.5	4.1512	-11.0	66.9596	7.5	102.6321	26.0	33.4828
-29.0	4.8815	-10.5	67.8439	8.0	98.1732	26.5	24.2568
-28.5	4.8815	-10.0	67.5372	8.5	99.4028	27.0	23.5263
-28.0	5.9962	-9.5	76.7619	9.0	100.6709	27.5	19.5284
-27.5	6.6112	-9.0	74.2637	9.5	98.6338	28.0	16.1071
-27.0	7.2646	-8.5	79.2998	10.0	108.6280	28.5	12.5319
-26.5	7.4184	-8.0	78.4544	10.5	109.9349	29.0	10.6099
-26.0	8.6868	-7.5	79.1471	11.0	113.8945	29.5	7.4962
-25.5	9.3018	-7.0	82.2987	11.5	124.5419	30.0	6.3045
-25.0	10.6855	-6.5	77.7253	12.0	119.1609	30.5	5.0358
-24.5	12.7996	-6.0	87.4129	12.5	119.7761	31.0	3.4214
-24.0	15.9515	-5.5	85.4138	13.0	126.6960	31.5	2.9985
-23.5	15.4902	-5.0	84.7600	13.5	120.0466	32.0	1.8837
-23.0	17.7964	-4.5	96.2543	14.0	129.7340	32.5	1.1149
-22.5	19.4493	-4.0	93.5631	14.5	123.6993	33.0	0.4613
-22.0	20.1411	-3.5	93.2563	15.0	133.6943	33.5	0.5766
-21.5	22.4474	-3.0	111.9380	15.5	142.5744	34.0	0.3460
-21.0	23.8311	-2.5	108.9410	16.0	128.8906	34.5	0.0000
-20.5	26.6755	-2.0	123.0869	16.5	140.3848	35.0	0.0000
-20.0	27.7133	-1.5	117.6284	17.0	125.7006	35.5	0.0769

Station information

WMO: 717300

Name: SUDBURY
State: ON
Country: CAN
Latitude: 46.6237°N
Longitude:
80.7939°W
Elevation: 348m
Month: Annual

Annual heating design dry bulb temperature

99.6%, -28.0 °C

99%, -24.8 °C

Annual cooling design dry bulb/wet bulb temperature

29.0/201 °C

Appendix B. Compressor coefficients

Data obtained from Emerson US Product Selection Software, PSS [114]

B 1. Copeland, ZF15K4E-TF5, R404A

	Cooling capacity	Absorbed power	Current, Amps	Mass flowrate
1	49776.18097	1167.893418	1.391856449	601.5548373
2	1102.862614	4.293590753	-0.017112138	11.89236551
3	-203.1770937	29.74158499	0.237796036	0.097510498
4	9.906756281	-0.134002363	-0.000641597	0.091341541
5	-3.765788503	0.160474882	0.0009178	0.005310798
6	-0.074565207	-0.070164729	-0.002047971	-0.004043319
7	0.02974346	-0.003070058	-5.08733E-06	0.000405269
8	-0.036951224	0.000492637	3.62418E-06	5.50857E-05
9	-0.008103739	0.000558808	-1.27476E-06	-6.25628E-05
10	-0.00121992	0.000668545	8.22678E-06	6.48869E-06

Total Subcooling (°F)	0
Constant Superheat (°F)	20
Min. Cond. (°F)	15
Max. Cond. (°F)	140
Min. Evap. (°F)	-40
Max. Evap. (°F)	45

B 3. Copeland, ZP24K6E-PFV, R410A

	Cooling capacity	Absorbed power	Current, Amps	Mass flowrate
1	19849.51386	-39.5885566	-1.446613435	187.9130613
2	380.976802	-3.995073492	-0.020929607	3.656461153
3	-135.8613743	25.67845403	0.153559661	-1.253037722
4	3.523794634	-0.005611462	-6.21708E-05	0.02150379
5	-0.584030576	0.028839238	0.000235652	-0.00390118
6	0.868964775	-0.196735377	-0.001296146	0.01463835
7	0.020558952	0.00054352	2.58254E-06	0.000243719
8	-0.018855906	-0.000847168	-3.29568E-06	-4.61303E-05
9	-0.00250202	0.000148504	-1.66788E-07	3.94462E-05
10	-0.004019895	0.001117562	6.40761E-06	-6.62996E-05

Total Subcooling (°F)	15
Constant Superheat (°F)	20
Min. Cond. (°F)	80
Max. Cond. (°F)	145
Min. Evap. (°F)	-10
Max. Evap. (°F)	55

B 4. Copeland, D6TA-150X, R404A

	Cooling Capacity	Power, W	Current, A	Mass flowrate
1	140861.3749	10874.52695	20.70898603	1616.470898
2	2626.53065	-42.13192271	-0.059176514	38.52894222
3	81.58586847	-30.16141047	-0.077570381	5.104658591
4	15.87579617	-0.882704621	-0.001329658	0.346829511
5	-0.73972503	1.630051692	0.001607856	0.054459084
6	-2.184573763	1.2693035	0.001667494	-0.035021357
7	0.02281893	-0.001146642	-2.09531E-06	0.001017218
8	-0.035691039	0.007775414	1.43549E-05	-0.000380031
9	-0.034634993	0.00059398	5.6615E-06	-0.000597239
10	-0.001685519	-0.003080038	-3.14478E-06	-3.08645E-05

Total Subcooling (°F)	0
Suction Gas Return (°F)	65
Min. Cond. (°F)	60
Max. Cond. (°F)	135
Min. Evap. (°F)	-90
Max. Evap. (°F)	-10

Appendix C. Calculations for SCOP

C 1. Whitehorse, YT single-stage heat pump system and electric element auxiliary heat

j	t_j	n_j/N	BL	HH	Q_{HP}	Q_{Aux}	Q_t	PLF
1	18	0.0294		244.9	354		354	0.75
2	16	0.0417	3	346.6	334		334	0.75
3	14	0.0530	6	441.2	315		315	0.75
4	12	0.0629	8	523.6	297		297	0.75
5	10	0.0700	11	582.3	279		279	0.76
6	8	0.0662	14	550.8	263		263	0.76
7	6	0.0592	17	492.2	248		248	0.76
8	4	0.0568	20	472.8	234		234	0.76
9	2	0.0652	23	542.0	220		220	0.76
10		0.0702	25	583.8	207		207	0.77
11	- 2	0.0626	28	520.5	195		195	0.77
12	- 4	0.0482	31	401.1	183		183	0.77
13	- 6	0.0440	34	366.0	171		171	0.77
14	- 8	0.0391	37	325.3	161		161	0.78
15	- 10	0.0340	39	283.2	150		150	0.78
16	- 12	0.0302	42	251.5	140		140	0.79
17	- 14	0.0301	45	250.1		45	45	1.00
18	- 16	0.0255	48	211.8		48	48	1.00
19	- 18	0.0214	51	177.7		51	51	1.00
20	- 20	0.0174	54	144.5		54	54	1.00
21	- 22	0.0165	56	137.0		56	56	1.00
22	- 24	0.0139	59	115.9		59	59	1.00
23	- 26	0.0114	62	94.6		62	62	1.00
24	- 28	0.0090	65	74.8		65	65	1.00
25	- 30	0.0067	68	55.5		68	68	1.00
26	- 32	0.0045	70	37.2		70	70	1.00
27	- 34	0.0036	73	30.2		73	73	1.00
28	- 36	0.0025	76	20.5		76	76	1.00
29	- 38	0.0016	79	13.3		79	79	1.00
30	- 40	0.0013	82	10.8		82	82	1.00
31	- 42	0.0010	85	8.6		85	85	1.00
32	- 44	0.0007	87	5.7		87	87	1.00
33	- 46	0.0003	90	2.2		90	90	1.00
34	- 48	-	93	-		93	93	1.00
35	- 50	-	96	-		96	96	1.00
36	- 52	-	99	-		99	99	1.00
Total				**8 318**				

τ	H	COP	P_{HP}	$Effy_{Aux}$	P_{aux}	P	E
-		7.57	47	1		62	
2.93	976	7.06	47	1		63	184
7.90	2 486	6.58	48	1		64	503
14.92	4 425	6.14	48	1		64	960
23.48	6 561	5.74	49	1		64	1 505
29.45	7 758	5.36	49	1		65	1 905
33.52	8 319	5.01	50	1		65	2 187
39.88	9 323	4.68	50	1		66	2 621
55.49	12 214	4.38	50	1		66	3 669
71.47	14 801	4.10	51	1		66	4 689
75.30	14 662	3.84	51	1		66	4 963
67.97	12 428	3.59	51	1		66	4 492
72.14	12 372	3.36	51	1		66	4 778
74.20	11 912	3.15	51	1		65	4 853
74.50	11 168	2.94	51	1		65	4 867
76.13	10 627	2.75	51	1		64	4 897
250.10	11 272	-		1	45	45	11 272
211.80	10 143	-		1	48	48	10 143
177.70	9 010	-		1	51	51	9 010
144.50	7 734	-		1	54	54	7 734
137.00	7 718	-		1	56	56	7 718
115.90	6 856	-		1	59	59	6 856
94.60	5 863	-		1	62	62	5 863
74.80	4 846	-		1	65	65	4 846
55.50	3 752	-		1	68	68	3 752
37.20	2 620	-		1	70	70	2 620
30.20	2 212	-		1	73	73	2 212
20.50	1 559	-		1	76	76	1 559
13.30	1 049	-		1	79	79	1 049
10.80	882	-		1	82	82	882
8.60	727	-		1	85	85	727
5.70	498	-		1	87	87	498
2.20	198	-		1	90	90	198
-		-		1	93	93	
-		-		1	96	96	
-		-		1	99	99	
	216 970						**124 013**
						SCOP	**1.750**

C 2. Whitehorse, YT, proposed heat pump system.

j	t_j	n_j/N	BL	HH	Q_{HP}	Q_{Aux}	Q_t	PLF
1	18	0.0294		244.9	354		354	0.75
2	16	0.0417	3	346.6	334		334	0.75
3	14	0.0530	6	441.2	315		315	0.75
4	12	0.0629	8	523.6	297		297	0.75
5	10	0.0700	11	582.3	279		279	0.76
6	8	0.0662	14	550.8	263		263	0.76
7	6	0.0592	17	492.2	248		248	0.76
8	4	0.0568	20	472.8	234		234	0.76
9	2	0.0652	23	542.0	220		220	0.76
10		0.0702	25	583.8	207		207	0.77
11	- 2	0.0626	28	520.5	195		195	0.77
12	- 4	0.0482	31	401.1	183		183	0.77
13	- 6	0.0440	34	366.0	123		123	0.78
14	- 8	0.0391	37	325.3	119		119	0.79
15	- 10	0.0340	39	283.2	116		116	0.79
16	- 12	0.0302	42	251.5	113		113	0.80
17	- 14	0.0301	45	250.1	109		109	0.80
18	- 16	0.0255	48	211.8	106		106	0.81
19	- 18	0.0214	51	177.7	103		103	0.81
20	- 20	0.0174	54	144.5	100		100	0.82
21	- 22	0.0165	56	137.0	97		97	0.82
22	- 24	0.0139	59	115.9	94		94	0.83
23	- 26	0.0114	62	94.6	91		91	0.83
24	- 28	0.0090	65	74.8	89		89	0.84
25	- 30	0.0067	68	55.5	86		86	0.85
26	- 32	0.0045	70	37.2	100		100	0.84
27	- 34	0.0036	73	30.2	100		100	0.84
28	- 36	0.0025	76	20.5	100		100	0.85
29	- 38	0.0016	79	13.3	100		100	0.85
30	- 40	0.0013	82	10.8	100		100	0.85
31	- 42	0.0010	85	8.6	100		100	0.86
32	- 44	0.0007	87	5.7	100		100	0.86
33	- 46	0.0003	90	2.2	100		100	0.86
34	- 48	-	93	-	100		100	0.87
35	- 50	-	96	-	100		100	0.87
36	- 52	-	99	-	100		100	0.87
Total				**8 318**				

τ	H	COP	P_{HP}	$Effy_{Aux}$	P_{aux}	P	E
-		7.57	47	1		62	
2.93	976	7.06	47	1		63	184
7.90	2 486	6.58	48	1		64	503
14.92	4 425	6.14	48	1		64	960
23.48	6 561	5.74	49	1		64	1 505
29.45	7 758	5.36	49	1		65	1 905
33.52	8 319	5.01	50	1		65	2 187
39.88	9 323	4.68	50	1		66	2 621
55.49	12 214	4.38	50	1		66	3 669
71.47	14 801	4.10	51	1		66	4 689
75.30	14 662	3.84	51	1		66	4 963
67.97	12 428	3.59	51	1		66	4 492
100.58	12 372	3.38	36	1		47	4 695
99.75	11 912	3.29	36	1		46	4 587
96.32	11 168	3.20	36	1		46	4 418
94.40	10 627	3.12	36	1		45	4 264
103.13	11 272	3.03	36	1		45	4 647
95.58	10 143	2.95	36	1		44	4 243
87.46	9 010	2.87	36	1		44	3 876
77.34	7 734	2.79	36	1		44	3 379
79.51	7 718	2.71	36	1		44	3 471
72.76	6 856	2.63	36	1		43	3 138
64.10	5 863	2.55	36	1		43	2 770
54.60	4 846	2.47	36	1		43	2 339
43.56	3 752	2.38	36	1		43	1 854
26.20	2 620	1.94	52	1		61	1 607
22.12	2 212	1.89	53	1		63	1 395
15.59	1 559	1.84	54	1		64	998
10.49	1 049	1.79	56	1		66	689
8.82	882	1.74	57	1		67	595
7.27	727	1.70	59	1		68	497
4.98	498	1.66	60	1		70	350
1.98	198	1.62	62	1		72	143
-		1.58	63	1		73	
-		1.54	65	1		75	
-		1.50	67	1		77	
	216 970						**81 636**
						SCOP	**2.658**

C 3. Sudbury, ON, single-stage heat pump system with auxiliary electric element heat

n_i/N	BL	HH	Q_{HP}	Q_{Aux}	Q_t	PLF
0.0652	1	494.1	354		354	0.75
0.0720	4	545.5	334		334	0.75
0.0660	8	500.2	315		315	0.75
0.0630	12	477.4	297		297	0.75
0.0551	15	417.9	279		279	0.76
0.0525	19	397.6	263		263	0.76
0.0519	23	393.7	248		248	0.76
0.0565	26	427.8	234		234	0.76
0.0659	30	499.5	220		220	0.77
0.0741	34	561.3	207		207	0.77
0.0609	37	461.6	195		195	0.77
0.0485	41	367.8	183		183	0.78
0.0439	45	332.8	171		171	0.78
0.0411	48	311.2	161		161	0.79
0.0368	52	279.1	150		150	0.79
0.0329	56	249.5	140		140	0.80
0.0288	59	218.1		59	59	1.00
0.0237	63	179.8		63	63	1.00
0.0189	67	142.9		67	67	1.00
0.0144	71	108.9		71	71	1.00
0.0105	74	79.8		74	74	1.00
0.0072	78	54.9		78	78	1.00
0.0043	82	32.7		82	82	1.00
0.0030	85	22.4		85	85	1.00
0.0019	89	14.7		89	89	1.00
0.0006	93	4.8		93	93	1.00
0.0003	96	2.1		96	96	1.00
0.0001	100	0.7		100	100	1.00
-	104	0.1		104	104	1.00
-	107	-		107	107	1.00
-	111	-		111	111	1.00
-	115	-		115	115	1.00
-	118	-		118	118	1.00
-	122	-		122	122	1.00
-	126	-		126	126	1.00
-	129	-		129	129	1.00
		7 579				

τ	H	COP	P_{HP}	$Effy_{Aux}$	P_{aux}	P	E
0.77	273	7.57	47	1.00		62	48
6.93	2 311	7.06	47	1.00		63	436
12.59	3 961	6.58	48	1.00		64	802
18.68	5 539	6.14	48	1.00		64	1 202
22.86	6 388	5.74	49	1.00		64	1 466
28.63	7 542	5.36	49	1.00		65	1 852
35.94	8 918	5.01	50	1.00		65	2 344
48.20	11 266	4.68	50	1.00		66	3 167
68.12	14 994	4.38	50	1.00		65	4 446
91.34	18 917	4.10	51	1.00		66	5 993
88.63	17 257	3.84	51	1.00		66	5 841
82.61	15 105	3.59	51	1.00		65	5 390
86.85	14 893	3.36	51	1.00		65	5 678
93.88	15 073	3.15	51	1.00		65	6 063
97.03	14 546	2.94	51	1.00		65	6 259
99.74	13 922	2.75	51	1.00		64	6 335
218.10	12 974	-		1.00	59	59	12 974
179.80	11 358	-		1.00	63	63	11 358
142.90	9 553	-		1.00	67	67	9 553
108.90	7 681	-		1.00	71	71	7 681
79.80	5 923	-		1.00	74	74	5 923
54.90	4 277	-		1.00	78	78	4 277
32.70	2 668	-		1.00	82	82	2 668
22.40	1 910	-		1.00	85	85	1 910
14.70	1 308	-		1.00	89	89	1 308
4.80	445	-		1.00	93	93	445
2.10	202	-		1.00	96	96	202
0.70	70	-		1.00	100	100	70
0.10	10	-		1.00	104	104	10
-		-		1.00	107	107	
-		-		1.00	111	111	
-		-		1.00	115	115	
-		-		1.00	118	118	
-		-		1.00	122	122	
-		-		1.00	126	126	
-		-		1.00	129	129	
	229 282						**115 699**

SCOP	**1.982**

C 4. Sudbury, ON, proposed heat pump system.

j	t_j	n_j/N	BL	HH	Q_{HP}	Q_{Aux}	Q_t	PLF
1	18	0.0652	1	494.1	354		354	0.75
2	16	0.0720	4	545.5	334		334	0.75
3	14	0.0660	8	500.2	315		315	0.75
4	12	0.0630	11	477.4	297		297	0.75
5	10	0.0551	15	417.9	279		279	0.76
6	8	0.0525	19	397.6	263		263	0.76
7	6	0.0519	22	393.7	248		248	0.76
8	4	0.0565	26	427.8	234		234	0.76
9	2	0.0659	30	499.5	220		220	0.77
10		0.0741	33	561.3	207		207	0.77
11	- 2	0.0609	37	461.6	195		195	0.77
12	- 4	0.0485	41	367.8	183		183	0.78
13	- 6	0.0439	44	332.8	123		123	0.80
14	- 8	0.0411	48	311.2	119		119	0.80
15	- 10	0.0368	52	279.1	116		116	0.81
16	- 12	0.0329	55	249.5	113		113	0.81
17	- 14	0.0288	59	218.1	109		109	0.82
18	- 16	0.0237	63	179.8	106		106	0.82
19	- 18	0.0189	66	142.9	103		103	0.83
20	- 20	0.0144	70	108.9	100		100	0.84
21	- 22	0.0105	74	79.8	97		97	0.84
22	- 24	0.0072	77	54.9	94		94	0.85
23	- 26	0.0043	81	32.7	91		91	0.86
24	- 28	0.0030	84	22.4	89		89	0.87
25	- 30	0.0019	88	14.7	86	2	88	1.00
26	- 32	0.0006	92	4.8	100		100	0.86
27	- 34	0.0003	95	2.1	100		100	0.87
28	- 36	0.0001	99	0.7	100		100	0.87
29	- 38	-	103	0.1	100	3	103	1.00
30	- 40	-	106	-	100	6	106	1.00
31	- 42	-	110	-	100	10	110	1.00
32	- 44	-	114	-	100	14	114	1.00
33	- 46	-	117	-	100	17	117	1.00
34	- 48	-	121	-	100	21	121	1.00
35	- 50	-	125	-	100	25	125	1.00
36	- 52	-	128	-	100	28	128	1.00
Total				**7 579**				

τ	H	COP_{HP}	P_{HP}	$Effy_{Aux}$	P_{aux}	P	E
0.76	270	7.57	47	1		62	48
6.86	2 290	7.06	47	1		63	433
12.48	3 925	6.58	48	1		64	795
18.51	5 488	6.14	48	1		64	1 191
22.65	6 330	5.74	49	1		64	1 452
28.37	7 473	5.36	49	1		65	1 836
35.61	8 837	5.01	50	1		65	2 323
47.76	11 163	4.68	50	1		66	3 138
67.50	14 857	4.38	50	1		65	4 405
90.51	18 744	4.10	51	1		66	5 939
87.82	17 099	3.84	51	1		66	5 788
81.86	14 967	3.59	51	1		65	5 341
119.98	14 757	3.38	36	1		46	5 461
125.06	14 935	3.29	36	1		45	5 680
124.30	14 413	3.20	36	1		45	5 561
122.55	13 795	3.12	36	1		45	5 468
117.62	12 855	3.03	36	1		44	5 171
106.06	11 254	2.95	36	1		44	4 651
91.89	9 466	2.87	36	1		43	3 974
76.11	7 611	2.79	36	1		43	3 246
60.45	5 869	2.71	36	1		43	2 576
44.97	4 238	2.63	36	1		42	1 894
28.90	2 643	2.55	36	1		42	1 205
21.32	1 893	2.47	36	1		41	882
14.70	1 296	2.38	36	1	2	38	561
4.41	441	1.94	52	1		60	264
2.00	200	1.89	53	1		61	122
0.69	69	1.84	54	1		63	43
0.10	10	1.79	56	1	3	59	6
-		1.74	57	1	6	64	
-		1.70	59	1	10	69	
-		1.66	60	1	14	74	
-		1.62	62	1	17	79	
-		1.58	63	1	21	84	
-		1.54	65	1	25	90	
-		1.50	67	1	28	95	
	227 190						**79 451**
						SCOP	**2.859**

C 5. Whitehorse, YT. GOODMAN single-stage heat pump system model GSZ160241B, AHRI Certificate # 201667130 and electric element auxiliary heat

j	t_j	n_j/N	BL	HH	Q_{HP}	Q_{Aux}	Q_t	PLF
1	18	0.0294	0.00	244.90	3.94	0.00	3.94	0.75
2	16	0.0417	0.03	346.60	3.79	0.00	3.79	0.75
3	14	0.0530	0.06	441.20	3.64	0.00	3.64	0.75
4	12	0.0629	0.08	523.60	3.48	0.00	3.48	0.75
5	10	0.0700	0.11	582.30	3.33	0.00	3.33	0.75
6	8	0.0662	0.14	550.80	3.18	0.00	3.18	0.76
7	6	0.0592	0.17	492.20	3.02	0.00	3.02	0.76
8	4	0.0568	0.20	472.80	2.87	0.00	2.87	0.76
9	2	0.0652	0.23	542.00	2.72	0.00	2.72	0.76
10		0.0702	0.25	583.80	2.57	0.00	2.57	0.76
11	- 2	0.0626	0.28	520.50	2.41	0.00	2.41	0.76
12	- 4	0.0482	0.31	401.10	2.26	0.00	2.26	0.77
13	- 6	0.0440	0.34	366.00	2.11	0.00	2.11	0.77
14	- 8	0.0391	0.37	325.30	1.95	0.00	1.95	0.77
15	- 10	0.0340	0.39	283.20	1.80	0.00	1.80	0.78
16	- 12	0.0302	0.42	251.50	1.65	0.00	1.65	0.78
17	- 14	0.0301	0.45	250.10	1.51	0.00	1.51	0.79
18	- 16	0.0255	0.48	211.80	1.34	0.00	1.34	0.79
19	- 18	0.0214	0.51	177.70	1.17	0.00	1.17	0.80
20	- 20	0.0174	0.54	144.50	1.00	0.00	1.00	0.82
21	- 22	0.0165	0.56	137.00	0.00	0.56	0.56	1.00
22	- 24	0.0139	0.59	115.90	0.00	0.59	0.59	1.00
23	- 26	0.0114	0.62	94.60	0.00	0.62	0.62	1.00
24	- 28	0.0090	0.65	74.80	0.00	0.65	0.65	1.00
25	- 30	0.0067	0.68	55.50	0.00	0.68	0.68	1.00
26	- 32	0.0045	0.70	37.20	0.00	0.70	0.70	1.00
27	- 34	0.0036	0.73	30.20	0.00	0.73	0.73	1.00
28	- 36	0.0025	0.76	20.50	0.00	0.76	0.76	1.00
29	- 38	0.0016	0.79	13.30	0.00	0.79	0.79	1.00
30	- 40	0.0013	0.82	10.80	0.00	0.82	0.82	1.00
31	- 42	0.0010	0.85	8.60	0.00	0.85	0.85	1.00
32	- 44	0.0007	0.87	5.70	0.00	0.87	0.87	1.00
33	- 46	0.0003	0.90	2.20	0.00	0.90	0.90	1.00
34	- 48	-	0.93	0.00	0.00	0.93	0.93	1.00
35	- 50	-	0.96	0.00	0.00	0.96	0.96	1.00
36	- 52	-	0.99	0.00	0.00	0.99	0.99	1.00
Total		**1.0001**		**8 318**				

τ	H	COP	P_{HP}	$Effy_{Aux}$	P_{aux}	P	E
0.00	0.00	4.14	0.95	1.00	0.00	1.27	0.00
2.58	9.76	4.00	0.95	1.00	0.00	1.26	3.26
6.84	24.86	3.85	0.94	1.00	0.00	1.26	8.61
12.70	44.25	3.70	0.94	1.00	0.00	1.25	15.94
19.70	65.61	3.56	0.94	1.00	0.00	1.25	24.61
24.42	77.58	3.41	0.93	1.00	0.00	1.23	29.95
27.51	83.19	3.26	0.93	1.00	0.00	1.22	33.57
32.47	93.23	3.11	0.92	1.00	0.00	1.21	39.39
44.94	122.14	2.97	0.92	1.00	0.00	1.21	54.17
57.70	148.01	2.82	0.91	1.00	0.00	1.20	69.06
60.79	146.62	2.67	0.90	1.00	0.00	1.19	72.17
55.02	124.28	2.53	0.89	1.00	0.00	1.16	63.90
58.75	123.72	2.38	0.89	1.00	0.00	1.15	67.54
61.00	119.12	2.23	0.88	1.00	0.00	1.14	69.31
61.94	111.68	2.08	0.87	1.00	0.00	1.11	68.97
64.25	106.27	1.92	0.86	1.00	0.00	1.11	71.07
74.90	112.72	1.76	0.86	1.00	0.00	1.08	81.12
75.47	101.43	1.58	0.85	1.00	0.00	1.07	81.05
76.88	90.10	1.39	0.84	1.00	0.00	1.05	80.91
77.34	77.34	1.20	0.83	1.00	0.00	1.02	78.60
137.00	77.18	0.00	0.00	1.00	0.56	0.56	77.18
115.90	68.56	0.00	0.00	1.00	0.59	0.59	68.56
94.60	58.63	0.00	0.00	1.00	0.62	0.62	58.63
74.80	48.46	0.00	0.00	1.00	0.65	0.65	48.46
55.50	37.52	0.00	0.00	1.00	0.68	0.68	37.52
37.20	26.20	0.00	0.00	1.00	0.70	0.70	26.20
30.20	22.12	0.00	0.00	1.00	0.73	0.73	22.12
20.50	15.59	0.00	0.00	1.00	0.76	0.76	15.59
13.30	10.49	0.00	0.00	1.00	0.79	0.79	10.49
10.80	8.82	0.00	0.00	1.00	0.82	0.82	8.82
8.60	7.27	0.00	0.00	1.00	0.85	0.85	7.27
5.70	4.98	0.00	0.00	1.00	0.87	0.87	4.98
2.20	1.98	0.00	0.00	1.00	0.90	0.90	1.98
0.00	0.00	0.00	0.00	1.00	0.93	0.93	0.00
0.00	0.00	0.00	0.00	1.00	0.96	0.96	0.00
0.00	0.00	0.00	0.00	1.00	0.99	0.99	0.00
	2 170						**1400.99**
						SCOP	**1.549**

C 6. Whitehorse, YT NEEP listed system MRCOOL plus auxiliary electric heat

j	t_j	n_j/N	BL	HH	Q_{HP}	Q_{Aux}	Q_t	PLF
1	18	0.0294	0.00	244.90	2.41	0.00	2.41	0.75
2	16	0.0417	0.03	346.60	2.31	0.00	2.31	0.75
3	14	0.0530	0.06	441.20	2.22	0.00	2.22	0.75
4	12	0.0629	0.08	523.60	2.12	0.00	2.12	0.75
5	10	0.0700	0.11	582.30	2.03	0.00	2.03	0.76
6	8	0.0662	0.14	550.80	1.94	0.00	1.94	0.76
7	6	0.0592	0.17	492.20	1.84	0.00	1.84	0.76
8	4	0.0568	0.20	472.80	1.75	0.00	1.75	0.76
9	2	0.0652	0.23	542.00	1.65	0.00	1.65	0.77
10		0.0702	0.25	583.80	1.56	0.00	1.56	0.77
11	- 2	0.0626	0.28	520.50	1.47	0.00	1.47	0.77
12	- 4	0.0482	0.31	401.10	1.37	0.00	1.37	0.78
13	- 6	0.0440	0.34	366.00	1.28	0.00	1.28	0.78
14	- 8	0.0391	0.37	325.30	1.18	0.00	1.18	0.79
15	- 10	0.0340	0.39	283.20	1.17	0.00	1.17	0.79
16	- 12	0.0302	0.42	251.50	1.17	0.00	1.17	0.80
17	- 14	0.0301	0.45	250.10	1.17	0.00	1.17	0.80
18	- 16	0.0255	0.48	211.80	1.13	0.00	1.13	0.80
19	- 18	0.0214	0.51	177.70	1.07	0.00	1.07	0.81
20	- 20	0.0174	0.54	144.50	1.00	0.00	1.00	0.82
21	- 22	0.0165	0.56	137.00	0.93	0.00	0.93	0.83
22	- 24	0.0139	0.59	115.90	0.86	0.00	0.86	0.84
23	- 26	0.0114	0.62	94.60	0.80	0.00	0.80	0.85
24	- 28	0.0090	0.65	74.80	0.73	0.00	0.73	0.86
25	- 30	0.0067	0.68	55.50	0.66	0.02	0.68	1.00
26	- 32	0.0045	0.70	37.20	0.00	0.70	0.70	1.00
27	- 34	0.0036	0.73	30.20	0.00	0.73	0.73	1.00
28	- 36	0.0025	0.76	20.50	0.00	0.76	0.76	1.00
29	- 38	0.0016	0.79	13.30	0.00	0.79	0.79	1.00
30	- 40	0.0013	0.82	10.80	0.00	0.82	0.82	1.00
31	- 42	0.0010	0.85	8.60	0.00	0.85	0.85	1.00
32	- 44	0.0007	0.87	5.70	0.00	0.87	0.87	1.00
33	- 46	0.0003	0.90	2.20	0.00	0.90	0.90	1.00
34	- 48	-	0.93	0.00	0.00	0.93	0.93	1.00
35	- 50	-	0.96	0.00	0.00	0.96	0.96	1.00
36	- 52	-	0.99	0.00	0.00	0.99	0.99	1.00
Total		**1.0001**		**8 318**				

τ	H	COP	P_{HP}	$Effy_{Aux}$	P_{aux}	P	E
0.00	0.00	3.76	0.64	1.00	0.00	0.85	0.00
4.22	9.76	3.64	0.64	1.00	0.00	0.85	3.58
11.21	24.86	3.51	0.63	1.00	0.00	0.84	9.44
20.83	44.25	3.38	0.63	1.00	0.00	0.84	17.43
32.32	65.61	3.26	0.62	1.00	0.00	0.82	26.50
40.07	77.58	3.13	0.62	1.00	0.00	0.81	32.60
45.16	83.19	3.01	0.61	1.00	0.00	0.81	36.43
53.33	93.23	2.88	0.61	1.00	0.00	0.80	42.62
73.85	122.14	2.75	0.60	1.00	0.00	0.78	57.64
94.88	148.01	2.63	0.59	1.00	0.00	0.77	73.22
100.01	146.62	2.50	0.59	1.00	0.00	0.76	76.23
90.59	124.28	2.37	0.58	1.00	0.00	0.74	67.18
96.81	123.72	2.25	0.57	1.00	0.00	0.73	70.65
100.61	119.12	2.12	0.56	1.00	0.00	0.71	71.16
95.54	111.68	2.15	0.54	1.00	0.00	0.69	65.82
90.90	106.27	2.21	0.53	1.00	0.00	0.66	60.24
96.51	112.72	2.26	0.52	1.00	0.00	0.65	62.29
89.44	101.43	2.24	0.51	1.00	0.00	0.63	56.73
84.52	90.10	2.13	0.50	1.00	0.00	0.62	52.32
77.44	77.34	2.02	0.50	1.00	0.00	0.60	46.76
82.91	77.18	1.91	0.49	1.00	0.00	0.59	48.76
79.43	68.56	1.80	0.48	1.00	0.00	0.57	45.39
73.70	58.63	1.69	0.47	1.00	0.00	0.55	40.84
66.60	48.46	1.58	0.46	1.00	0.00	0.54	35.69
55.50	37.52	1.47	0.45	1.00	0.02	0.47	25.81
37.20	26.20	0.00	0.00	1.00	0.70	0.70	26.20
30.20	22.12	0.00	0.00	1.00	0.73	0.73	22.12
20.50	15.59	0.00	0.00	1.00	0.76	0.76	15.59
13.30	10.49	0.00	0.00	1.00	0.79	0.79	10.49
10.80	8.82	0.00	0.00	1.00	0.82	0.82	8.82
8.60	7.27	0.00	0.00	1.00	0.85	0.85	7.27
5.70	4.98	0.00	0.00	1.00	0.87	0.87	4.98
2.20	1.98	0.00	0.00	1.00	0.90	0.90	1.98
0.00	0.00	0.00	0.00	1.00	0.93	0.93	0.00
0.00	0.00	0.00	0.00	1.00	0.96	0.96	0.00
0.00	0.00	0.00	0.00	1.00	0.99	0.99	0.00
	2 170						**1222.78**
						SCOP	**1.774**

C 7. Whitehorse, YT. Proposed system fan power considered.

j	t_j	n_j/N	BL	HH	Q_{HP}	Q_{Aux}	Q_t	PLF
1	18	0.0294		244.9	204		204	0.75
2	16	0.0417	3	346.6	194		194	0.75
3	14	0.0530	6	441.2	185		185	0.75
4	12	0.0629	8	523.6	176		176	0.76
5	10	0.0700	11	582.3	167		167	0.76
6	8	0.0662	14	550.8	158		158	0.76
7	6	0.0592	17	492.2	150		150	0.76
8	4	0.0568	20	472.8	142		142	0.77
9	2	0.0652	23	542.0	135		135	0.77
10		0.0702	25	583.8	128		128	0.77
11	- 2	0.0626	28	520.5	121		121	0.78
12	- 4	0.0482	31	401.1	114		114	0.78
13	- 6	0.0440	34	366.0	107		107	0.79
14	- 8	0.0391	37	325.3	101		101	0.80
15	- 10	0.0340	39	283.2	95		95	0.80
16	- 12	0.0302	42	251.5	93		93	0.81
17	- 14	0.0301	45	250.1	103		103	0.80
18	- 16	0.0255	48	211.8	101		101	0.81
19	- 18	0.0214	51	177.7	100		100	0.81
20	- 20	0.0174	54	144.5	99		99	0.82
21	- 22	0.0165	56	137.0	99		99	0.82
22	- 24	0.0139	59	115.9	98		98	0.83
23	- 26	0.0114	62	94.6	98		98	0.83
24	- 28	0.0090	65	74.8	97		97	0.83
25	- 30	0.0067	68	55.5	96		96	0.84
26	- 32	0.0045	70	37.2	93		93	0.84
27	- 34	0.0036	73	30.2	93		93	0.85
28	- 36	0.0025	76	20.5	93		93	0.85
29	- 38	0.0016	79	13.3	93		93	0.86
30	- 40	0.0013	82	10.8	93		93	0.86
31	- 42	0.0010	85	8.6	93		93	0.86
32	- 44	0.0007	87	5.7	93		93	0.87
33	- 46	0.0003	90	2.2	93		93	0.87
34	- 48	-	93	-	93		93	0.87
35	- 50	-	96	-	93	3	96	1.00
36	- 52	-	99	-	93	5	99	1.00
Total				**8 318**				

τ	H	COP	P_{HP}	$Effy_{Aux}$	P_{aux}	P	E
-		5.10	40	1.00		53	
5.02	976	4.93	39	1.00		53	264
13.45	2 486	4.76	39	1.00		52	696
25.19	4 425	4.60	38	1.00		50	1 266
39.32	6 561	4.43	38	1.00		50	1 949
48.98	7 758	4.26	37	1.00		49	2 394
55.38	8 319	4.10	37	1.00		48	2 670
65.49	9 323	3.94	36	1.00		47	3 076
90.60	12 214	3.78	36	1.00		46	4 201
116.04	14 801	3.62	35	1.00		46	5 311
121.62	14 662	3.47	35	1.00		45	5 425
109.19	12 428	3.31	34	1.00		44	4 808
115.29	12 372	3.17	34	1.00		43	4 945
117.92	11 912	3.02	33	1.00		42	4 924
117.82	11 168	2.88	33	1.00		41	4 849
114.67	10 627	2.85	33	1.00		40	4 607
109.97	11 272	2.22	46	1.00		58	6 350
100.64	10 143	2.19	46	1.00		57	5 728
90.10	9 010	2.17	46	1.00		57	5 136
77.79	7 734	2.15	46	1.00		56	4 391
78.10	7 718	2.13	46	1.00		57	4 419
69.79	6 856	2.11	47	1.00		56	3 913
60.04	5 863	2.09	47	1.00		56	3 380
49.93	4 846	2.07	47	1.00		57	2 822
38.89	3 752	2.05	47	1.00		56	2 184
28.11	2 620	1.90	49	1.00		59	1 645
23.73	2 212	1.86	50	1.00		59	1 399
16.73	1 559	1.82	51	1.00		60	1 006
11.26	1 049	1.79	52	1.00		61	683
9.47	882	1.75	53	1.00		62	587
7.80	727	1.71	54	1.00		63	494
5.34	498	1.67	56	1.00		64	342
2.13	198	1.64	57	1.00		66	139
-		1.60	58	1.00		67	
-		1.56	60	1.00	3	62	
-		1.56	60	1.00	5	65	
	216 970						**96 001**
						SCOP	**2.260**

C 8. Sudbury, ON, GOODMAN single-stage heat pump system model GSZ160241B, AHRI Certificate # 201667130 and electric element auxiliary heat

j	t_j	n_j/N	BL	HH	Q_{HP}	Q_{Aux}	Q_t	PLF
1	18	0.0652	0.01	494.1	3.94	0.00	3.94	0.75
2	16	0.0720	0.04	545.5	3.79	0.00	3.79	0.75
3	14	0.0660	0.08	500.2	3.64	0.00	3.64	0.75
4	12	0.0630	0.11	477.4	3.48	0.00	3.48	0.75
5	10	0.0551	0.15	417.9	3.33	0.00	3.33	0.76
6	8	0.0525	0.19	397.6	3.18	0.00	3.18	0.76
7	6	0.0519	0.22	393.7	3.02	0.00	3.02	0.76
8	4	0.0565	0.26	427.8	2.87	0.00	2.87	0.76
9	2	0.0659	0.30	499.5	2.72	0.00	2.72	0.76
10		0.0741	0.33	561.3	2.57	0.00	2.57	0.77
11	- 2	0.0609	0.37	461.6	2.41	0.00	2.41	0.77
12	- 4	0.0485	0.41	367.8	2.26	0.00	2.26	0.77
13	- 6	0.0439	0.44	332.8	2.11	0.00	2.11	0.78
14	- 8	0.0411	0.48	311.2	1.95	0.00	1.95	0.78
15	- 10	0.0368	0.52	279.1	1.80	0.00	1.80	0.79
16	- 12	0.0329	0.55	249.5	1.65	0.00	1.65	0.79
17	- 14	0.0288	0.59	218.1	1.51	0.00	1.51	0.80
18	- 16	0.0237	0.63	179.8	1.34	0.00	1.34	0.81
19	- 18	0.0189	0.66	142.9	1.17	0.00	1.17	0.82
20	- 20	0.0144	0.70	108.9	1.00	0.00	1.00	0.84
21	- 22	0.0105	0.74	79.8	0.00	0.74	0.74	1.00
22	- 24	0.0072	0.77	54.9	0.00	0.77	0.77	1.00
23	- 26	0.0043	0.81	32.7	0.00	0.81	0.81	1.00
24	- 28	0.0030	0.84	22.4	0.00	0.84	0.84	1.00
25	- 30	0.0019	0.88	14.7	0.00	0.88	0.88	1.00
26	- 32	0.0006	0.92	4.8	0.00	0.92	0.92	1.00
27	- 34	0.0003	0.95	2.1	0.00	0.95	0.95	1.00
28	- 36	0.0001	0.99	0.7	0.00	0.99	0.99	1.00
29	- 38	-	1.03	0.1	0.00	1.03	1.03	1.00
30	- 40	-	1.06	-	0.00	1.06	1.06	1.00
31	- 42	-	1.10	-	0.00	1.10	1.10	1.00
32	- 44	-	1.14	-	0.00	1.14	1.14	1.00
33	- 46	-	1.17	-	0.00	1.17	1.17	1.00
34	- 48	-	1.21	-	0.00	1.21	1.21	1.00
35	- 50	-	1.25	-	0.00	1.25	1.25	1.00
36	- 52	-	1.28	-	0.00	1.28	1.28	1.00
Total				**7 579**				

τ	H	COP_{HP}	P_{HP}	$Effy_{Aux}$	P_{aux}	P	E
0.69	3	4.14	0.95	1.00	0.00	1.27	0.87
6.04	23	4.00	0.95	1.00	0.00	1.26	7.64
10.79	39	3.85	0.94	1.00	0.00	1.26	13.60
15.76	55	3.70	0.94	1.00	0.00	1.25	19.77
19.01	63	3.56	0.94	1.00	0.00	1.23	23.43
23.52	75	3.41	0.93	1.00	0.00	1.23	28.85
29.22	88	3.26	0.93	1.00	0.00	1.22	35.66
38.88	112	3.11	0.92	1.00	0.00	1.21	47.17
54.66	149	2.97	0.92	1.00	0.00	1.21	65.89
73.08	187	2.82	0.91	1.00	0.00	1.18	86.32
70.89	171	2.67	0.90	1.00	0.00	1.17	83.08
66.26	150	2.53	0.89	1.00	0.00	1.16	76.95
70.07	148	2.38	0.89	1.00	0.00	1.13	79.53
76.47	149	2.23	0.88	1.00	0.00	1.12	85.79
79.94	144	2.08	0.87	1.00	0.00	1.10	87.88
83.41	138	1.92	0.86	1.00	0.00	1.09	91.09
85.42	129	1.76	0.86	1.00	0.00	1.07	91.35
83.73	113	1.58	0.85	1.00	0.00	1.05	87.71
80.77	95	1.39	0.84	1.00	0.00	1.03	82.93
76.11	76	1.20	0.83	1.00	0.00	0.99	75.51
79.80	59	-	0.00	1.00	0.74	0.74	58.69
54.90	42	-	0.00	1.00	0.77	0.77	42.38
32.70	26	-	0.00	1.00	0.81	0.81	26.43
22.40	19	-	0.00	1.00	0.84	0.84	18.93
14.70	13	-	0.00	1.00	0.88	0.88	12.96
4.80	4	-	0.00	1.00	0.92	0.92	4.41
2.10	2	-	0.00	1.00	0.95	0.95	2.00
0.70	1	-	0.00	1.00	0.99	0.99	0.69
0.10		-	0.00	1.00	1.03	1.03	0.10
-		-	0.00	1.00	1.06	1.06	0.00
-		-	0.00	1.00	1.10	1.10	0.00
-		-	0.00	1.00	1.14	1.14	0.00
-		-	0.00	1.00	1.17	1.17	0.00
-		-	0.00	1.00	1.21	1.21	0.00
-		-	0.00	1.00	1.25	1.25	0.00
-		-	0.00	1.00	1.28	1.28	0.00
	2 272						**1 338**
						SCOP	**1.698**

C 9. Sudbury, ON, NEEP listed system MRCOOL plus auxiliary electric heat

j	t_j	n_j/N	BL	HH	Q_{HP}	Q_{Aux}	Q_t	PLF
1	18	0.0652	0.01	494.1	2.41	0.00	2.41	0.75
2	16	0.0720	0.04	545.5	2.31	0.00	2.31	0.75
3	14	0.0660	0.08	500.2	2.22	0.00	2.22	0.75
4	12	0.0630	0.11	477.4	2.12	0.00	2.12	0.76
5	10	0.0551	0.15	417.9	2.03	0.00	2.03	0.76
6	8	0.0525	0.19	397.6	1.94	0.00	1.94	0.76
7	6	0.0519	0.22	393.7	1.84	0.00	1.84	0.77
8	4	0.0565	0.26	427.8	1.75	0.00	1.75	0.77
9	2	0.0659	0.30	499.5	1.65	0.00	1.65	0.77
10		0.0741	0.33	561.3	1.56	0.00	1.56	0.78
11	- 2	0.0609	0.37	461.6	1.47	0.00	1.47	0.78
12	- 4	0.0485	0.41	367.8	1.37	0.00	1.37	0.79
13	- 6	0.0439	0.44	332.8	1.28	0.00	1.28	0.79
14	- 8	0.0411	0.48	311.2	1.18	0.00	1.18	0.80
15	- 10	0.0368	0.52	279.1	1.17	0.00	1.17	0.81
16	- 12	0.0329	0.55	249.5	1.17	0.00	1.17	0.81
17	- 14	0.0288	0.59	218.1	1.17	0.00	1.17	0.81
18	- 16	0.0237	0.63	179.8	1.13	0.00	1.13	0.82
19	- 18	0.0189	0.66	142.9	1.07	0.00	1.07	0.83
20	- 20	0.0144	0.70	108.9	1.00	0.00	1.00	0.84
21	- 22	0.0105	0.74	79.8	0.93	0.00	0.93	0.85
22	- 24	0.0072	0.77	54.9	0.86	0.00	0.86	0.86
23	- 26	0.0043	0.81	32.7	0.80	0.01	0.81	1.00
24	- 28	0.0030	0.84	22.4	0.73	0.12	0.84	1.00
25	- 30	0.0019	0.88	14.7	0.66	0.22	0.88	1.00
26	- 32	0.0006	0.92	4.8	0.00	0.92	0.92	1.00
27	- 34	0.0003	0.95	2.1	0.00	0.95	0.95	1.00
28	- 36	0.0001	0.99	0.7	0.00	0.99	0.99	1.00
29	- 38	-	1.03	0.1	0.00	1.03	1.03	1.00
30	- 40	-	1.06	-	0.00	1.06	1.06	1.00
31	- 42	-	1.10	-	0.00	1.10	1.10	1.00
32	- 44	-	1.14	-	0.00	1.14	1.14	1.00
33	- 46	-	1.17	-	0.00	1.17	1.17	1.00
34	- 48	-	1.21	-	0.00	1.21	1.21	1.00
35	- 50	-	1.25	-	0.00	1.25	1.25	1.00
36	- 52	-	1.28	-	0.00	1.28	1.28	1.00
Total				**7 579**				

τ	H	COP_{HP}	P_{HP}	$Effy_{Aux}$	P_{aux}	P	E
1.12	3	3.76	0.64	1.00	0.00	0.85	0.96
9.90	23	3.64	0.64	1.00	0.00	0.85	8.39
17.70	39	3.51	0.63	1.00	0.00	0.84	14.91
25.84	55	3.38	0.63	1.00	0.00	0.83	21.34
31.18	63	3.26	0.62	1.00	0.00	0.82	25.56
38.60	75	3.13	0.62	1.00	0.00	0.81	31.41
47.97	88	3.01	0.61	1.00	0.00	0.80	38.19
63.86	112	2.88	0.61	1.00	0.00	0.79	50.37
89.83	149	2.75	0.60	1.00	0.00	0.78	70.11
120.15	187	2.63	0.59	1.00	0.00	0.76	91.55
116.64	171	2.50	0.59	1.00	0.00	0.75	87.76
109.09	150	2.37	0.58	1.00	0.00	0.73	79.87
115.47	148	2.25	0.57	1.00	0.00	0.72	83.21
126.14	149	2.12	0.56	1.00	0.00	0.70	88.10
123.30	144	2.15	0.54	1.00	0.00	0.67	82.84
118.01	138	2.21	0.53	1.00	0.00	0.65	77.24
110.06	129	2.26	0.52	1.00	0.00	0.64	70.16
99.24	113	2.24	0.51	1.00	0.00	0.62	61.41
88.80	95	2.13	0.50	1.00	0.00	0.60	53.64
76.21	76	2.02	0.50	1.00	0.00	0.59	44.92
63.04	59	1.91	0.49	1.00	0.00	0.57	36.20
49.09	42	1.80	0.48	1.00	0.00	0.56	27.41
32.70	26	1.69	0.47	1.00	0.01	0.48	15.82
22.40	19	1.58	0.46	1.00	0.12	0.58	12.95
14.70	13	1.47	0.45	1.00	0.22	0.67	9.85
4.80	4	-	0.00	1.00	0.92	0.92	4.41
2.10	2	-	0.00	1.00	0.95	0.95	2.00
0.70	1	-	0.00	1.00	0.99	0.99	0.69
0.10		-	0.00	1.00	1.03	1.03	0.10
-		-	0.00	1.00	1.06	1.06	0.00
-		-	0.00	1.00	1.10	1.10	0.00
-		-	0.00	1.00	1.14	1.14	0.00
-		-	0.00	1.00	1.17	1.17	0.00
-		-	0.00	1.00	1.21	1.21	0.00
-		-	0.00	1.00	1.25	1.25	0.00
-		-	0.00	1.00	1.28	1.28	0.00
	2 272						**1 191**
						SCOP	**1.907**

C 10. Sudbury, ON, Proposed system fan power considered.

j	t_j	n_j/N	BL	HH	Q_{HP}	Q_{Aux}	Q_t	PLF
1	18	0.0652	1	494.1	204		204	0.75
2	16	0.0720	4	545.5	194		194	0.75
3	14	0.0660	8	500.2	185		185	0.76
4	12	0.0630	11	477.4	176		176	0.76
5	10	0.0551	15	417.9	167		167	0.76
6	8	0.0525	19	397.6	158		158	0.76
7	6	0.0519	22	393.7	150		150	0.77
8	4	0.0565	26	427.8	142		142	0.77
9	2	0.0659	30	499.5	135		135	0.78
10		0.0741	33	561.3	128		128	0.78
11	- 2	0.0609	37	461.6	121		121	0.79
12	- 4	0.0485	41	367.8	114		114	0.79
13	- 6	0.0439	44	332.8	107		107	0.80
14	- 8	0.0411	48	311.2	101		101	0.81
15	- 10	0.0368	52	279.1	95		95	0.82
16	- 12	0.0329	55	249.5	93		93	0.82
17	- 14	0.0288	59	218.1	103		103	0.82
18	- 16	0.0237	63	179.8	101		101	0.83
19	- 18	0.0189	66	142.9	100		100	0.83
20	- 20	0.0144	70	108.9	99		99	0.84
21	- 22	0.0105	74	79.8	99		99	0.84
22	- 24	0.0072	77	54.9	98		98	0.85
23	- 26	0.0043	81	32.7	98		98	0.85
24	- 28	0.0030	84	22.4	97		97	0.86
25	- 30	0.0019	88	14.7	96		96	0.86
26	- 32	0.0006	92	4.8	93		93	0.87
27	- 34	0.0003	95	2.1	93	2	95	1.00
28	- 36	0.0001	99	0.7	93	6	99	1.00
29	- 38	-	103	0.1	93	10	103	1.00
30	- 40	-	106	-	93	13	106	1.00
31	- 42	-	110	-	93	17	110	1.00
32	- 44	-	114	-	93	20	114	1.00
33	- 46	-	117	-	93	24	117	1.00
34	- 48	-	121	-	93	28	121	1.00
35	- 50	-	125	-	93	31	125	1.00
36	- 52	-	128	-	93	35	128	1.00
Total				**7 579**				

τ	H	COP_{HP}	P_{HP}	$Effy_{Aux}$	P_{aux}	P	E
1.33	270	5.10	40	1.00		53	71
11.78	2 290	4.93	39	1.00		53	619
21.24	3 925	4.76	39	1.00		51	1 084
31.24	5 488	4.60	38	1.00		50	1 571
37.94	6 330	4.43	38	1.00		50	1 880
47.18	7 473	4.26	37	1.00		49	2 306
58.83	8 837	4.10	37	1.00		48	2 800
78.42	11 163	3.94	36	1.00		47	3 683
110.20	14 857	3.78	36	1.00		46	5 044
146.96	18 744	3.62	35	1.00		45	6 640
141.84	17 099	3.47	35	1.00		44	6 247
131.49	14 967	3.31	34	1.00		43	5 717
137.52	14 757	3.17	34	1.00		42	5 825
147.84	14 935	3.02	33	1.00		41	6 097
152.05	14 413	2.88	33	1.00		40	6 105
148.87	13 795	2.85	33	1.00		40	5 907
125.42	12 855	2.22	46	1.00		56	7 065
111.67	11 254	2.19	46	1.00		56	6 203
94.66	9 466	2.17	46	1.00		56	5 265
76.56	7 611	2.15	46	1.00		55	4 218
59.38	5 869	2.13	46	1.00		55	3 280
43.14	4 238	2.11	47	1.00		55	2 362
27.07	2 643	2.09	47	1.00		55	1 488
19.50	1 893	2.07	47	1.00		55	1 064
13.43	1 296	2.05	47	1.00		55	737
4.73	441	1.90	49	1.00		57	267
2.10	200	1.86	50	1.00	2	52	110
0.70	69	1.82	51	1.00	6	57	40
0.10	10	1.79	52	1.00	10	62	6
-		1.75	53	1.00	13	66	
-		1.71	54	1.00	17	71	
-		1.67	56	1.00	20	76	
-		1.64	57	1.00	24	81	
-		1.60	58	1.00	28	86	
-		1.56	60	1.00	31	91	
-		1.56	60	1.00	35	95	
	227 190						**93 701**
							2.425

Appendix D. ccASHP listed on the NEEP website.

Manufacturer Name	AHRI #	Indoor model #	Outdoor model #	HSPF Region (IV)	COP at Max. Cap. @ 5°F	Max Cap @5 °F	Rated Cap @47°F	Cap @5/ Cap @47°F
1HVAC	210857353	ACIQ-60HPB	ACIQ-60AHB	10.5	1.91	54356	59000	92%
ACIQ	210857356	ACIQ-60HPB	ACIQ-60AHB	10.5	1.91	54356	59000	92%
DIYCOOL	210857359	ACIQ-60HPB	ACIQ-60AHB	10.5	1.91	54356	59000	92%
CTMORLEY	210191035	MOU-A55VH-4	MIU-A60V-4	10.5	1.91	54356	59000	92%
MOOVAIR	210295923	DMA60HOS20230E7	FMA60HIAHUU230X7	10.5	1.91	54356	59000	92%
LBG PRODUCTS	208136301	LCHB24DO	LCHB24DHNI	11.3	2.1	19400	26000	75%
INNOVAIR	208106859	SEV24H2R19	DEV24H2R19	11.3	2.1	19400	26000	75%
COMFORTSTAR	208142953	CPR24CD(O)	AHU24-SG2	11.3	2.1	19400	26000	75%
TRUST AIR CONDITIONERS	208284009	AH24H/O44P	AH24H/I44P	11.3	2.1	19400	26000	75%
CTMORLEY	209847221	MOU-A24V-4	MIU-A24V-4	11.3	2.1	19400	26000	75%
BREEZE33	208130311	BZ33-HYP18OUT2-G2-P	BZ33-MSAHU18-G2-P	10.8	2	18295	19000	96%
ACIQ	210857357	ACIQ-18ZPL-HP230B	ACIQ-18AHB-HH-M	10.8	2	18295	19000	96%
1HVAC	210857354	ACIQ-18ZPL-HP230B	ACIQ-18AHB-HH-M	10.8	2	18295	19000	96%
DIYCOOL	210857360	ACIQ-18ZPL-HP230B	ACIQ-18AHB-HH-M	10.8	2	18295	19000	96%
DIYCOOL	210857361	ACIQ-24ZPL-HP230B	ACIQ-24AHB-HH-M	11.6	1.9	24252	26000	93%
ACIQ	210857358	ACIQ-24ZPL-HP230B	ACIQ-24AHB-HH-M	11.6	1.9	24252	26000	93%
1HVAC	210857355	ACIQ-24ZPL-HP230B	ACIQ-24AHB-HH-M	11.6	1.9	24252	26000	93%
BREEZE33	208130312	BZ33-HYP24OUT2-G2-P	BZ33-MSAHU24-G2-P	11.6	1.9	24252	26000	93%
MRCOOL	208960636	CENTRAL-24-HP-C-23025	CENTRAL-24-HP-MUAH-23025	10	2.29	18100	24000	75%
CTMORLEY	209865028	MOU-A48VH-4	MIU-A48V-4	10	1.9	46000	50000	92%
INNOVAIR	210343157	SHV48H2R20	DEV48H2R19	10	1.9	46000	50000	92%

Manufacturer Name	AHRI #	Indoor model #	Outdoor model #	HSPF Region (IV)	COP at Max. Cap. @ 5°F	Max Cap @5 °F	Rated Cap @47°F	Cap @5/ Cap @47°F
TRUST AIR CONDITIONERS	208284018	AA48H/O44P	AH48H/I44P	10	1.9	46000	50000	92%
1HVAC	208106640	ACIQ-48-HPB	ACIQ-48-AHB	10	1.9	46000	50000	92%
ACIQ	208106637	ACIQ-48-HPB	ACIQ-48-AHB	10	1.9	46000	50000	92%
MOOVAIR	207706562	DMA48HOS20230E7	FMA48HIAHUU230X7	10	1.9	46000	50000	92%
CANAIR	207706572	CDH2048C21	CDH2048F21	10	1.9	46000	50000	92%
DIRECT AIR	207706567	DIRM-48MAGICPRO20-OU	DIRM-48MAGICPRO20-AH	10	1.9	46000	50000	92%
DIYCOOL	208106634	ACIQ-48-HPB	ACIQ-48-AHB	10	1.9	46000	50000	92%
DIYCOOL	208106633	ACIQ-36-HPB	ACIQ-36-AHB	10.5	1.96	36876	40000	92%
DIRECT AIR	207706566	DIRM-36MAGICPRO20-OU	DIRM-36MAGICPRO20-AH	10.5	1.96	36876	40000	92%
CANAIR	207706571	CDH2036C21	CDH2036F21	10.5	1.96	36876	40000	92%
MOOVAIR	207706561	DMA36HOS20230E7	FMA36HIAHUU230X7	10.5	1.96	36876	40000	92%
DETTSON	210365427	MHD-18	MHD-CC2.0-17.5-M	10.1	2.19	14600	19500	75%
BLUERIDGE	210025757	BMAH6016C	BMAH6016I	10.5	1.91	54356	59000	92%
MAXI AIR	210426581	MAXS-4260	AHMS-6020	10.5	1.91	54356	59000	92%
COMFORT-AIRE	210568228	A-VCD60SA-1	B-VCD60SA-1	10.5	1.91	54356	59000	92%
KERR	210857424	A-KCD60SA-1	B-KCD60SA-1	10.5	1.91	54356	59000	92%
COOPER&HUNTER	208141208	CH-NHPR48LCU-230VO	CH-48AHU	10	1.8	46443	48000	97%
COOPER&HUNTER	208141207	CH-NHPR36LCU-230VO	CH-36AHU	10.6	1.9	39357	40000	98%
ALSETRIA	208130386	MOX430U-24HFN1-MR0	MVC-24HWFN1-M	11.3	2.1	19400	26000	75%
ECO-AIR	208130397	MOX430U-24HFN1-MR0	MVC-24HWFN1-M	11.3	2.1	19400	26000	75%
AC PRO.COM	209748109	AOX430-24HFN1-MR0	AVC-24HWFN1-M	11.3	2.1	19400	26000	75%
COMFORT-AIRE	208136322	A-VMH18SV-1	B-VMH18AV-1	10.8	2	18295	19000	96%
COOPER&HUNTER	208141205	CH-HPR18-230VO	CH-M18AHU	10.8	2	18295	19000	96%
COMFORT-AIRE	208136323	A-VMH24SV-1	B-VMH24AV-1	11.6	1.9	24252	26000	93%

Manufacturer Name	AHRI #	Indoor model #	Outdoor model #	HSPF Region (IV)	COP at Max. Cap. @ 5°F	Max Cap @5 °F	Rated Cap @47°F	Cap @5/ Cap @47°F
COOPER&HUNTER	208101232	CH-HPR24-230VO	CH-M24AHU	11.6	1.9	24252	26000	93%
COMFORT-AIRE	210568232	A-VCD48SA-1	B-VCD48SA-1	10	1.9	46000	50000	92%
DETTSON	210365435	EVD-48-O	EVD-48-I	10	1.9	46000	50000	92%
ECO-AIR	208130406	MOE30U-48HFN1-M-[X1]	MVC-48HWFN1-M	10	1.9	46000	50000	92%
ALSETRIA	208130395	MOE30U-48HFN1-M-[X1]	MVC-48HWFN1-M	10	1.9	46000	50000	92%
BLUERIDGE	208101246	BMAH4816C	BMAH4816I	10	1.9	46000	50000	92%
BLUERIDGE	208101245	BMAH3618C	BMAH3618I	10.5	1.96	36876	40000	92%
ALSETRIA	208130394	MOE31U-36HFN1-M	MVC-36HWFN1-M	10.5	1.96	36876	40000	92%
ECO-AIR	208130405	MOE31U-36HFN1-M	MVC-36HWFN1-M	10.5	1.96	36876	40000	92%
DETTSON	210365434	EVD-36-O	EVD-36-I	10.5	1.96	36876	40000	92%
SENVILLE	210426579	SENDC-36HF-OM	SENDC-36HF-IM	10.5	1.96	36876	40000	92%
COMFORT-AIRE	210568227	A-VCD36SA-1	B-VCD36SA-1	10.5	1.96	36876	40000	92%
COMFORT-AIRE	210568226	A-VCD30SA-1	B-VCD30SA-1	10.5	1.77	25757	33000	78%
MAXI AIR	210426580	MAXS-2430	AHMS-3015	10.5	1.77	25757	33000	78%
DETTSON	210365433	EVD-30-O	EVD-30-I	10.5	1.77	25757	33000	78%
ECO-AIR	208130404	MOD30U-30HFN1-MR0(X)	MVC-30HWFN1-M	10.5	1.77	25757	33000	78%
ALSETRIA	208130393	MOD30U-30HFN1-MR0(X)	MVC-30HWFN1-M	10.5	1.77	25757	33000	78%
BLUERIDGE	208101244	BMAH3018C	BMAH3018I	10.5	1.77	25757	33000	78%
BLUERIDGE	208101243	BMAH2420C	BMAH2420I	12	1.91	24071	24000	100%
COOPER&HUNTER	211246029	CH-NHPR60LCU-230VO	CH-60AHU	10.5	1.96	57600	60000	96%
PERFECTAIRE	211253528	3PAHHSD60-SZO	3PAHHSD60-AHU	10.5	1.91	54356	59000	92%
SEA BREEZE+	211126514	CSZ36H424ZMO	AH36H424ZMI	10.6	1.9	39357	40000	98%
PERFECTAIRE	211253527	3PAHHSD48-SZO	3PAHHSD48-AHU	10	1.9	46000	50000	92%
PERFECTAIRE	211253526	3PAHHSD36-SZO	3PAHHSD36-AHU	10.5	1.96	36876	40000	92%

Manufacturer Name	AHRI #	Indoor model #	Outdoor model #	HSPF Region (IV)	COP at Max. Cap. @ 5°F	Max Cap @5 °F	Rated Cap @47°F	Cap @5/ Cap @47°F
PERFECTAIRE	211253525	3PAHHSD30-SZO	3PAHHSD30-AHU	10.5	1.77	25757	33000	78%
PERFECTAIRE	211253524	3PAHHSD24-SZO	3PAHHSD24-AHU	12	1.91	24071	24000	100%
PERFECTAIRE	211253523	3PAHHSD18-SZO	3PAHHSD18-AHU	11	2.04	18629	19000	98%
PIONEER	207028597	YH4248GHFD18R2	DR048GHFD18HT2	10	1.9	33600	47000	71%
PIONEER	207028595	YH3036GHFD18R2	DR036GHFD18HT2	11	2.1	25200	35000	72%
PIONEER	207028594	YH1824GHFD18R2	DR024GHFD18HT2	10	2.16	16800	23000	73%
SAMSUNG	207465470	AC048BXADCH	AC048BNZDCH	9.8	1.81	41000	53000	77%
SAMSUNG	207465467	AC042BXADCH	AC042BNZDCH	9.6	1.75	39500	47000	84%
SAMSUNG	207465464	AC036BXADCH	AC036BNZDCH	10.2	1.95	33000	40000	83%
SAMSUNG	207465452	AC018BXADCH	AC018BNZDCH	10	1.8	18200	20000	91%
SAMSUNG	210273924	AC036BXUPCH	AV360CT	10.5	2.17	37900	34600	110%
SAMSUNG	210299847	AC048BXUPCH	AV480CT	10	1.92	44300	44000	101%
SAMSUNG	210273925	AC060BXUPCH	AV600CT	10.5	2.06	53100	53000	100%
SAMSUNG	210273923	AC036BXUDCH	AV360CT	9.5	1.93	34600	34600	100%
SAMSUNG	210299846	AC024BXUPCH	AV240BT	10	1.9	26000	26000	100%
ECOER	208141153	EODA18H-4860B	GNC3036BPT	10	2.1	28000	35000	80%
ECOER	208141152	EODA18H-4860B	GNC3036BPT	10	2.1	28000	35000	80%
ECOER	208141147	EODA18H-2436B	GNC2430BPT	10	2.1	19200	24000	80%
ECOER	208141145	EODA18H-2436B	GNC2430BPT	10	2.1	19200	24000	80%
ECOER	207861759	EODA18H-4860B	EAHATN-48B	10	1.98	34400	47000	73%
ECOER	207861758	EODA18H-4860B	EAHATN-36B	10.5	2.1	29200	36000	81%
ECOER	207861756	EODA18H-2436B	EAHATN-24B	10.5	2.1	19600	24000	82%
ECOER	202110529	EODA18H-4860	EAHATN-36	10	2.1	28000	36000	78%
ECOER	202337969	EODA18H-2436	EAHATN-24	10	2.04	19200	24000	80%
HONEYWELL	207698174	HOH16S-60AA	HVTAN-36A	10	2	28400	35400	80%
HONEYWELL	207698173	HOH16S-36AA	HVTAN-24A	10	2.11	17600	24000	73%

Manufacturer Name	AHRI #	Indoor model #	Outdoor model #	HSPF Region (IV)	COP at Max. Cap. @ 5°F	Max Cap @5 °F	Rated Cap @47°F	Cap @5/ Cap @47°F
INVERTERCOOL	207742360	COH16S-60AA	CVTAN-36A	10	2	28400	35400	80%